TECHNICAL REPORT ITL-88-3

LOCK AND DAM NO. 26 (REPLACEMENT) COFFERDAM EXPERIMENTAL AND ANALYTICAL STUDY

Report 5

TENSILE TESTS OF STEEL SHEET PILES

by

Edward F. O'Neil, Willie E. McDonald

Structures Laboratory

DEPARTMENT OF THE ARMY
Waterways Experiment Station, Corps of Engineers
PO Box 631, Vicksburg, Mississippi 39181-0631

September 1988

Report 5 of a Series

Prepared for DEPARTMENT OF THE ARMY
US Army Engineer District, St. Louis
St Louis, Missouri 63101-1986

Monitored by Information Technology Laboratory
US Army Engineer Waterways Experiment Station
PO Box 631, Vicksburg, Mississippi 39181-0631

Unclassified

SECURITY CLASSIFICATION OF THIS PAGE

REPORT DOCUMENTATION PAGE

Form Approved
OMB No. 0704-0188

1a. REPORT SECURITY CLASSIFICATION Unclassified	1b. RESTRICTIVE MARKINGS
2a. SECURITY CLASSIFICATION AUTHORITY 2b. DECLASSIFICATION / DOWNGRADING SCHEDULE	3. DISTRIBUTION / AVAILABILITY OF REPORT Approved for public release; distribution unlimited.
4. PERFORMING ORGANIZATION REPORT NUMBER(S)	5. MONITORING ORGANIZATION REPORT NUMBER(S) Technical Report ITL-88-3
6a. NAME OF PERFORMING ORGANIZATION USAEWES Structures Laboratory 6b. OFFICE SYMBOL (If applicable) CEWES-SC	7a. NAME OF MONITORING ORGANIZATION USAEWES Information Technology Laboratory
6c. ADDRESS (City, State, and ZIP Code) PO Box 631 Vicksburg, MS 39181-0631	7b. ADDRESS (City, State, and ZIP Code) PO Box 631 Vicksburg, MS 39181-0631
8a. NAME OF FUNDING / SPONSORING ORGANIZATION US Army Engineer District, St. Louis 8b. OFFICE SYMBOL (If applicable) CE-LMS	9. PROCUREMENT INSTRUMENT IDENTIFICATION NUMBER
8c. ADDRESS (City, State, and ZIP Code) 210 Tucker Blvd, N. St. Louis, MO 63101-1986	10. SOURCE OF FUNDING NUMBERS PROGRAM ELEMENT NO. / PROJECT NO. / TASK NO. / WORK UNIT ACCESSION NO.

11. TITLE (Include Security Classification)
Lock and Dam No. 26 (Replacement) Cofferdam Experimental and Analytical Study; Tensile Tests of Steel Sheet Piles

12. PERSONAL AUTHOR(S)
O'Neil, Edward F., McDonald, Willie E.

13a. TYPE OF REPORT	13b. TIME COVERED	14. DATE OF REPORT (Year, Month, Day)	15. PAGE COUNT
Report 5 of a series	FROM ______ TO ______	September 1988	164

16. SUPPLEMENTARY NOTATION
Available from National Technical Information Service, 5285 Port Royal Road, Springfield, VA 22161.

17. COSATI CODES			18. SUBJECT TERMS (Continue on reverse if necessary and identify by block number)	
FIELD	GROUP	SUB-GROUP	Axial strains	Cofferdams
			Bending strains	Cracks
			Brittleness	Deformations (Continued)

19. ABSTRACT (Continue on reverse if necessary and identify by block number)

A comprehensive tensile testing and analysis program for steel sheet pile specimens was conducted to develop useful data characterizing the failure mechanisms. Analysis of the behavior of individual sheet piles as well as sheet piles combined as a system are described. Particular attention was given to the interlock joints connecting the sheet pile specimens.

A total of 10 sheet pile tensile tests were performed using steel material from two manufacturers. Five of the sheet pile specimens were of standard-strength steel and five were of high-strength steel. Extensive documentation of the tests included strain gages with XY plots, linear variable displacement transducer displacement readings, before and after tracings of the configurations of the sheet pile specimens as tested, photographic deformation histories, and video cassette recordings of the tests.

(Continued)

20. DISTRIBUTION / AVAILABILITY OF ABSTRACT ☐ UNCLASSIFIED/UNLIMITED ☒ SAME AS RPT. ☐ DTIC USERS	21. ABSTRACT SECURITY CLASSIFICATION Unclassified
22a. NAME OF RESPONSIBLE INDIVIDUAL	22b. TELEPHONE (Include Area Code) / 22c. OFFICE SYMBOL

DD Form 1473, JUN 86 Previous editions are obsolete. SECURITY CLASSIFICATION OF THIS PAGE

Unclassified

18. SUBJECT TERMS (Continued).

Ductility
Failure mechanism
Finite element analysis
Gross strain
High-strength steel
Interlock joints
Linear variable displacement transducer (LVDT)
Modulus of elasticity
Moment diagram
Photographic stress analysis
Platen movement
Regression analysis
Sheet piles
Standard-strength steel
Strain gages
Tensile testing
Web strain
XY plots

19. ABSTRACT (Continued).

Failure of each sheet pile specimen was a result of separation of the connecting interlock joints due to bending deformations. A regression analysis of the data was conducted to provide a best fit equation of the load versus deformation to provide input for a finite element code on sheet pile cofferdams being developed by the US Army Engineer Waterways Experiment Station and Virginia Polytechnic Institute.

PREFACE

The investigation described in this report was conducted by the Concrete Technology Division (CTD), Structures Laboratory (SL), US Army Engineer Waterways Experiment Station (WES) for the Computer-Aided Engineering Division (CAED), formerly the Engineering Application Office (EAO), Information Technology Laboratory (ITL), WES. This study is a part of the project entitled "Lock and Dam No. 26 (Replacement) Cofferdam Experimental and Analytical Study" authorized by the US Army District, St. Louis (LMS). This is Report 5 of seven reports on the project. Mr. Reed Mosher, CAED, is the Project Manager for the project under the general supervision of Dr. Edward Middleton, Chief, CAED, and Dr. N. Radhakrishnan, Chief, ITL. Technical Monitors for the LMS were Messrs. Edward Demsky and Tom Mudd.

The investigation was performed at SL, WES, under general supervision of Messrs. Bryant Mather, Chief,; John M. Scanlon, former Chief, CTD; and Henry Thornton, Chief, Evaluation and Monitoring Unit (EMU); and the direct supervision of Messrs. Edward F. O'Neil and Willie E. McDonald, both of EMU, as Principal Investigators. Instrumentation and laboratory testing assistance were provided by Messrs. Percy Collins, Concrete and Grouting Unit, and Dan E. Wilson, EMU. Mr. Mosher provided many thoughtful insights during this investigation. Final editing and coordination of text and figure layout were coordinated by Mmes. Gilda Miller and Chris Habeeb, editor and editorial assistant, respectively, Information Products Division, ITL, WES.

COL Dwayne G. Lee, EN, is the Commander and Director of WES. Dr. Robert W. Whalin is Technical Director.

CONTENTS

CONVERSION FACTORS, NON-SI TO SI (METRIC) UNITS OF MEASUREMENT

Non-SI units of measurement used in this report can be converted to SI (metric) units as follows:

Multiply	By	To Obtain
feet	0.3048	metres
inches	25.4	millimetres
microinch per inch	254.0	metres
pounds (force)	4.44822	newtons
pounds per inch	1.129848	newton metre
pounds per square inch	0.006894757	megapascals

LOCK AND DAM NO. 26 (REPLACEMENT) COFFERDAM EXPERIMENTAL AND ANALYTICAL STUDY: TENSILE TESTING OF STEEL SHEET PILES

PART I: INTRODUCTION

Background

1. The Engineering Applications Group, Information Technology Laboratory (ITL), US Army Engineer Waterways Experiment Station (WES), requested that the Concrete Technology Division of the Structures Laboratory, WES, conduct tensile tests on sections of steel-sheet piling linked together. These tests provide technical data on the deformation of pile systems, as input to a larger project on cofferdam modeling WES is conducting for the US Army Engineer District, St. Louis.

2. ITL, in conjunction with Virginia Polytechnic Institute (VPI), has been developing a three-dimensional, finite element, cofferdam-cell model for predicting the behavior of cofferdam structures. To correlate the mathematical model with tests, tensile tests of sheet piles coupled together were conducted, and deformation data of the system as a whole was collected. A previous set of tests similar to those recorded in this report were performed in 1983 by Shannon and Wilson.* In that series of tests, deformation data at the interlocks between pile sections indicated that there was significant bending of the interlocks and sheet piles during the tensile loading. As a result, the present set of tests was undertaken, and a different method of monitoring the deformations at the interlocks was used to account for the bending in the piles and interlocks.

Objectives

3. It is the objective of this test program to develop data that describe the load-deformation relationships for regular- and high-strength

* Shannon and Wilson. 1983 (Mar). "Sheet Pile Interlock Testing," Lock and Dam No. 26, unpublished research report submitted to sponsor agency.

load-carrying differences between sheet piles of the two manufacturers, the load-deformation relationships, and a comparison of the modulus of elasticity of the steel in the sheet pile to the modulus of elasticity of the piles connected together as a system. The load-deformation relationships requested are the deformation of a system of three sections of sheet piles coupled together and tested in uniaxial tension. This, in effect, is measuring the deformation (or strain) of three sections of steel, and the two interlocks between them. Additionally, the tests are conducted in a configuration and environment (a tensile testing frame) which subjects the piles to a different loading condition from that which they would experience under field conditions. It represents the measurement of a very complicated system, and care should be exercised when applying the results to mathematical models.

Scope

4. This investigation consisted of sheet pile preparation, instrumentation, testing, documentation, and data collection and reduction for 10 sheet-pile specimens using steel from two manufacturers. Additionally, deformation descriptions and regression equations were generated in support of steel sheet pile cofferdam modeling efforts.

PART II: DESCRIPTION OF TESTS

Specimen Preparation

Initial pile preparation

5. The piles were received by WES in the form of lengths of sheet pile ranging from approximately 1 to more than 3 ft* long. They were first spray painted to color code them by type, and then sent to the WES machine shop to be prepared for testing.

6. The large pieces of pile were cut across each longitudinal axis to produce test sections which were approximately 3 in. wide. This preparation produced 30 sections of pile which would be configured into 10 tests consisting of 3 sections of pile each. Figure 1 shows a sketch of the configuration of the test specimens.

7. Each cut face of the 30 sections was machined to 3.00 in. ±0.05 in., and polished to receive further specimen preparation. Each section then received a surface grid as described in the following paragraphs.

Specimen gridding

8. Historical record. To maintain a historical record of the deformation of the sheet piles during testing, a method was devised to record the movement of each pile as the tensile load was applied. Of particular interest in the testing was a record of the interlock deformation under load to failure. Previous testing by Shannon and Wilson** determined that there was considerable bending associated with the tensile tests, and that any mechanical method of gaging the interlocks would be compromised by the bending movement. As a result, it was decided to record the deformation by photography. To accomplish this, a reference grid was placed on the face of the piles to be photographed.

9. Method of gridding. The pile sections received the grid by laser burning of the polished surface. This produced a rectangular trough in the surface approximately 0.015 in. wide and 0.008 in. deep. The grid, shown in Figure 1, was scribed on 0.125-in. centers, longitudinally and laterally, in

---

* A table of factors for converting non-SI units of measurement to SI (metric) units is presented on page 3.

** Op. cit., p 4.

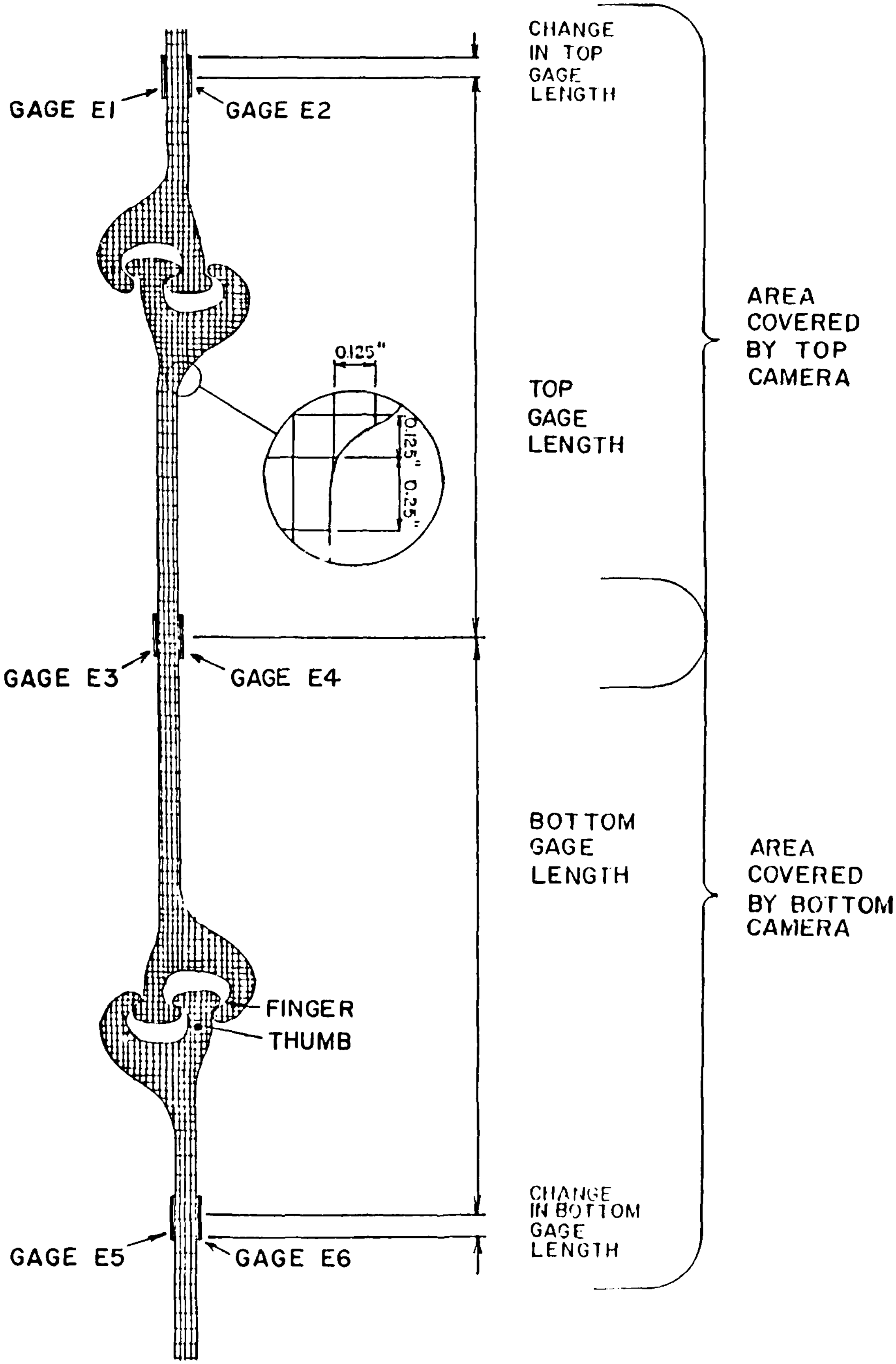

Figure 1. Sketch of the test configuration

the vicinity of the interlocks, and 0.125 in. longitudinally, and 0.25 in. laterally in the vicinity of the web of the pile. The sections of pile were secured on a computer driven platen and moved beneath the laser beam in the pattern described above. This technique provided the most accurate method of gridding.

10. One section of pile was returned from gridding with the grid scribed on the wrong side. This section was turned over, spray painted with black paint, and a grid of approximately the same dimensions scribed into the black paint to reveal the bright metal beneath.

11. Specimen identifiers. Table 1 identifies the type of piles and the number of tests of each type. Throughout the report, the specimens are

Table 1

Characterization of Sheet Pile Types

Sheet Pile Description	Number of Tests	Alternate Description
PS31 standard strength	4	BET01 through BET04
PS31 high strength	4	BETB5 through BETB8
PS32 standard strength	1	USR10
PSX32 high strength	1	USY9

referred to by the above descriptions. However, in the graphs and tables in the appendixes, they are sometimes referred to by the alternate identifiers listed in Table 1.

Final pile preparation

12. Pile section tracing. After the sections were scribed, final preparations were made for testing. Outline tracings of a cross section of each pile in the as-tested configuration were scribed in a mylar material before and after the tests were conducted for comparison of before and after test shapes.

13. The piles were set on the mylar in the configuration they would take in the test machine, the center section carefully removed, and a steel scribe drawn around the outline of each end pile section, thus tracing the outline in the mylar. The center section was then carefully replaced, the end sections removed, and the center section traced. This procedure involved only

the pile section being scribed and did not disturb the orientation of the other sections.

14. Configuring the test specimens. The test configuration consisted of one entire pile section interlocked with two modified pile sections on either side. Each of the sections acting as end pieces was cut in the web section just inside the unused interlock. This was done to allow the outside pile sections to fit into the testing machine. Figure 2 shows the pile sections in the final test configuration.

15. Strain gaging. Bending and axial strains were recorded by monitoring strain gages bonded to the surface of the webs of the pile specimens. In each test six strain gages were bonded to the steel as shown in Figure 1. Two gages were mounted on each section of pile on opposite sides of the web, and were oriented in the direction of the longitudinal axis of the test specimen. The gages on the center section of the test assembly were located at the longitudinal and lateral center lines. The gages on the end pieces were located approximately 3 in. from the beginning of the interlocks. This location was chosen to keep the gages away from the jaws of the gripping device which holds the end pieces in the test machine.

16. The gages used were micromeasurement type EA-06-500BH-120. The gage resistance was 120.0 ±0.3 percent ohm, with a gage factor of 2.04 ± 0.5 percent ohm.

Test Procedure

Test description

17. The tests were conducted by increasing the tensile load monotonically to failure, while recording strains on the three sections of pile and photo-recording movement of the grid scribed on the edge of the sections. Failure was determined to be that load at which the steel yielded, the steel failed in a brittle manner, or the interlocks separated. Yielding was defined as continued deformation without any increase in the load carried by the piles, and separation of the interlocks defined as that point when there was no longer any load transferring capacity between the interlock of one section and its adjacent section.

Test pile setup

18. The 10 tests were conducted in the same manner with only minor

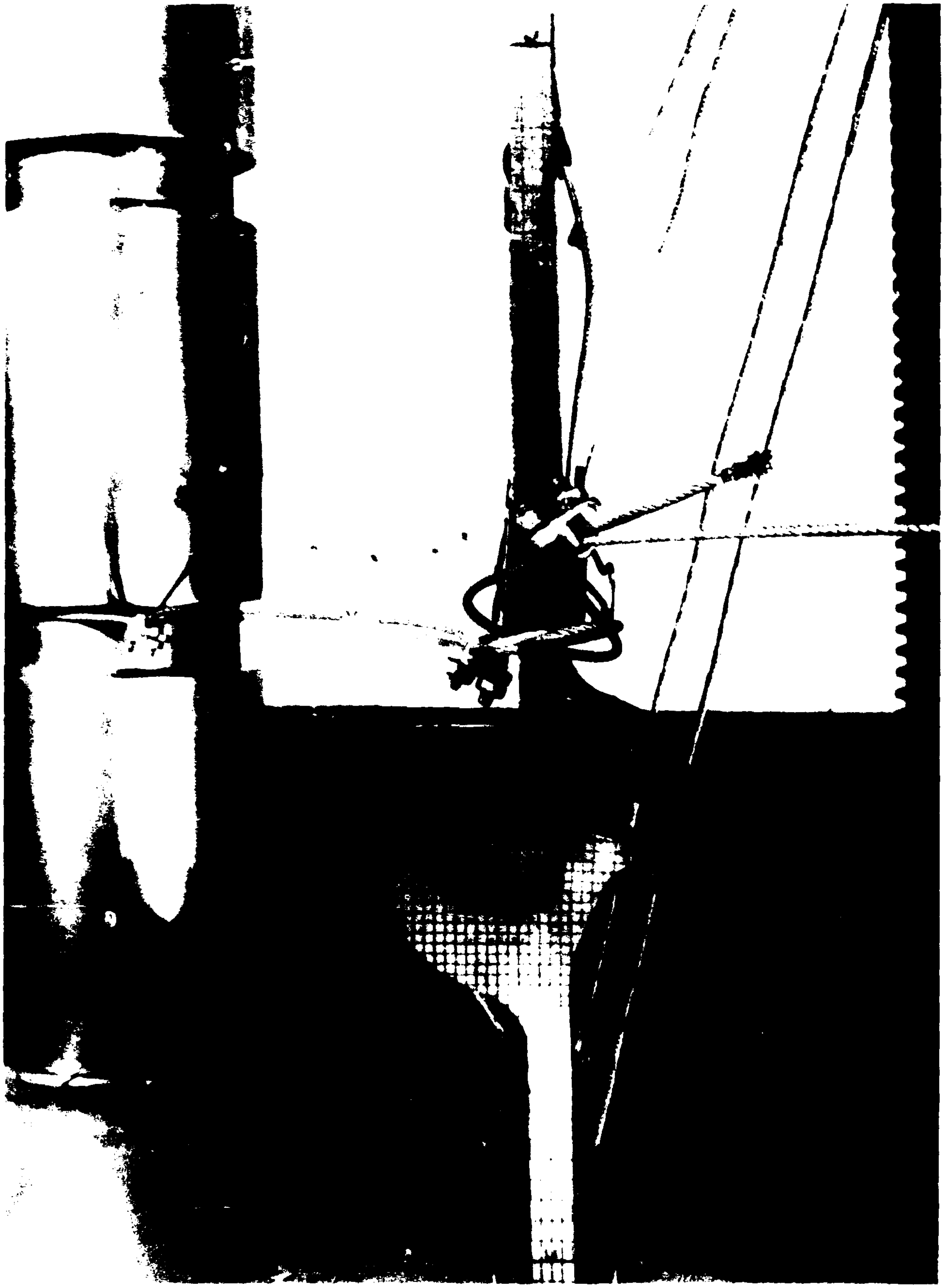

Figure 2. Final test setup

alterations. Initially, the specimens were fitted into the test machine one section at a time. The section that was to be held in the top testing machine grips was mounted first.

19. Approximately 6 in. of the web of the top piece was inserted into the grips. A plumb line was attached to the edge of the top test piece at the point where it emerged from the grips, and the edge of the pile section was aligned with the plumb-line string. The top grips were then tightened.

20. With the plumb line still in place, the bottom test section was set in place. The edge of the bottom section was aligned with the plumb-line string, allowing 6 in. of the pile web to be inserted in the lower grips. The two grips of the test machine were brought together so that the interlocks of the two outside sections of the test specimen touched, and the alignment of the sections were checked to ensure that the two edges aligned by plumb line were still in the same plane.

21. The center test section was placed in the test setup by lowering the testing machine head until the center section could be inserted into the interlocks of the two end sections. The edges of the center section were aligned with the edges of the two end sections.

22. The three sections were mounted with the grids facing the same side and the camera set up. The strain gages were connected to the x-y recorders and the recorders zeroed.

Alternate setup

23. Several of the tests were set up in an alternate manner to note if the setup had any bearing on the outcome of the tests. Rather than loading the top section of the test in the top grips first, the bottom section was first loaded into the bottom grips. Its vertical alignment was certified by use of the plumb line attached to the top grips and the lower section aligned against the plumb line. The top section was then inserted and aligned to the plumb-line string and secured. The middle section was installed as previously described.

Pile seating

24. When the piles were set in the testing machine they were subjected to two load-unload cycles of 1,000 lb. This was done to seat the piles in the grips prior to the test, and to eliminate any major misalignment of the bearing points of the interlocks. It was noted upon placing the center pile in the test setup that the bearing of one interlock section on the other was

not always continuous along the entire 3-in. length of the interlock. This resulted from the variation of the interlock surface during fabrication. The small load was intended to improve the bearing across the entire width of the test specimen.

Loading rate

25. All tests were conducted at the same loading rate and interval between photographs recording the change in deformation of the grid etched on the pile cross section.

26. The specimens were loaded at 5,000 lb per min, from zero load to failure, using a Baldwin 440,000-lb universal testing machine.

27. Photographic records of the deformation of the interlocks and pile webs were recorded at zero load, at each 1,500-lb increment from zero load to 6,000 lb, and at every 3,000-lb increment of load thereafter to failure. A photograph was taken at the failure load, and the remaining frames in the cameras were exposed as rapidly as the shutter would allow during the postfailure portion of the test.

Posttest tracing

28. The piles were removed from the test machine and taken to a laboratory for posttest tracing of the cross section of the test setup. A scribing technique similar to the pretest scribing was used except that one interlock of the test setup (the failure end) could not be repositioned exactly, and it was scribed in a position as close to failure as could be achieved.

Instrumentation

Strain

29. Strains were measured in all tests as described in paragraphs 15 and 16. The six gages used in each test were connected to three separate x-y recorders with the capability of recording two y-variables (strain) and one x-variable. The x-variable of all three x-y recorders was connected to the load cell output of the Baldwin testing machine.

Deformation

30. Photographic record of interlock movement. Cameras were used to record the deformation of the interlocks and webs of the piles. Since the piles would be subjected to bending movements, it was decided that the best

way to record all movement, bending and elongation, was to photograph the test while in progress.

31. Two Hasselblad 2- by 2-in. format cameras were mounted on a ladder, one at the elevation of each interlock of the test specimens. The cameras were completely isolated from the test machine so as not to experience any movement during the test. The cameras contained motor drives, activating the shutters by a remote handheld button.

32. Each camera was positioned to focus on one of the interlocks on the pile cross section. The field of view was adjusted to include the interlock with a reference mark placed on the edge of the pile at the center line of the gages above the interlock and at the center line of the gages below the interlock. The two cameras were also oriented to overlap on the reference mark at the center of the middle pile section so that there would be a record of deformation over the two interlocks.

33. A reference board was placed behind the piles and in line with the field of view of the cameras to act as a reference that did not move with the pile. The reference board was secured to a frame free of the testing environment and was painted with six targets that could be seen in the field of view of each camera.

34. When the piles had been set in the testing machine and had been seated, reference photographs were taken as a record of the pile orientation at zero load, and as a template for a reference grid that would be made after the tests were completed. The pile setup was then loaded to 1,500 lb and a second pair of photographs were taken. This process continued with pairs of photographs being taken at 1,500-lb and 3,000-lb intervals until the pile system failed.

35. Photographic grids. When the photographs were processed, the resulting pictures provided a detailed description of the movement of all areas of the pile. To measure this movement, a reference grid, a duplication of the configuration of the grid prior to testing, could be overlaid on each of the photographs describing the configuration at any given load, and a description of the relative movement of any point on the pile could be easily recorded.

36. The reference grid was produced by placing a sheet of clear acetate over the photograph that was taken just prior to beginning the test and inking a copy of the pile outline and its grid on the acetate. Since the six targets

on the background reference board were also present in the reference photograph, they were also inked onto the acetate so that they could be matched with the targets in the photographs at the various loads to record the original location of the reference pile.

37. The photographs were enlarged to 8 by 10 in. from the 2- by 2-in. negatives; therefore, the deformations taken from the photographs were not at a true scale. To determine the scale, the web of the pile was measured in the photographs, and a corresponding measurement was made on the actual piece of sheet pile. Measurements were made above the interlock, below the interlock, and averaged. This process was repeated for each set of photographs until there was a scale factor for every set. The scale factors for the tests are given in Table 2.

Table 2

Scale Factors Calculated for Photographic Data

Designation on Photograph	Test Descriptor	Scale Factor
1/T	USY9 Top	1.112
1/B	USY9 Bottom	1.112
2/T	USR10 Top	1.113
2/B	USR10 Bottom	1.137
3/T	BET01 Top	1.584
3/B	BET01 Bottom	1.594
4/T	BET02 Top	1.504
4/B	BET02 Bottom	1.518
5/T	BET03 Top	1.597
5/B	BET03 Bottom	1.607
6/T	BET04 Top	1.532
6/B	BET04 Bottom	1.529
7/T	BETB5 Top	1.544
7/B	BETB5 Bottom	1.594
8/T	BETB6 Top	1.513
8/B	BETB6 Bottom	1.521
9/T	BETB7 Top	1.474
9/B	BETB7 Bottom	1.530
10/T	BETB8 Top	1.524
10/B	BETB8 Bottom	1.519

38. Videotape. Three of the tests were videotaped using 0.75-in. video cassette tape. The tapes were recorded from zero load through failure. There was only one tape per test, the field of view was set to include the entire test specimen up to the point in which it was apparent which interlock would be the one to fail. At this point the focus of the taping was shifted to the failing interlock, and the field of view was enlarged and confined to the interlock itself to provide a more detailed view of the failure.

PART III: RESULTS

Failure Mode

39. The 10 pile tests failed by separation of the interlocks. Four tests had failures in the upper interlock, and six tests failed in the lower interlock. Table 3 gives the locations of failure for the 10 tests.

Table 3

Location of Interlock Failure

Test Specimen	Failure Interlock	Cracking Present
PS31 standard strength, Test 1	Bottom	No
PS31 standard strength, Test 2	Bottom	No
PS31 standard strength, Test 3	Top	No
PS31 standard strength, Test 4	Bottom	No
PS31 high strength, Test 5	Top	Yes
PS31 high strength, Test 6	Top	Yes
PS31 high strength, Test 7	Top	Yes
PS31 high strength, Test 8	Bottom	Yes
PSX32 high strength, Test 9	Bottom	No
PS32 standard strength, Test 10	Bottom	No

40. The nonfailure interlocks showed some signs of bending, but the major bending was seen in the thumb and finger portion of the failure interlock. All of the failure interlocks from the high-strength PS31 piles showed cracking of the steel across the inside of the finger of the interlock as a result of the tensile stresses set up by the bending. This cracking was not seen in the standard-strength PS31 piles or either of the PS32 or PSX32 piles.

Load Versus Platen Movement

41. Load versus platen movement plots are presented in Appendix A, Figures A1 through A3. These plots describe the platen movement in inches, measured by a linear variable displacement transducer (LVDT) and the load, and in pounds per inch of specimen width, taken from the load cell of the test machine. The three figures are grouped as tests of: PS31 standard-strength piles, four plots: PS31 high-strength piles, four plots: and PS32

standard-strength and PSX32 high-strength, two plots. One end of the LVDT was attached to the stable base of the test machine and the other end was placed on the movable crosshead. This is shown in Figure 3.

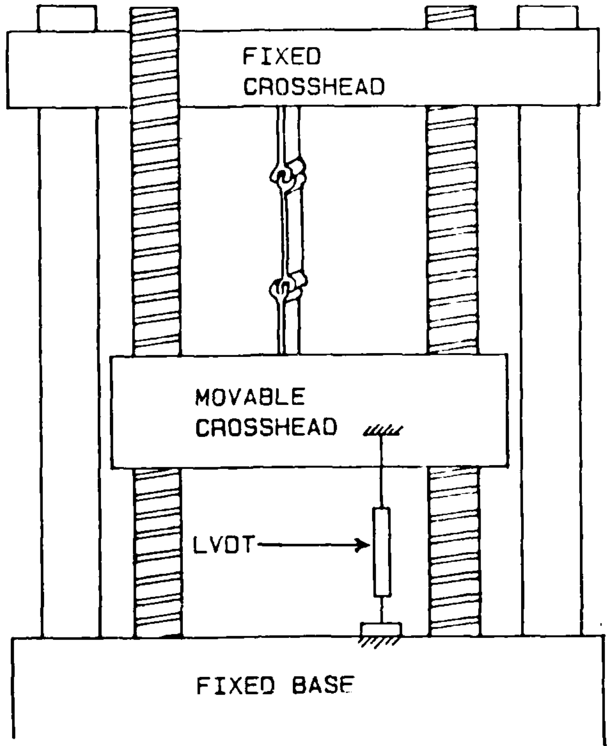

Figure 3. Sketch of LVDT orientation

42. Plots for the PS31 standard-strength piles, Figure A1, show very consistent load-deformation behavior for all of the piles. These curves can be broken into three segments of different load-deformation behavior. Initially, there is a nonlinear segment with significant deformation due to increase in load. With loads of above 5,000 lb/in., a segment of approximately linear load and deformation dominates the curves up to near the failure loads. Finally, near the failure loads, nonlinear behavior of increased deformation with loading occurs as the interlocks begin to separate due to the very high localized strains in the interlock area.

43. The plots for the PS31 high-strength tests, Figure A2, indicate a greater rate of initial deformation than did those for the PS31 standard-strength tests. However, from the early stages of loading to near failure loading, the load-deformation relationship was characterized by near linear behavior. The relationship at failure was nonlinear and not as well defined as the interlocks began to slip rapidly. Also, this phenomena occurred very

shortly before failure as opposed to the condition in the PS31 standard-strength tests. As would be expected for high-strength piles, the ultimate load and deformation were higher than for the PS31 standard-strength tests. It should be noted that the deformation data for the last six data points on Gage 2 in Figure A2 are in error due to a malfunction of the LVDT.

44. The plots for the PS32 piles, both standard- and high-strength, are recorded on Figure A3. The early deformation data for Gage 1 on that plot did not record due to a malfunction of the LVDT. The assumed load deformation for that region has been shown as a dashed line on this plot. Initial deformation in the PS32 standard-strength test, Gage 2, was small, similar to that in the PS31 standard-strength tests. Both graphs began to show a linear load-deformation relationship at early loadings and continued this pattern up to near the failure loads, where the deformations began to increase as failure took place. The tables of the load-deformation data for these tests are given in Appendix A, Tables A1 through A10.

Load Versus Deformation

45. The plots of load versus deformation are given in Figures B1 through B10 in Appendix B. These plots were generated from the photographic raw data taken of both interlocks in each test. They represent the deformation under load that was experienced between the extremes of the two gage lengths shown on Figure 1. There are three curves plotted on each figure. Gage 1 plots the load versus deformation of the top gage length: Gage 2 plots that of the bottom gage length: and Gage 3 is a plot of load versus the sum of deformations of Gage 1 and Gage 2. The load which is plotted against the deformations is the load per unit width of the test pieces (P/W).

46. The data, when plotted, gave a saw-toothed plot rather than a smooth curve. The results of this type of analysis gave deformations which were smaller than those at equal loads using the LVDT data. The data in Figures B1 through B10 appear to be linear or very slightly nonlinear from early loading levels up to immediately before failure. At initial load and at failure there is a higher rate of deformation per load increment than during the middle portions of the test. The combined deformations for the top and bottom gage lengths ranged from 0.29 to 0.48 in. for the PS31 standard-strength piles, and from 0.34 to 0.44 in. for the PS31 high-strength piles.

The largest deformation for both the PS32 and the PSX32 tests was 0.26 in.

47. It is difficult to tell the linearity of the data from the scattered nature of the data points, and an evaluation of the data using regression analysis indicated the data fit best to a third-order polynomial equation. A discussion of the regression analysis is given in Appendix E. The tables of the generated data taken from the photographs are given in Tables B1 through B10 in Appendix B.

Load Versus Bending Strain

48. The plots of load versus bending strain are given in Appendix C, Figures C1 through C10. There are three curves for each test. Curves marked Gage 1 represent the bending strain for the top two gages (Gages E1 and E2 in Figure 1), the curves marked Gage 2 represent the middle two gages (Gages E3 and E4 in Figure 1), and the curves marked Gage 3 represent the bottom two gages (Gages E5 and E6). The data in these plots are, of course, the bending strain as calculated by taking the average of the difference of the two strain gage recordings. A positive result represents bending in one direction, and a negative result represents bending in the other direction. The bending strain is plotted against the load per unit width of test specimen (P/W).

49. The curves generally showed bending that increased rapidly with load early in the loading history, and then became more linear during the majority of the test history. The bending strain was generally below 380 μin./in. for the PS31 standard-strength pile tests, with one exception of Test BET01 at 590 μin./in., and below 485 μin./in. for the PS31 high-strength tests. For the PS32 and PSX32 tests, the maximum bending strains were 325 and 1,733 μin./in., respectively. Whether the strain was positive or negative was a function of how the individual sections of pile were oriented in the test configuration during the test. Approaching the failure load, one of the curves representing the outer pile sections would generally begin to show signs of decreasing bending strain as load increased.

50. The bending strain in the PS31 high-strength piles was characteristically large in one end section, and small in the other end section for the first half of the test. However, by the middle of the loading history, the strain in the two end sections became similar and remained so to the end of the test.

51. The bending strain in the end opposite the failure end generally demonstrated smaller strains than in the end that supported the failure. Further bending details are reported in the discussion of the bending versus load in paragraphs 76 and 77. Tables C1 through C10 in Appendix C give the individual, calculated bending strain and load data for the 10 tests.

Average Web Strain Versus Gross Strain

52. Web strain versus gross strain was computed using the data from the strain gages mounted on the web of the pile and the deformation data taken from the photographs of the test. The web strain is taken as the elongation strain in the center pile section, and is calculated by averaging the strains from Gages E3 and E4 (Figure 1). The gross strain is taken from the photographic data and is defined as the sum of the deformations of both the top and bottom gage lengths, divided by the sum of the original lengths of the top and bottom gage lengths. The top and bottom gage lengths are defined in Figure 1.

53. It should be noted that the gross strain includes deformations associated with two interlocks and the web strain is purely the strain in the steel. Therefore, it should be observed that the gross strain will be much larger than the web strain.

54. Figures D1 through D4 in Appendix D are the plots of web strain versus gross strain for the PS31 standard-strength tests. The four plots give a relatively linear relationship from a web strain of approximately 100 to 1,150 μin./in., with the maximum gross strain within this region ranging from about 3,500 to 7,000 μin./in. Beyond 1,150 μin./in. of web strain, the gross strain increases rapidly to a final value of between 9,000 and 15,000 μin./in. The web strain at failure was between 1,200 and 1,300 μin./in.

55. Figures D5 through D8 show the data for the PS31 high-strength tests. These plots also gave a linear relationship which extended from about 100 μin./in. of web strain out until the tests failed. There was no sharp point in the curve where the piles began to show large increases of gross strain before failure. The gross strain at failure was higher than the PS31 standard-strength tests, ranging from 5,300 to 14,195 μin./in. The web strain at failure was also somewhat higher than the PS31 standard-strength tests, ranging from 1,575 to 1,760 μin./in.

56. The curves for the PS32 standard-strength test and the PSX32 high-strength test are given in Figures D9 and D10, respectively. Both curves were essentially linear out to a web strain of about 1,000 μin./in. At this point the gross strain was the same for both tests at approximately 6,000 μin./in. The standard-strength piles then began to exhibit a large gross strain increase to 12,165 μin./in. at a failure web strain of 1,075 μin./in., while the high-strength test specimens continued to strain linearly to a failure gross strain of 10,960 μin./in. and a web strain of 1,475 μin./in. The tabular data for all these curves are given in Tables D1 through D10 in Appendix D.

PART IV: DISCUSSION

Load Versus Deformation

Data analysis

57. Measurement of deformation. During the testing, the deformation data were recorded by two methods. An LVDT was attached to the crosshead of the testing machine and recorded the movement of the crosshead over the length of the test. This provided a record of all movement between the two crossheads of the testing frame. The other method of recording movement was to photograph the specimens as they were being loaded and use the photographs to determine the deformation.

58. The deformations recorded by the LVDT were read directly from the raw data x-y recorder plots of load versus deformation. The deformations that were taken from the photographs were made by choosing two points on the reference photograph and measuring the distance between them, using a steel rule with graduations to $1/100^{th}$ in. This was called the reference gage length. The same two points were then measured on each of the photographs representing the different load intervals, and the reference length subtracted from each of these measurements to determine the change in length. The two gage lengths chosen extended from the top strain gage pair to the middle strain gage pair, including the top interlock for the first gage length, and from the middle strain gage pair to the bottom strain gage pair, including the bottom interlock for the other.

59. The convention used to display the load-deformation data throughout this report is opposite from standard conventions for displaying load-deformation or stress-strain data. That is, where strain or deformation is normally reported on the y-axis of a graph, here it has been placed on the x-axis. This was done to allow the deformation to be the dependent variable in the regression analysis equations presented in Appendix E.

60. Plots using crosshead data. Figures A1 through A3 give the load versus deformation plots created using the crosshead deformation data. Figure A1 shows the plots of all the PS31 standard-strength tests, Figure A2 shows all the PS31 high-strength tests, and Figure A3 shows the PS32 and the PSX32 tests. As stated in paragraphs 45, 46, and 47, the PS31 standard-strength piles show an area of high deformation under a small load increase

from a load of about 500 to 3,000 lb/in. This high amount of deformation is attributed to the seating of the piles during the early portions of the test. Part of the deformation in this region of the curve is due to bending of the thumb and fingers of the interlocks as they attempt to seat themselves under load. Another part of the deformation in this region is attributed to slippage of the pile sections in the test machine grips, as the grips were beginning to develop a hold on the specimen. This caused additional deformation in a given increment of load.

61. The LVDT records every movement between the crossheads, including strain in the steel, deformation of the interlocks, and slippage of the test machine grips. This deformation, due to slippage of the grips, is included in these plots although it is not a normal component of sheet-pile deformation due to load on the specimens.

62. Beyond approximately 3,000 lb/in., the plots begin to behave as typical load-deflection plots for tensile testing of steel coupons. That is, in the range of approximately 3,000 to 15,000 lb/in. the plots are relatively straight, reflecting elastic strain in the steel. Above 15,000 lb/in. the plots begin to describe the nonlinear behavior that is indicative of the pile sections separating as a result of bending failure in the interlock region. The failure mechanism is discussed in paragraphs 89 through 101.

63. The four plots shown in Figure A2 are those of the PS31 high-strength tests. Their behavior is similar to the standard-strength tests with the exceptions that the linear elastic portion of the curves is longer and the onset of bending failure is at a higher load, around 23,000 lb/in. The plots are not as tightly grouped as the standard-strength tests, but they are all within the expected range of deformation for a given load. The last six deformation data points for Gage 2 in this figure were not recorded properly by the x-y recorder and as such show no deformation with increasing load.

64. Figure A3 gives the load-deformation data for both the PS32 and the PSX32 piles. These two piles also behaved in a manner similar to the PS31 piles. The lower-strength PS32 pile exhibited lower ultimate strength than the PS31 piles as well as lower initial deformation in the range attributed to seating and slippage movement. The deformation at the early stages of the test of the PSX32 pile was lost due to x-y recorder malfunction, but it exhibited greater initial slip and seating deformation than did the PS32 pile. The PSX32 also failed at a lower ultimate strength than the PS31 high-strength

piles. Tables A1 through A10 give the tabular data for these graphs.

65. Plots using photographic data. Figures B1 through B10 give the load versus deformation data that were collected by analyzing the photographs of the testing. The data are presented differently in these plots because it was possible to separate the deformation associated with each interlock as a function of the load. These figures refer to deformation for top and bottom gage lengths. The top gage length extends from the lateral center line of the gage pair above the top interlock to the lateral center line of the central gage pair; the bottom gage length extends from the lateral center line of the central gage pair to the lateral center line of the gage pair beneath the bottom interlock.

66. Each figure represents one test. Gage 1 in the figures represents the load-deflection history within the top gage length, Gage 2 represents the history of the bottom gage length, and Gage 3 is the summation of the two deformations to represent the deformation of the entire test as a function of load. Figure 4 shows a sketch of the areas covered by each plot. The overall deformation length used with the photographic data does not correspond with the deformation length that was used when the deformation was calculated using the crosshead movement. Since the use of the photographic grids to determine deformation would exclude any movement outside of the length of the grid that was used as a reference, the deformation due to slippage of the specimens in the testing machine grips would not be included. The deformations due to the seating of the interlocks and the strain in the pile would be seen, since they are between the gage marks.

67. It should be noted that the nonlinear, early seating portion of the load-deformation plots shown in Figure A1 are no longer present in these plots and that the relationship here tends to be linear or close to it from early loading to close to failure.

68. Figures B1 through B4 are the plots of PS31 standard-strength piles. The data for all four figures show a relatively linear load-deformation relationship until very close to failure. At the failure load for all four tests, which is approximately 18,000 lb/in., one of the gage lengths increases rapidly, indicating that gage length contained the failed interlock. It is important to observe that up until failure both gage lengths showed similar deformation, and that the movement was not concentrated in the interlock that was ultimately to fail. It is also interesting to note that the

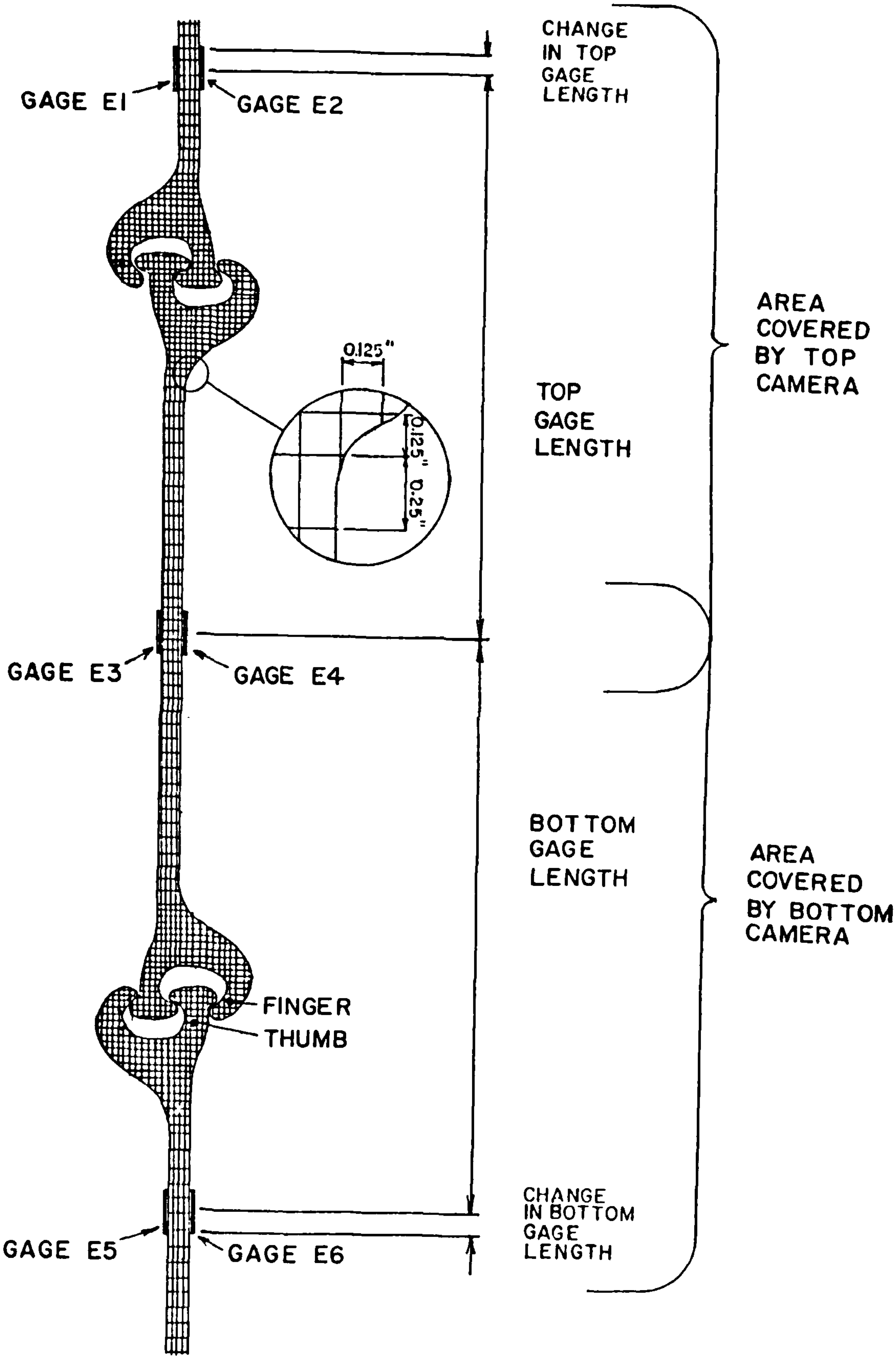

Figure 4. Test setup showing gage lengths

total deformation just before failure is in the range of 0.15 to 0.24 in. as compared to the range of deformation of 0.33 to 0.55 in. just prior to failure in the data taken from the LVDT measurements. This indicates that there is from 0.15 to 0.3 in. of slip associated with seating of the specimens in the test machine grips.

69. Figures B5 through B8 are plots of the PS31 high-strength piles. Their behavior is similar to the PS31 standard-strength piles except that their failure loads are greater than the standard piles by approximately 33 percent. They also showed deformation at both interlocks throughout the test with the failure interlock increasing in deformation only near the failure load. Their total deformation just before failure ranges between 0.24 to 0.36 in., whereas the LVDT measured data indicate between 0.39 and 0.48 in. total deformation. This relates a deformation due to slip in the range of 0.12 to 0.15 in.

70. Figures B9 and B10 show the data taken from the photographs for piles PS32 and PSX32. The graphs show essentially linear deformation up until near failure as with the other specimens. Their maximum deformations are both about the same, at 0.26 in., whereas the maximum deformations in the LVDT data differ by about 0.30 in. (Figure A3).

71. These plots give load-deformation graphs that are not smooth, as were those obtained using the LVDT data. The saw-tooth effect, sometimes indicating that with increasing load there was decreasing deflection, reflects some of the limitations of obtaining data from photographs. It is obvious that in this type of loading configuration, increases in load cannot be accompanied by decreases in deformation. The method allows the measurement of deformations within any subset of the total test length: however, it is difficult to obtain a high degree of accuracy since the measurement rule used only had divisions to 0.01 in., and accuracy beyond that level would have been possible only with more detailed instruments. There is also the possibility of minute variations in the photographic scale from photograph to photograph due to processing deficiencies. The overall trends of the data are nevertheless valid, and the data should be considered as scatter plots to be fitted with a smoothed curve (or straight line).

72. From the comparisons of the LVDT data and the photographic data, it can be stated that the analyses using the LVDT data contain deformations that include slippages between the test specimens and the test frame grips. These

data are eliminated by using data taken from the photographs. It can also be stated that the load-deformation relationships for the 10 tests were nonlinear when the data near the failure load are included, but up to failure the relationship is nearly linear. Paragraphs 73, 74, and 75 summarize the regression analysis undertaken to fit the data to families of curves, with detailed discussion given in Appendix E.

Regression analysis

73. Approach. The regression analysis consisted of applying standard curve fitting techniques to the load versus deformation data to provide the curve that best fit the data. The data were separated into groups according to the type of pile. This gave four groups of data, PS31 standard strength, PS31 high strength, PS32, and PSX32.

74. Data subgroups. The data within each group were separated into two subgroups, those data that represented load deformation at the failure interlock, and those data that represented load deformation at the nonfailure interlock.

75. Analyses results. The results of those regression analyses are presented in detail in Appendix E. In all groups and subgroups an exponential or a third-order polynomial curve best fit the data. The correlation coefficients and sum of the squares of the residuals were close in all respects, however in a majority of cases, the third-order polynomial equation better fit the data. It can be seen from Figures E1 through E16 that even though a third-order polynomial equation better fit the data, the shape of the resulting curve was not characteristic of the behavior of a sheet pile system under a load to failure environment. Since the differences of the correlation coefficients and residuals between curve types were so small, further analysis of the shapes of the suggested curves might indicate that the acceptance of an exponential curve might better represent the overall behavior of a sheet pile system.

Bending Strain Versus Load

Plots

76. Figures C1 through C10 are plots of the 10 tests of bending strain

versus load. These data were compiled from the raw data of strain versus load using the following relationship:

$$\text{Bending strain} = \frac{(e1 - e2)}{2}$$

where e1 and e2 are the strains recorded from gages mounted on opposite sides of the web of the piles. Positive bending strain in these plots indicates curvature of the pile in one direction while negative strain indicates curvature in the opposite direction.

77. The three curves on each plot represent the gage pairs on the top, middle, and bottom sections of pile in the test configuration. The gage pairs are identified in the legend on each plot.

PS31 Tests

78. Figures C1 through C4 are the plots of bending strain for the PS31 standard-strength pile tests. The bending strain in these tests were not evenly distributed. One end carried more strain than the other (with the exception of the strains in Figure C2), as is evident by the plots. In two of the four tests, the strain in the end that was associated with the interlock failure began to decrease rapidly just before the interlock failed. This condition can be explained by realizing that just before the interlock fails, the thumb and fingers each slip out of the other's restraints. This release of restraint allows the interlock to rotate to relieve the moment on the connection, and also relieve the strain in the web.

79. Figures C5 through C8 give the bending strains for the PS31 high-strength specimens. The overall behavior of the strains is essentially the same as the PS31 standard-strength specimens, except the magnitude of the strains is marginally higher. In these four tests, at any given load, the largest bending strain fluctuated between one end pile section, and the middle section. The failure interlock was always the interlock that was between the two sections experiencing the highest strain. The failures were more abrupt than the PS31 standard-strength piles primarily because of the brittle nature of the higher-strength steel. It will be recalled from Table 3 that all of the high-strength piles had developed cracking in the inside of the finger of the interlock. This cracking is a function of the increased brittleness of the material. In all four cases the strain in the end sections of the test

began with differing bending strains, but by the middle of the test, they had become nearly the same and remained so for the rest of the test. This redistribution of bending strain is possibly a function of the cracking in the steel. As the steel began to stress beyond its load carrying capacity, the cracks developed, and the bending moments redistributed. The redistribution increased the load in the nonfailure end, and decreased it in the failure end, to the point where they eventually became similar. The failure end would then be the one that had cracked.

PS32 tests

80. Figures C9 and C10 give the bending curves for the PS32 and PSX32 tests, respectively. The curves in Figure C9 indicate that there was only a very small amount of bending present in any of the sections of the piles. In this figure, the top section exhibited bending in one direction while the middle and bottom showed bending in the other direction. The bending in the bottom section was very small in the same direction as the middle section, and was similar in shape to the top section. At failure, this bottom section showed an increase in bending just before it failed. The graph for the PSX32 pile shows the condition seen in the majority of the PS31 piles, the top and bottom sections bending in one direction, and the middle bending in the other. This set of curves, however, is greatly out of scale with the rest of the tests. The maximum bending strain is in the vicinity of 1,700 μin./in. where the maximum for any other test is in the vicinity of 600 μin./in. The data look correct but is too large to be compared with the rest of the piles. Although it cannot be confirmed, it is suspected that the x-y recorder was incorrectly set when taking the raw data.

Bending behavior

81. There was one bending characteristic which was common to nine of the ten tests. In these nine tests (the exception was PS32), the top and bottom gage pairs exhibited bending in one direction while the middle gage pair exhibited bending in the opposite direction. This characteristic produced an "S" shape in the pile setup which was a result of the webs of the individual sections of pile being out of longitudinal alignment as a function of their interlock geometry. Whether or not the top and bottom pairs exhibited positive or negative bending strain was a function of how the interlocks were oriented when the sections were placed in the testing frame, and do not particularly affect the test results.

82. Several other characteristics were observed in a majority of the tests. As load increased, the change in bending in the middle pile section began to get more linear than did the bending in either the top or bottom section. Close to the failure load, the magnitude of the bending in the middle section was typically smaller than the magnitude of the outer sections.

83. As the loading proceeded to the failure load, the top or bottom gage pair, or both, exhibited a drop in magnitude of the strain. In six of the eight tests of the PS31 piles, the interlock which failed was associated with the section which exhibited the greatest drop in magnitude of the bending strain. This is attributed to the failure mechanism. At the point of failure, the slip between the thumb and fingers in the failure interlock would allow rotation of the piles to relieve the bending moment in the piles affected. This, in turn, would reduce the bending strain in the web of the piles.

84. It was also observed in the same six of the eight PS31 tests, that the interlock which eventually failed was associated with the top or bottom section showing the greatest magnitude of bending strain during the conduct of the test. The higher amount of bending in the web of that pile section during the test could account for additional bending force on the thumbs and fingers of the associated interlock, thereby causing them to open wider than the other interlock and eventually be the interlock that failed.

Web Strain Versus Gross Strain

85. The web strain versus gross strain data suggest that the PS31 standard-strength tests had more ductility than the PS31 high-strength tests because they showed more deformation (increase of gross strain) very near failure. The high-strength specimens did not show this trend. The high-strength tests failed more rapidly when failure was imminent and did not allow the same magnitude of straining. This can be explained by the greater brittle nature of the high-strength steels. The inside faces of all the fingers of the high-strength interlocks (at the failure end) were cracked which attests to the brittle nature of the higher strength steels.

86. The curves of web strain versus gross strain give an indication of how the entire system is deforming (straining) as a function of the strain in the steel. Both graph axes contain data of strain. If the entire system were

straining in the same manner and magnitude as the steel, then the slope of the graph would be unity. However, the gross strain contains deformations which are not present in the web strain, such as interlock slip, so the slope of the graph should be an indication of how the interlocks are deforming in relationship to the strain in the steel. All the graphs were essentially linear up to a web strain close to the failure web strain suggesting a linear relationship in this area. The slope of the line through the data in this region was determined, and the slopes for all the piles in one group averaged. The PS31 standard-strength tests had an average slope of 3.2 while the PS31 high-strength tests had an average of 4.5. These averages indicate that the piles as a system strained about four times more than the steel itself. The high-strength tests indicated a higher ratio because the strain in the steel was smaller, and when applied in the ratio equation would yield a larger ratio.

Stress Versus Gross Strain

87. Plots of stress versus gross strain were generated for the 10 tests in order to compute moduli of elasticity for the test systems. These plots are shown in Figures F1 through F10 in Appendix F. Values of stress were calculated by dividing the load, in pounds per inch, by the average thickness of the individual piles in a test; and the gross strain was calculated by dividing the deformations taken from the photographic data by the original gage length (the sum of top and bottom gage lengths as defined in Figure 4).

88. Linear regression analysis was applied to the individual data points in Figures F1 through F10 to give the best fit straight line through the data points. The slope of this linear equation was used as the modulus and these results are shown in Table 4. The final data points in Figures F1, F2, F3, F4, and F9 were eliminated from the regression analyses because they represented strain close to the failure load where the behavior was nonlinear, and it was felt that if these data points were included it would give a misrepresentation at the slope of the line through the linear portion of the graphs.

Failure Mechanism

Shape of the specimens under load

89. As tensile load was applied to the three sections under test, the

Table 4

Moduli of Elasticity for Sheet Pile Systems

Test Descriptor	Modulus, psi
BET01	5.711376E 06
BET02	7.148397E 06
BET03	6.420222E 06
BET04	8.072899E 06
BETB5	5.090473E 06
BETB6	4.366393E 06
BETB7	4.492315E 06
BETB8	3.285813E 06
USY9	5.002395E 06
USR10	5.392804E 06

geometry of the pile sections caused bending to take place such that the specimens took on a characteristic deformed shape. This was observable in the photographs, as well as from the strain data obtained from the applied strain gages.

90. Observation of the raw strain data for any given gage pair on opposite sides of the pile web shows that one gage experienced greater strain at any given load than its pair. The gage experiencing the greatest tensile strain was always situated on the convex face of the pile, and the gage showing the least tensile strain (in some cases, compressive strain) was always on the concave face of the web. It was also observed that the three sections that made up any test deformed into a characteristic "S" shape in which the top and bottom sections bent in one direction while the middle section bent in the opposite direction, with the points of inflection occurring near the interlocks. This characteristic shape is sketched in Figure 5. If a large number of pile sections were connected, and placed in tension (as in a sheet-pile cofferdam), a serpentine deflected shape with minor modifications, due to the curved line of action in the circular cell would result.

91. This characteristic shape is a function of the misalignment of the longitudinal center lines of the three sections of pile that compose each test. Since the top and bottom jaws of the testing machine are both aligned longitudinally, the center lines of the webs of the piles locked in these jaws are also aligned. The center line of the middle section in the test is always

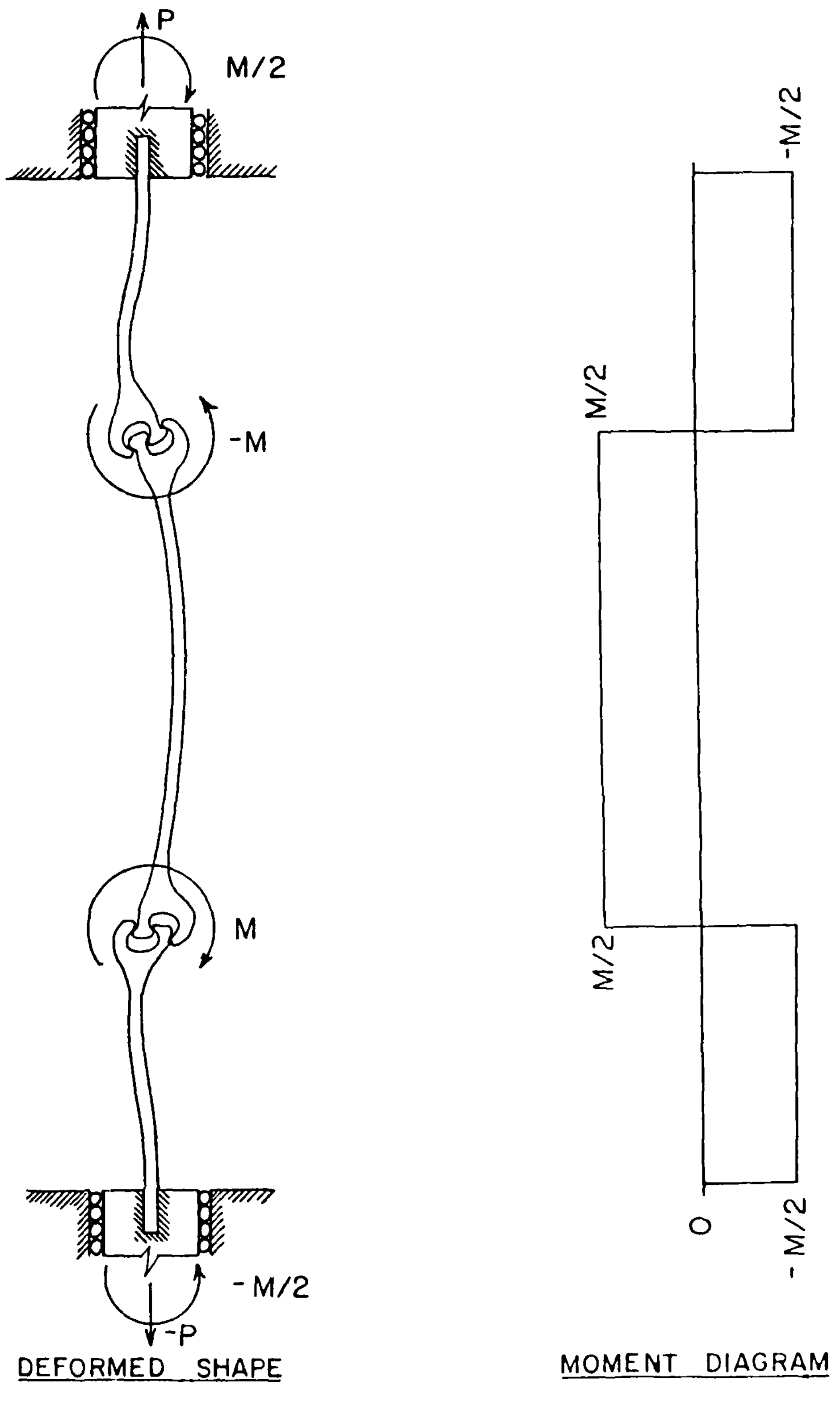

Figure 5. Sketch of deformed shape and idealized moment diagram

offset to one side of these center lines or the other, depending upon how the interlocks were coupled together. When a tensile load is placed on the three sections, the line of action of the load tries to follow the center line of the sections. A couple is formed where the center lines of the adjacent sections deviate from colinearity (at the interlocks), and produces a pure bending moment. Under ideal conditions, the couples at the two interlocks are of equal magnitude and opposite sign.

Moment diagram

92. An idealized moment diagram of the sections as tested is also shown in Figure 5. Since the center line of each web is offset from its neighbor by a slight amount, the effect is to apply a couple at each interlock. This causes the pile group to bend as described in the previous paragraph. Since the end piles are fixed in the grips of the test machine and are not allowed to rotate, each couple at the interlocks, in turn, causes a moment at its gripped end. The shape of the resulting moment diagram is that shown in the figure.

Location of failure

93. In all 10 tests failure resulted from separation of the interlocks. This separation was caused by both the thumb and finger portions of both halves of the interlock bending outward, and allowing the interlocks to separate. Significant deformation in the interlocks began to occur at approximately 80 percent of the final separation load.

94. The sequence of separation was taken from the photographic record of the failure. From the beginning of the loading, the major transfer path that the load would tend to take was from one thumb in the interlock to the other. Some of the load would pass around the fingers and into the fingers and thumb of the other half of the interlock, but the majority of load would pass directly from one thumb to the other. This is because the two thumbs fall closest to the line of action between the two webs.

95. Since the bearing faces between the two thumbs in an interlock slope with respect to each other, they have a tendency to try to slide off one another under tensile load. This sliding is resisted by the confining pressure exerted by the finger on the heel side of each thumb, and the result is that the thumb tries to wedge its way through the thumb and finger on the opposite half of the interlock. As load increases, the thumb wedges its way through the opposite thumb and finger, and they are bent outward, allowing

further slippage of the two thumbs and a smaller bearing surface for the transfer of the load.

96. At the moment before the failure occurs, the heel of the thumb, which was bearing on the inside of the finger of the interlock, has lost all of its bearing surface and is now only confined from horizontal movement by the edge of the finger. The only bearing through the interlock is through a small bearing surface remaining between the two thumbs. Further tensile load on the interlock causes the thumb to slide further off the surface of the opposing thumb and the heel of the thumb to slide out of the confines of the finger. This allows the heel of the thumb to slide sideways, and the remaining bearing between the two thumbs to be lost. This description can be observed in the photographs of the failure interlocks at the higher load pictures.

97. The shape in which the piles deformed was a function of how they were arranged in the testing machine. When load was applied, they deflected into a characteristic "S" shape with the center pile bending one direction and the two outside piles bending in the opposite direction. The interlocks served as points of inflection between the curved sections of the test. These points of inflection serve to point out a phenomenon that occurred in all the tests.

98. At each interlock there are two pile thumbs which bear on each other, and the heels of these thumbs bear on the fingers of the interlock. In the failure mechanism, the heel of one of the thumbs would slip off its finger before the other would, and that would be the beginning of the failure.

99. Relating this back to the point of inflection of the curved "S" shape at the two interlocks, if one were to draw a tangent to the curves at the interlocks, one thumb heel and finger would lie above the tangent, and one would lie below the tangent. In all cases, the thumb heel and finger that slipped first, and thereby began the failure, was the one above the tangent line. This phenomenon is not properly understood since the interlocks would be expected to rotate as a unit when the bending moment was applied.

Interlock position and failure

100. Throughout the tests the failure mechanism was by slippage at the interlocks, but one observable phenomenon points to a reasonable explanation as to which interlock would be the failure interlock. In most of the tests, when one would observe the piles as set up for testing, the relative position

of the two thumbs in the interlock gave a clue as to which interlock would be the failure interlock.

101. Referring to Figure 2 in the text, one notices that the two thumbs of the upper interlock are overlapped more thoroughly than the thumbs of the bottom interlock. This, of course, is where the major load transfer between sections of pile occurs. The load that transfers through this point can be thought of as a load vector, and this load vector causes a bending moment around the root of the thumb. This, in turn, causes the thumb to bend outward under the load. The magnitude of this bending moment is a function of the perpendicular distance between this load vector and the center of bending in the thumb. The larger the distance between the load vector and the center of bending, the larger the moment. Since the top two thumbs in Figure 2 overlap to a greater extent than the thumbs in the bottom interlock, the load vector is closer to the center of bending, and the bending moment in that interlock will be smaller than the bending moment in the bottom interlock. Because the bottom interlock experiences a larger benjing moment, it will experience greater bending and will eventually fail first. Examination of the reference photographs for six of the ten tests confirmed this hypothesis: two of the tests were not possible to determine because the interlocks were so similar, and in two of the tests, the other interlock was the one to fail. This is a contributing factor to the cause of failure; it is not suggested that this is the only mechanism, but one that would make a significant difference.

PART V: CONCLUSIONS

Load Versus Deformation

102. From the comparisons of the load versus LVDT data and the load versus photographic data, it can be stated that the LVDT data contain deformations that include slippages between the test specimens and the test frame grips due to seating of the specimens. These slippages amount to between 0.15 and 0.3 in.

103. From the plots of load versus deformation it was shown that the deformations were similar for the failure end and the nonfailure end up until the failure point, indicating that deformation was distributed throughout the two interlocks of the test.

104. In the analysis of the web strain versus gross strain it can be stated that the overall deformation of the system, to include deformation of the interlocks, was on an average, four times greater than the strain in the web of the pile itself.

105. From the regression analyses, it can be said that the best fit of the raw data is described by both third-order polynomial and exponential curves. On the whole, the third-order polynomials represent the data more closely than the exponential curves. Only where the polynomial curve exhibits decreasing deformation with increasing load does it become inappropriate. Further, the coefficients of the different equations are nearly the same in describing the behavior of each end, indicating that both failure and nonfailure interlocks deformed in a similar manner, up until near failure.

106. As a general deformation conclusion, it can be stated that the PS31 high-strength piles showed less ductility in their behavior near the failure load than the PS31 standard-strength piles. They were also the only specimens in the 10 sets of tests which exhibited cracking of the steel in the fingers of the interlocks.

Bending Strain

107. From the relationships developed of load versus bending strain, the following conclusions can be drawn. Due to the design of the interlock, the longitudinal center lines of adjacent pile webs do not fall on the same line,

and a bending couple is formed at each interlock. This couple then induces bending strain and rotation in each of the pile sections.

108. The configuration of the deformed pile group under the influence of the couples formed at the interlocks is that of a serpentine shape in which every other pile section exhibits bending in the opposite direction.

109. In the tests conducted in this study, generally it can be stated that the pile end section that experienced the greatest bending strain during the conduct of the testing would be connected to the interlock that eventually failed. Also, just prior to failure that end would begin to show a decrease in bending strain. The central section of the test exhibited the smallest bending strain of all sections, but this is due to the geometry of the test.

Failure Mechanism

110. From the tension testing of 10 pile groups, it can be stated that the method of failure in every test was by separation of the interlocks. The overriding cause of the separation was due to the bending failure of the thumbs and fingers of the failure interlock, allowing the interlocked members to separate. The failure always occurred between the heel of the thumb and the finger which restrained that thumb from moving.

111. In a majority of the tests, the failure interlock was the interlock where the two thumbs of opposing halves of the interlock were not as well overlapped and thereby created a larger internal moment in the root of the thumb of the interlock.

APPENDIX A: PLOTS AND DATA TABLES OF LOAD VERSUS PLATEN MOVEMENT

Load versus platen movement plots are presented in Figures A1 through A3, grouped as tests of PS31 standard- and high-strength, PS32 standard-strength and PSX32 high-strength piles. Tables A1 through A10 present the load-deformation data for these tests.

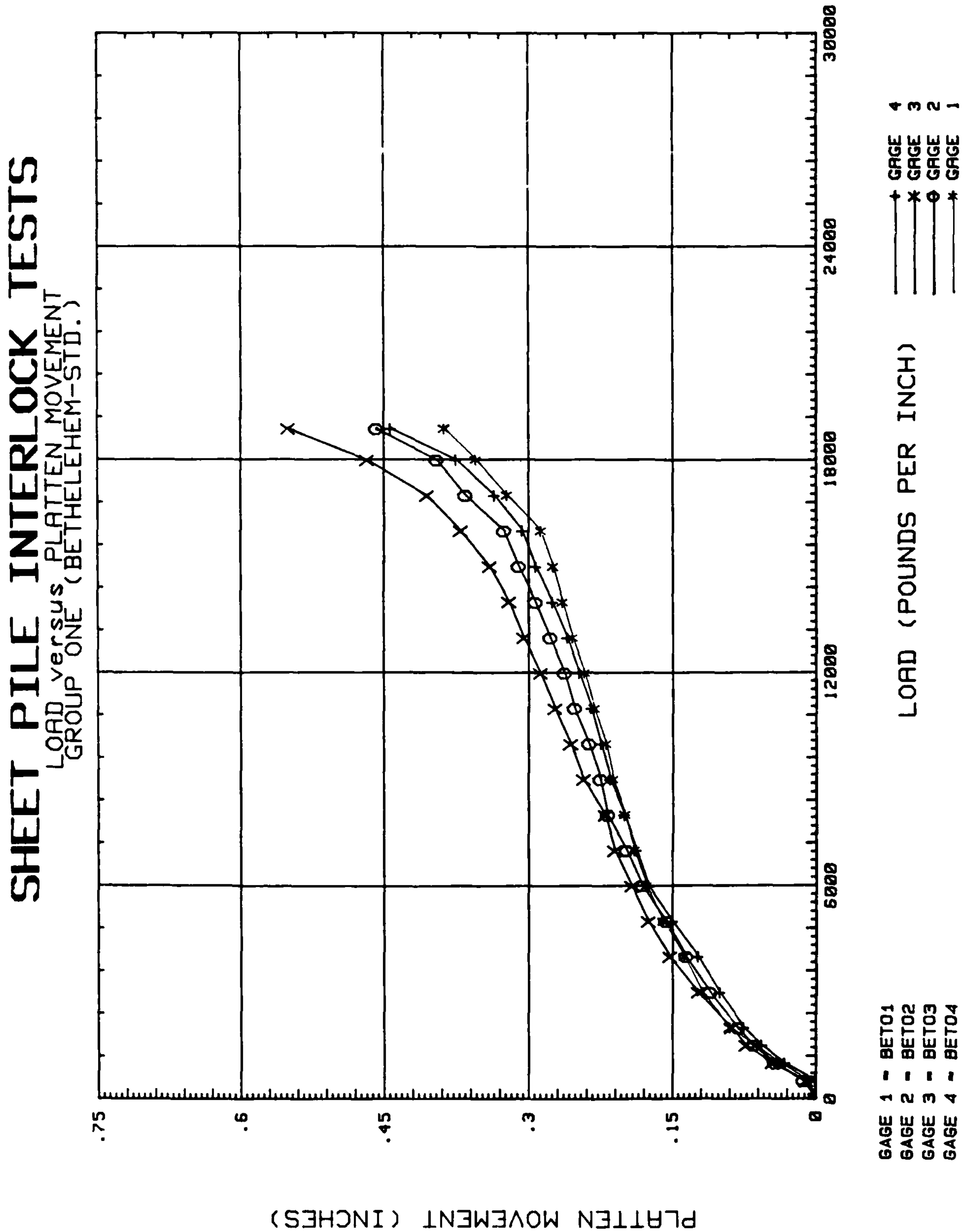

SHEET PILE INTERLOCK TESTS
LOAD versus PLATTEN MOVEMENT
GROUP ONE (BETHELEHEM-STD.)
PLATTEN MOVEMENT (INCHES)
LOAD (POUNDS PER INCH)
0
.15
.3
.45
.6
.75
6000
12000
18000
24000
30000
GAGE 1 - BETO1
GAGE 2 - BETO2
GAGE 3 - BETO3
GAGE 4 - BETO4
GAGE 4
GAGE 3
GAGE 2
GAGE 1

FIGURE A1

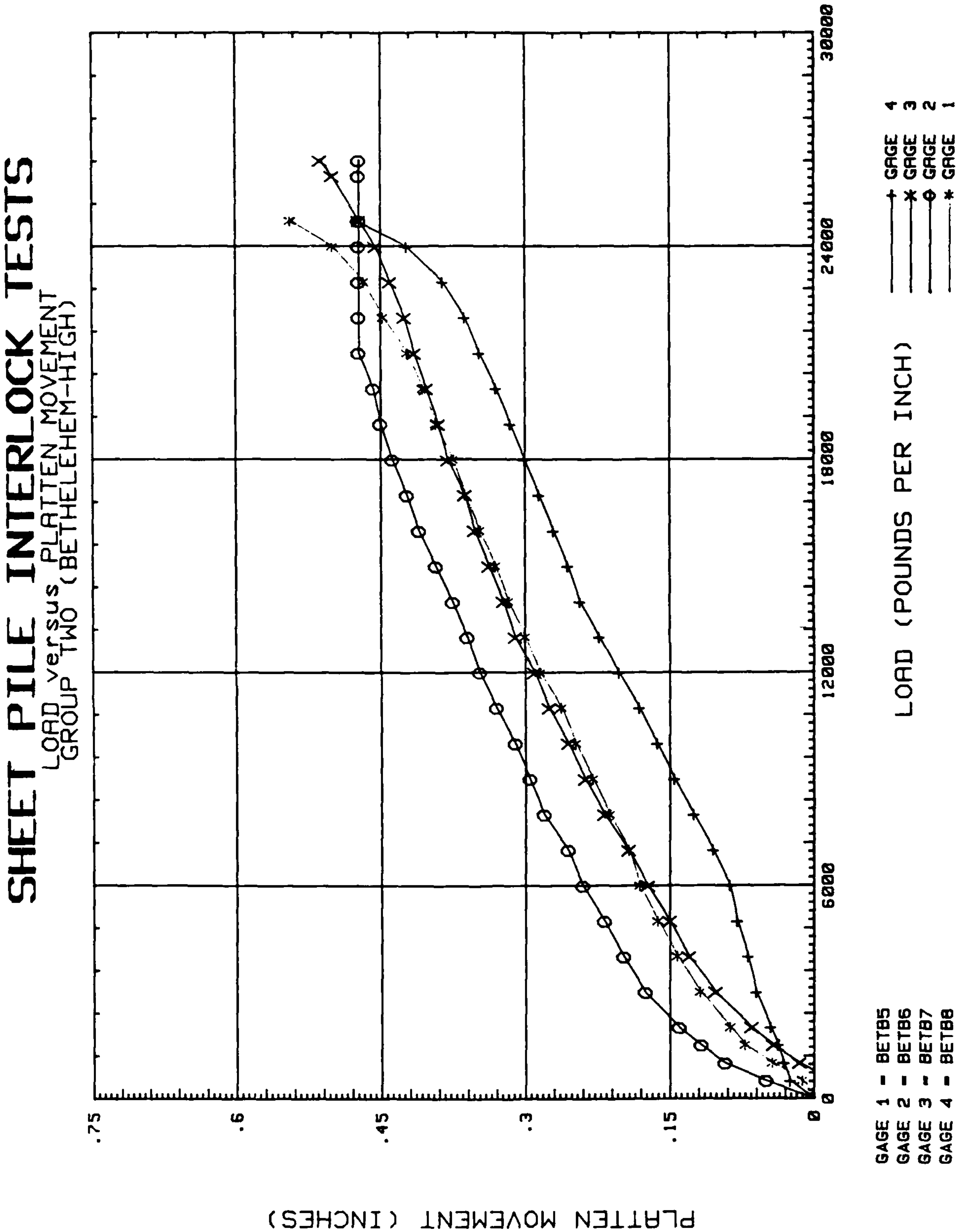

SHEET PILE INTERLOCK TESTS
LOAD versus PLATTEN MOVEMENT
GROUP TWO (BETHELEHEM-HIGH)
PLATTEN MOVEMENT (INCHES)
LOAD (POUNDS PER INCH)
0
.15
.3
.45
.6
.75
6000
12000
18000
24000
30000
GAGE 1 - BETB5
GAGE 2 - BETB6
GAGE 3 - BETB7
GAGE 4 - BETB8
GAGE 4
GAGE 3
GAGE 2
GAGE 1

FIGURE A2

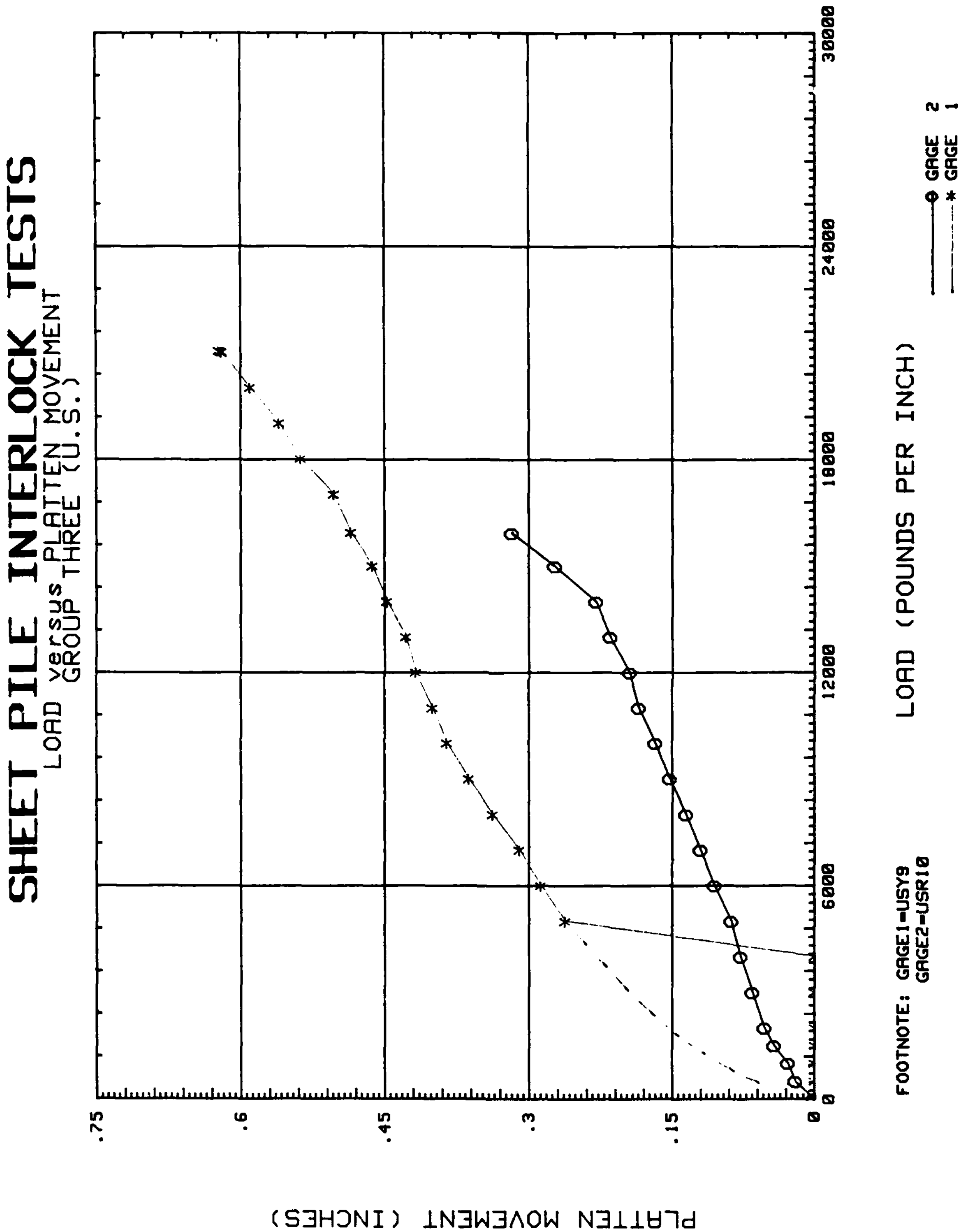

SHEET PILE INTERLOCK TESTS
LOAD versus PLATTEN MOVEMENT
GROUP THREE (U.S.)
PLATTEN MOVEMENT (INCHES)
.75
.6
.45
.3
.15
0
0
6000
12000
18000
24000
30000
LOAD (POUNDS PER INCH)
FOOTNOTE: GAGE1-USY9
GAGE2-USR10
GAGE 2
GAGE 1

FIGURE A3

Table A1

Sheet Pile Interlock Tests

Load Versus Platen Movement

Specimen No. BET01 (Bethelehem-Standard)

Average Pile Width = 3.001 in.

Load		Platen Movement
lb	lb/in.	in.
0	0	0.0000
1,500	500	0.0075
3,000	1,000	0.0375
4,500	1,500	0.0650
6,000	2,000	0.0900
9,000	2,999	0.1188
12,000	3,999	0.1375
15,000	4,999	0.1600
18,000	5,999	0.1775
21,000	6,998	0.1900
24,000	7,998	0.2000
27,000	8,998	0.2125
30,000	9,998	0.2200
33,000	10,998	0.2325
36,000	11,997	0.2425
39,000	12,997	0.2550
42,000	13,997	0.2650
45,000	14,997	0.2750
48,000	15,996	0.2875
51,000	16,996	0.3225
54,000	17,996	0.3550
56,200	18,729	0.3875

Table A2

Sheet Pile Interlock Tests

Load Versus Platen Movement

Specimen No. BET02 (Bethelehem-Standard)

Average Pile Width = 3.003 in.

Load lb	Load lb/in.	Platen Movement in.
0	0	0.0000
1,500	500	0.0125
3,000	999	0.0425
4,500	1,499	0.0650
6,000	1,998	0.0813
9,000	2,997	0.1100
12,000	3,996	0.1350
15,000	4,995	0.1563
18,000	5,994	0.1813
21,000	6,993	0.1975
24,000	7,992	0.2175
27,000	8,991	0.2250
30,000	9,990	0.2375
33,000	10,989	0.2525
36,000	11,988	0.2625
39,000	12,987	0.2775
42,000	13,986	0.2925
45,000	14,985	0.3100
48,000	15,984	0.3250
51,000	16,983	0.3650
54,000	17,982	0.3950
56,950	18,964	0.4575

Table A3

Sheet Pile Interlock Tests

Load Versus Platen Movement

Specimen No. BET03 (Bethelehem-Standard)

Average Pile Width = 3.003 in.

Load lb	Load lb/in.	Platen Movement in.
0	0	0.0000
1,500	499	0.0100
3,000	999	0.0450
4,500	1,498	0.0725
6,000	1,998	0.0875
9,000	2,997	0.1225
12,000	3,996	0.1525
15,000	4,994	0.1750
18,000	5,993	0.1925
21,000	6,992	0.2100
24,000	7,991	0.2200
27,000	8,990	0.2425
30,000	9,989	0.2563
33,000	10,988	0.2725
36,000	11,987	0.2875
39,000	12,986	0.3050
42,000	13,984	0.3200
45,000	14,983	0.3400
48,000	15,982	0.3700
51,000	16,981	0.4050
54,000	17,980	0.4675
57,000	18,979	0.5500

Table A4

Sheet Pile Interlock Tests

Load Versus Platen Movement

Specimen No. BET04 (Bethelehem-Standard)

Average Pile Width = 3.002 in.

Load		Platen Movement
lb	lb/in.	in.
0	0	0.0000
1,500	500	0.0000
3,000	999	0.0325
4,500	1,499	0.0563
6,000	1,999	0.0750
9,000	2,998	0.1000
12,000	3,998	0.1225
15,000	4,997	0.1500
18,000	5,997	0.1750
21,000	6,996	0.1875
24,000	7,996	0.2000
27,000	8,995	0.2150
30,000	9,994	0.2250
33,000	10,994	0.2350
36,000	11,993	0.2475
39,000	12,993	0.2600
42,000	13,992	0.2750
45,000	14,992	0.2925
48,000	15,991	0.3063
51,000	16,991	0.3350
54,000	17,990	0.3750
56,400	18,790	0.4425

Table A5

Sheet Pile Interlock Tests

Load Versus Platen Movement

Specimen No. BETB5 (Bethelehem-High)

Average Pile Width = 3.001 in.

Load		Platen Movement
lb	lb/in.	in.
0	0	0.0000
1,500	500	0.0125
3,000	1,000	0.0438
4,500	1,500	0.0725
6,000	2,000	0.0875
9,000	2,999	0.1188
12,000	3,999	0.1425
15,000	4,999	0.1625
18,000	5,999	0.1813
21,000	6,998	0.1925
24,000	7,998	0.2125
27,000	8,998	0.2300
30,000	9,998	0.2475
33,000	10,998	0.2625
36,000	11,997	0.2850
39,000	12,997	0.3000
42,000	13,997	0.3175
45,000	14,997	0.3313
48,000	15,996	0.3475
51,000	16,996	0.3625
54,000	17,996	0.3750
57,000	18,996	0.3925
60,000	19,996	0.4063
63,000	20,995	0.4224
66,000	21,995	0.4475
69,000	22,995	0.4675
72,000	23,995	0.5000
73,500	24,495	0.5438

Table A6

Sheet Pile Interlock Tests

Load Versus Platen Movement

Specimen No. BETB6 (Bethelehem-High)

Average Pile Width = 3.005 in.

Load		Platen Movement
lb	lb/in.	in.
0	0	0.0000
1,500	499	0.0500
3,000	998	0.0925
4,500	1,498	0.1175
6,000	1,997	0.1400
9,000	2,995	0.1750
12,000	3,993	0.1975
15,000	4,992	0.2175
18,000	5,990	0.2400
21,000	6,988	0.2550
24,000	7,987	0.2800
27,000	8,985	0.2950
30,000	9,983	0.3100
33,000	10,982	0.3300
36,000	11,980	0.3475
39,000	12,978	0.3600
42,000	13,977	0.3750
45,000	14,975	0.3925
48,000	15,973	0.4100
51,000	16,972	0.4225
54,000	17,970	0.4375
57,000	18,968	0.4500
60,000	19,967	0.4575
63,000	20,965	0.4725
66,000	21,963	0.4725
69,000	22,962	0.4725
72,000	23,960	0.4725
75,000	24,958	0.4725
78,000	25,957	0.4725
80,300	26,722	0.4725

Table A7

Sheet Pile Interlock Tests

Load Versus Platen Movement

Specimen No. BETB7 (Bethelehem-High)

Average Pile Width = 3.002 in.

Load		Platen Movement
lb	lb/in.	in.
0	0	0.0000
1,500	500	-0.0175
3,000	999	0.0150
4,500	1,499	0.0425
6,000	1,999	0.0650
9,000	2,998	0.1025
12,000	3,997	0.1300
15,000	4,997	0.1500
18,000	5,996	0.1725
21,000	6,995	0.1925
24,000	7,995	0.2175
27,000	8,994	0.2375
30,000	9,993	0.2550
33,000	10,993	0.2750
36,000	11,992	0.2900
39,000	12,991	0.3100
42,000	13,991	0.3225
45,000	14,990	0.3375
48,000	15,989	0.3525
51,000	16,989	0.3625
54,000	17,988	0.3800
57,000	18,987	0.3900
60,000	19,987	0.4025
63,000	20,986	0.4150
66,000	21,985	0.4250
69,000	22,985	0.4400
72,000	23,984	0.4550
75,000	24,983	0.4725
78,000	25,983	0.5000
78,300	26,083	0.5125

Table A8

Sheet Pile Interlock Tests

Load Versus Platen Movement

Specimen No. BETB8 (Bethelehem-High)

Average Pile Width = 3.002 in.

Load		Platen Movement
lb	lb/in.	in.
0	0	0.0000
1,500	500	0.0250
3,000	999	0.0313
4,500	1,499	0.0375
6,000	1,999	0.0450
9,000	2,998	0.0600
12,000	3,997	0.0688
15,000	4,997	0.0800
18,000	5,996	0.0875
21,000	6,995	0.1050
24,000	7,995	0.1250
27,000	8,994	0.1450
30,000	9,993	0.1625
33,000	10,993	0.1813
36,000	11,992	0.2025
39,000	12,991	0.2225
42,000	13,991	0.2425
45,000	14,990	0.2550
48,000	15,989	0.2700
51,000	16,989	0.2850
54,000	17,988	0.3000
57,000	18,987	0.3150
60,000	19,987	0.3300
63,000	20,986	0.3475
66,000	21,985	0.3625
69,000	22,985	0.3850
72,000	23,984	0.4225
73,200	24,384	0.4750

Table A9

Sheet Pile Interlock Tests

Load Versus Platen Movement

Specimen No. USY9 (US-High)

Average Pile Width = 2.998 in.

Load		Platen Movement
lb	lb/in.	in.
0	0	0.0000
1,500	500	0.0000
3,000	1,001	0.0000
4,500	1,501	0.0000
6,000	2,001	0.0000
9,000	3,002	0.0000
12,000	4,002	0.0000
15,000	5,003	0.2625
18,000	6,003	0.2875
21,000	7,004	0.3100
24,000	8,004	0.3375
27,000	9,005	0.3625
30,000	10,006	0.3850
33,000	11,006	0.4000
36,000	12,007	0.4175
39,000	13,007	0.4275
42,000	14,008	0.4475
45,000	15,008	0.4625
48,000	16,009	0.4850
51,000	17,009	0.5025
54,000	18,010	0.5375
57,000	19,011	0.5600
60,000	20,011	0.5900
63,000	21,012	0.6200
63,100	21,045	0.6225

Table A10

Sheet Pile Interlock Tests

Load Versus Platen Movement

Specimen No. USR10 (US-Standard)

Average Pile Width = 3.002 in.

Load		Platen Movement
lb	lb/in.	in.
0	0	0.0000
1,500	500	0.0200
3,000	999	0.0275
4,500	1,499	0.0425
6,000	1,999	0.0525
9,000	2,998	0.0650
12,000	3,998	0.0775
15,000	4,997	0.0875
18,000	5,997	0.1050
21,000	6,996	0.1200
24,000	7,996	0.1350
27,000	8,995	0.1525
30,000	9,994	0.1675
33,000	10,994	0.1850
36,000	11,993	0.1950
39,000	12,993	0.2150
42,000	13,992	0.2300
45,000	14,992	0.2725
47,600	15,858	0.3175

APPENDIX B: PLOTS AND DATA TABLES OF LOAD VERSUS DEFORMATION

Plots of load versus deformation are given in Figures B1 through B10. These plots were generated from the photographic raw data taken of both interlocks in each test of PS31 standard- and high-strength, PS32 standard-strength, and PSX32 high-strength piles. The generated data taken from the photographs of each of these tests are given in Tables B1 through B10.

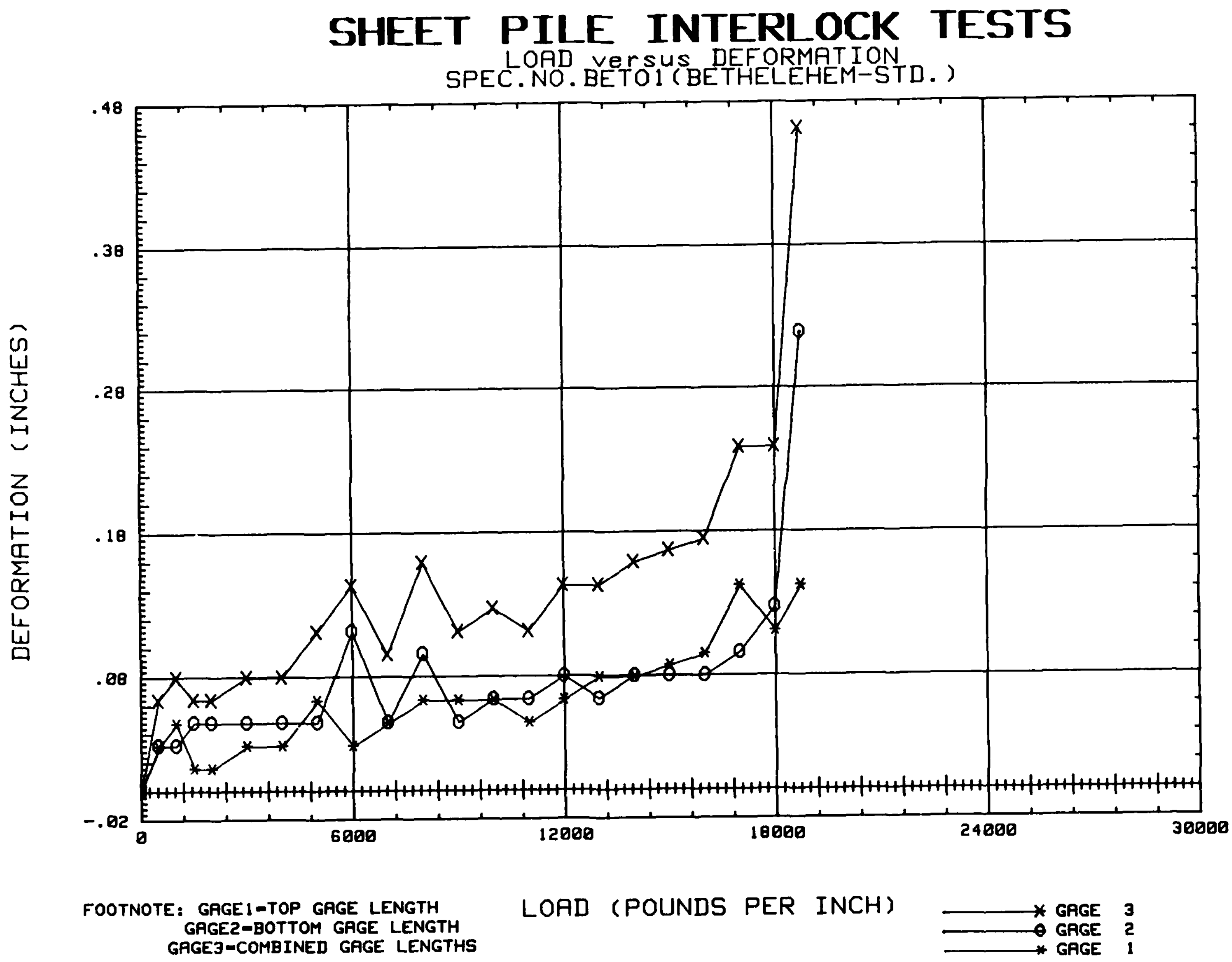
SHEET PILE INTERLOCK TESTS
LOAD versus DEFORMATION
SPEC.NO.BET01(BETHELEHEM-STD.)
DEFORMATION (INCHES)
.48
.38
.28
.18
.08
-.02
0
6000
12000
18000
24000
30000
LOAD (POUNDS PER INCH)
FOOTNOTE: GAGE1-TOP GAGE LENGTH
GAGE2-BOTTOM GAGE LENGTH
GAGE3-COMBINED GAGE LENGTHS
GAGE 3
GAGE 2
GAGE 1

FIGURE B1

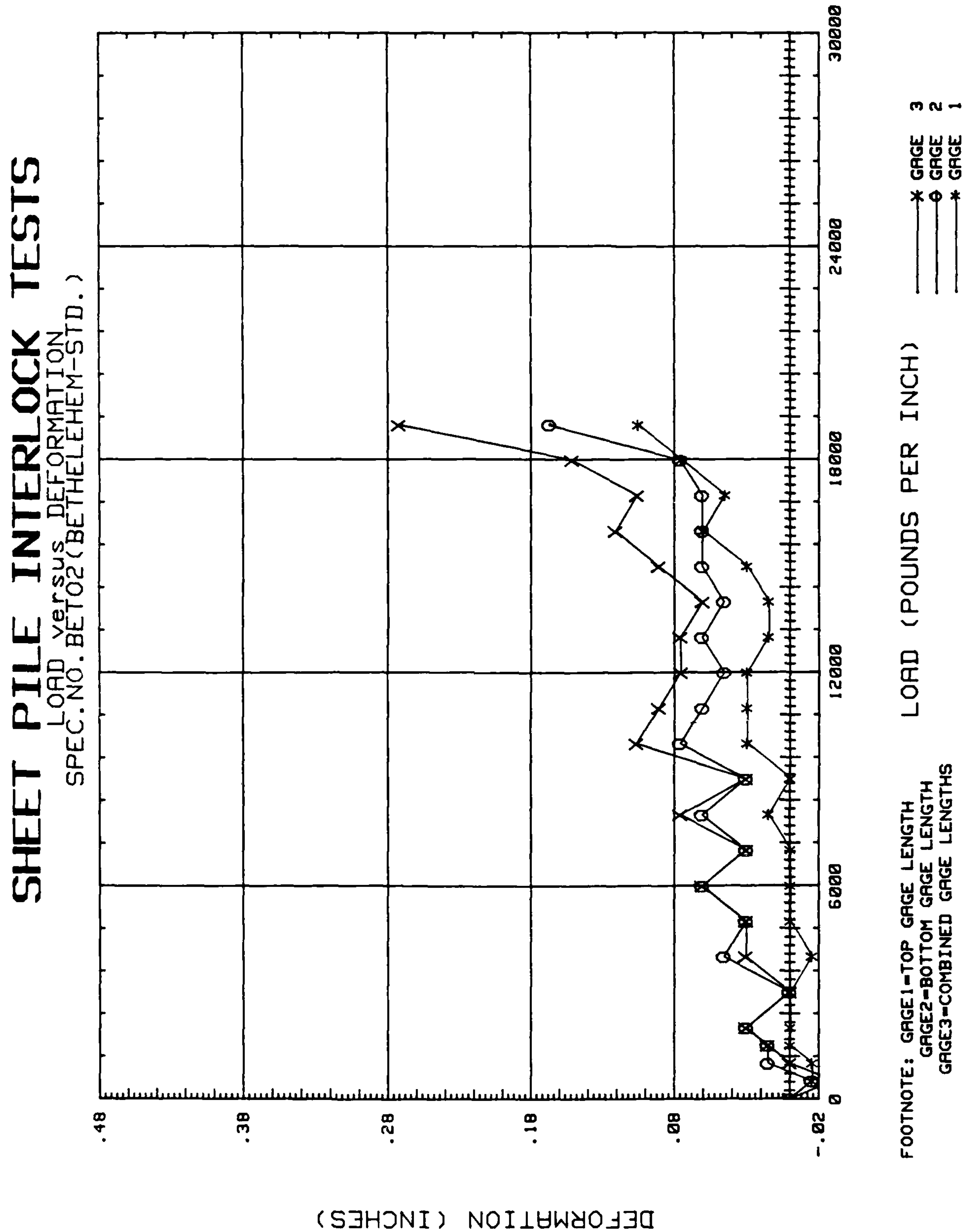
SHEET PILE INTERLOCK TESTS
LOAD versus DEFORMATION
SPEC.NO.BETO2(BETHELEHEM-STD.)
DEFORMATION (INCHES)
.48
.38
.28
.18
.08
-.02
0
6000
12000
18000
24000
30000
LOAD (POUNDS PER INCH)
GAGE 3
GAGE 2
GAGE 1
FOOTNOTE: GAGE1=TOP GAGE LENGTH
GAGE2=BOTTOM GAGE LENGTH
GAGE3=COMBINED GAGE LENGTHS

FIGURE B2

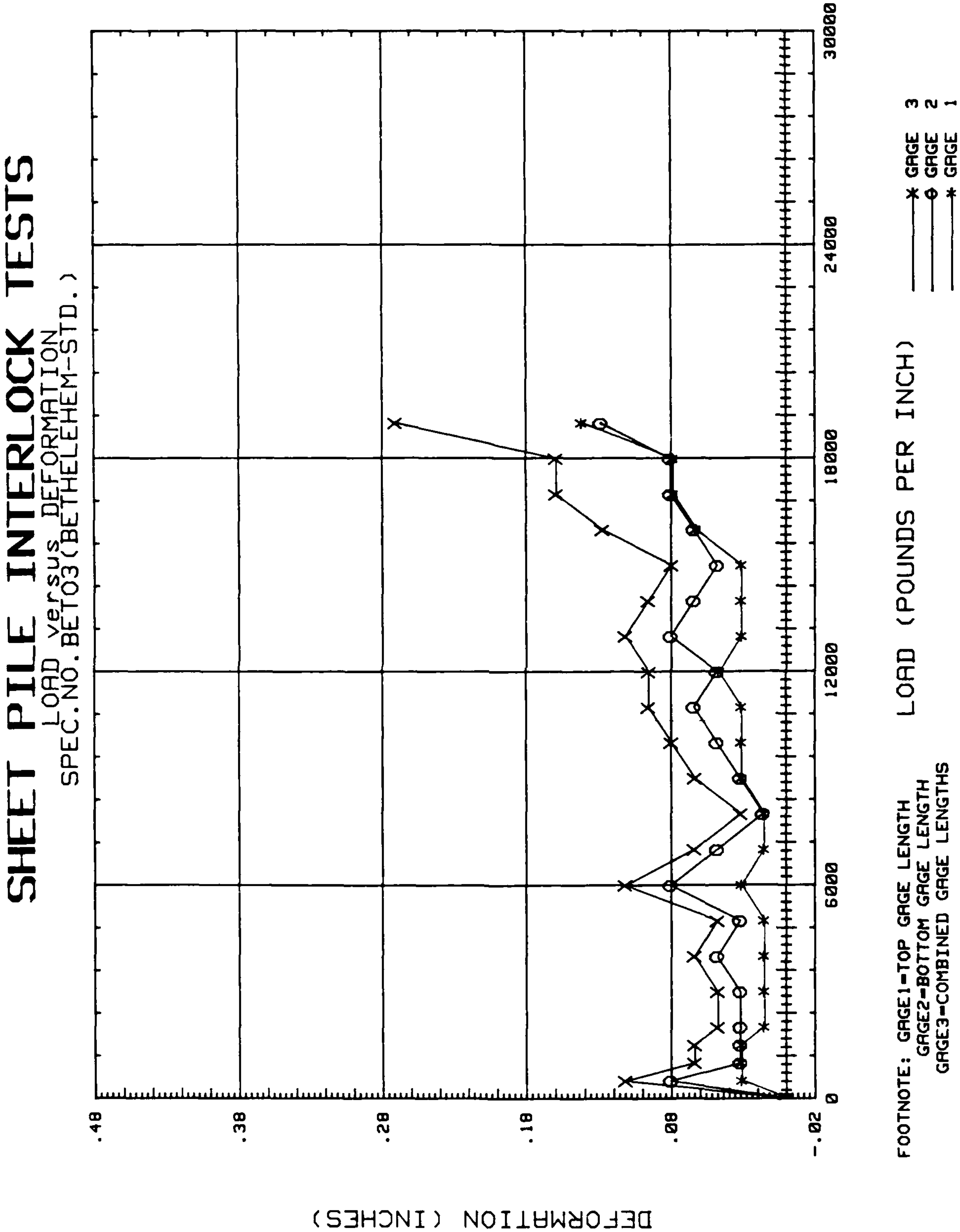

SHEET PILE INTERLOCK TESTS
LOAD versus DEFORMATION
SPEC.NO.BETO3(BETHELEHEM-STD.)
DEFORMATION (INCHES)
.48
.38
.28
.18
.08
-.02
LOAD (POUNDS PER INCH)
0
6000
12000
18000
24000
30000
FOOTNOTE: GAGE1-TOP GAGE LENGTH
GAGE2-BOTTOM GAGE LENGTH
GAGE3-COMBINED GAGE LENGTHS
GAGE 3
GAGE 2
GAGE 1

FIGURE B3

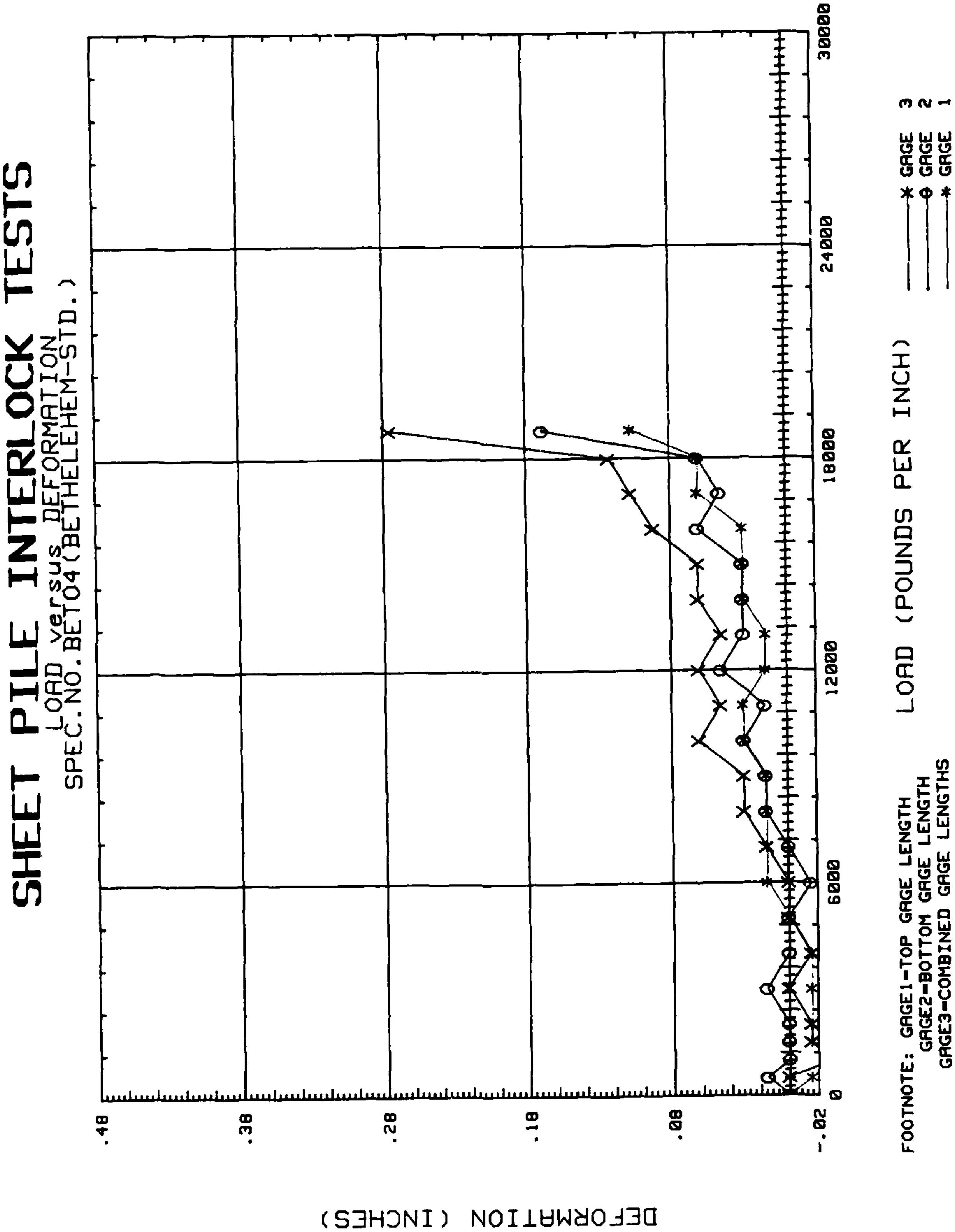
SHEET PILE INTERLOCK TESTS
LOAD versus DEFORMATION
SPEC.NO.BET04(BETHELEHEM-STD.)
LOAD (POUNDS PER INCH)
DEFORMATION (INCHES)
0
6000
12000
18000
24000
30000
-.02
.08
.18
.28
.38
.48
GAGE 3
GAGE 2
GAGE 1
FOOTNOTE: GAGE1-TOP GAGE LENGTH
GAGE2-BOTTOM GAGE LENGTH
GAGE3-COMBINED GAGE LENGTHS

FIGURE B4

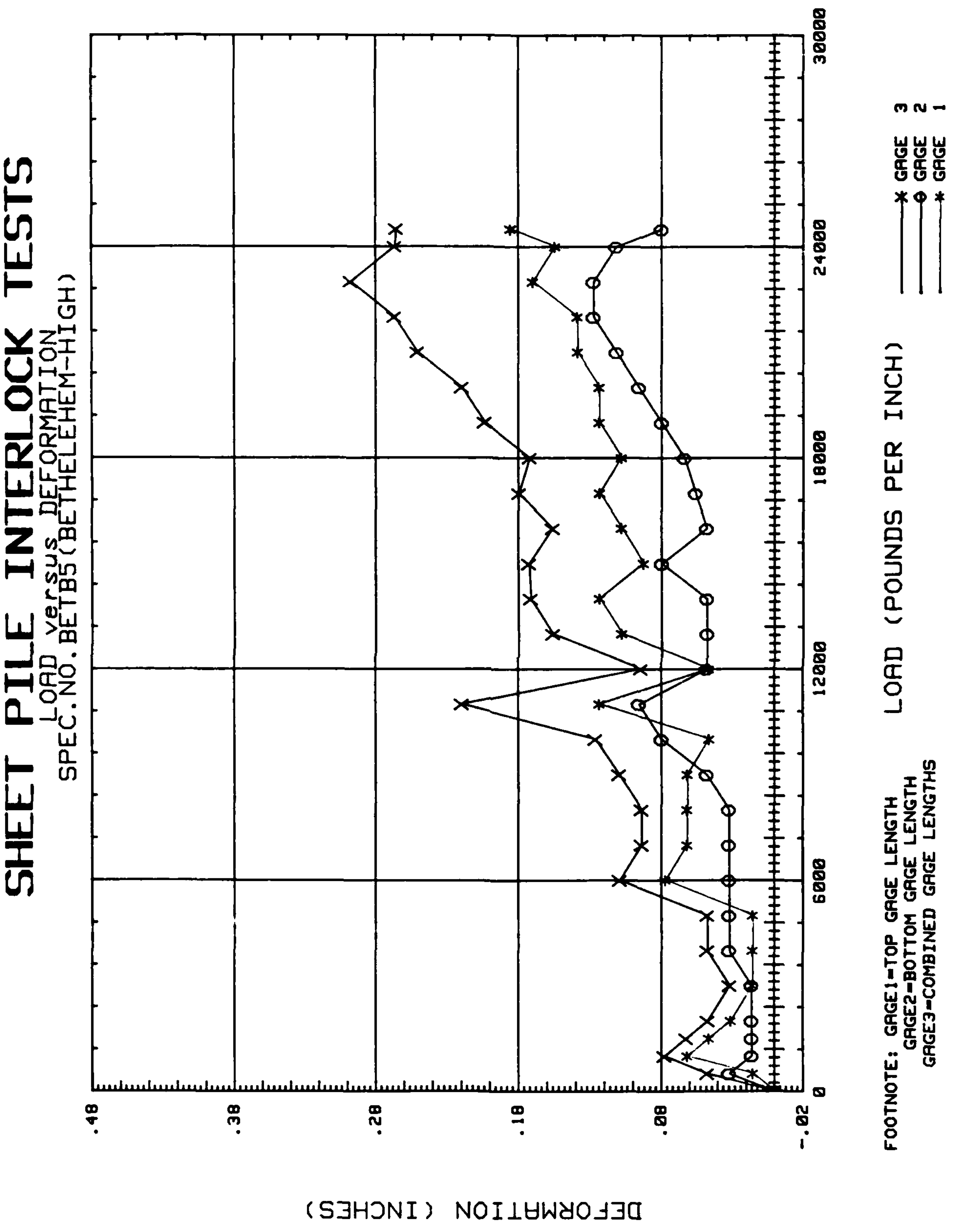

SHEET PILE INTERLOCK TESTS
LOAD versus DEFORMATION
SPEC.NO.BETB5(BETHELEHEM-HIGH)
LOAD (POUNDS PER INCH)
DEFORMATION (INCHES)
.48
.38
.28
.18
.08
-.02
0
6000
12000
18000
24000
30000
GAGE 3
GAGE 2
GAGE 1
FOOTNOTE: GAGE1=TOP GAGE LENGTH
GAGE2=BOTTOM GAGE LENGTH
GAGE3=COMBINED GAGE LENGTHS

FIGURE B5

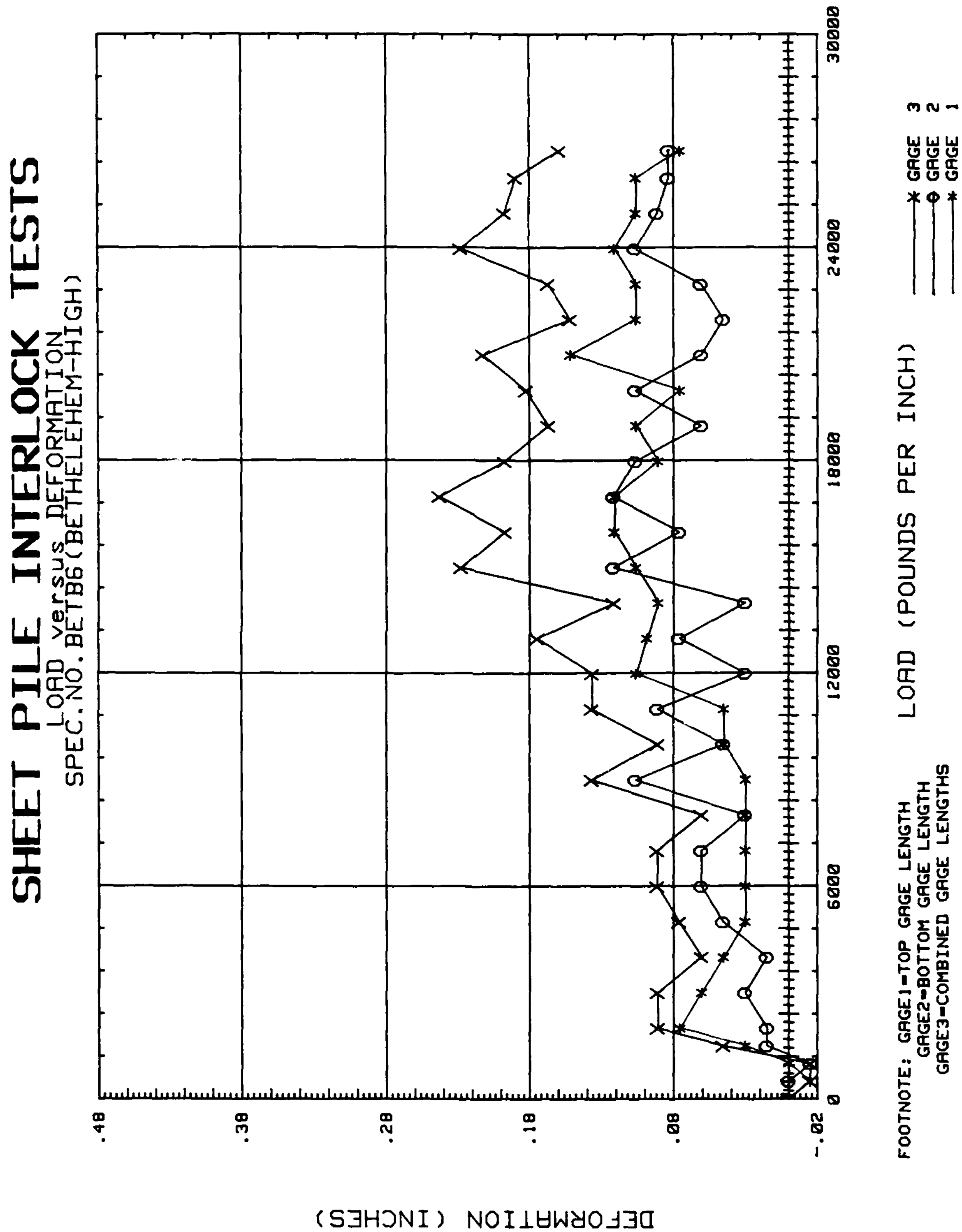
SHEET PILE INTERLOCK TESTS
LOAD versus DEFORMATION
SPEC.NO.BETB6(BETHELEHEM-HIGH)
.48
.38
.28
.18
.08
-.02
0
6000
12000
18000
24000
30000
DEFORMATION (INCHES)
LOAD (POUNDS PER INCH)
FOOTNOTE: GAGE1=TOP GAGE LENGTH
GAGE2=BOTTOM GAGE LENGTH
GAGE3=COMBINED GAGE LENGTHS
GAGE 3
GAGE 2
GAGE 1

FIGURE B6

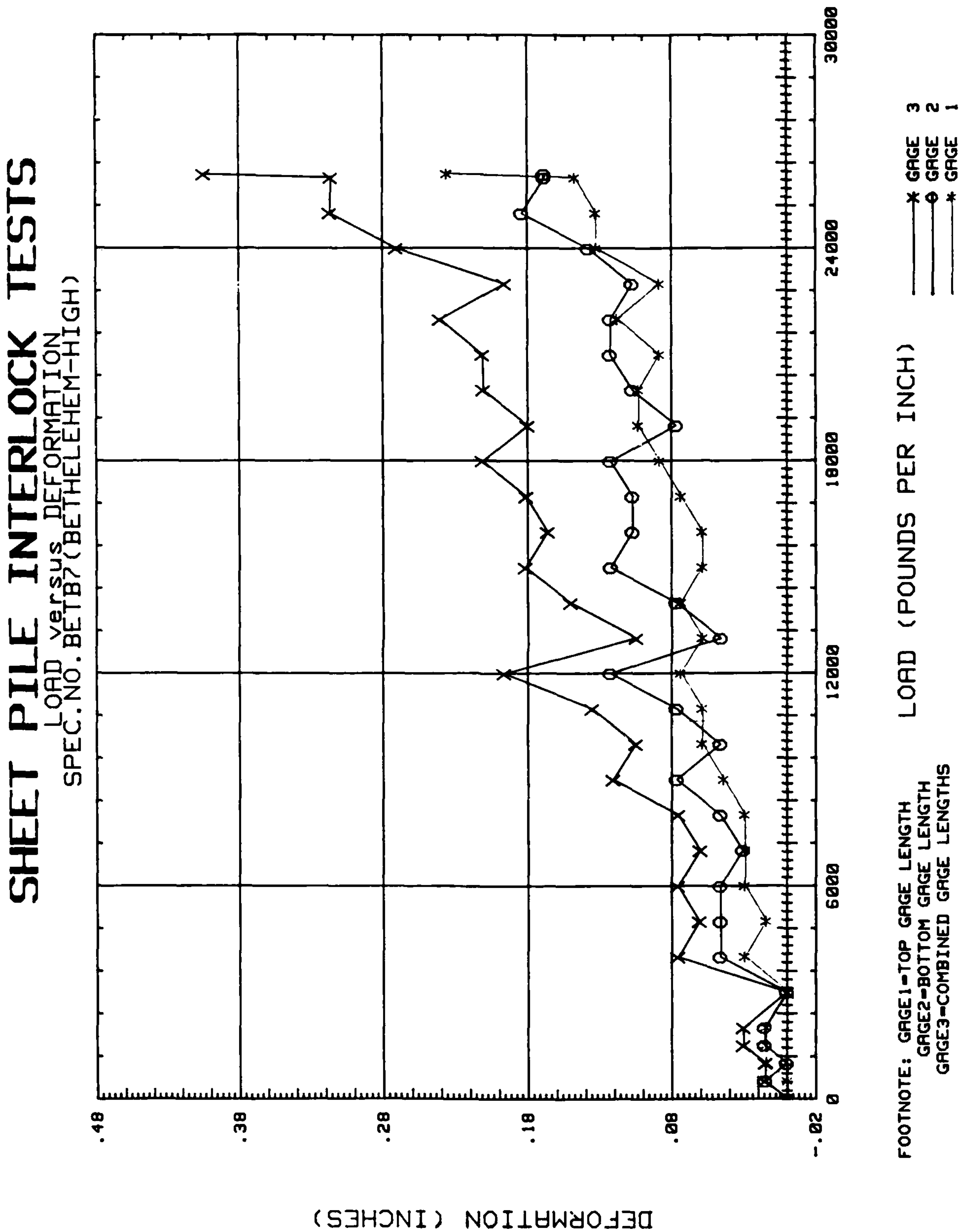

SHEET PILE INTERLOCK TESTS
LOAD versus DEFORMATION
SPEC.NO.BETB7(BETHELEHEM-HIGH)
.48
.38
.28
.18
.08
-.02
0
6000
12000
18000
24000
30000
LOAD (POUNDS PER INCH)
DEFORMATION (INCHES)
GAGE 3
GAGE 2
GAGE 1
FOOTNOTE: GAGE1-TOP GAGE LENGTH
GAGE2-BOTTOM GAGE LENGTH
GAGE3-COMBINED GAGE LENGTHS

FIGURE B7

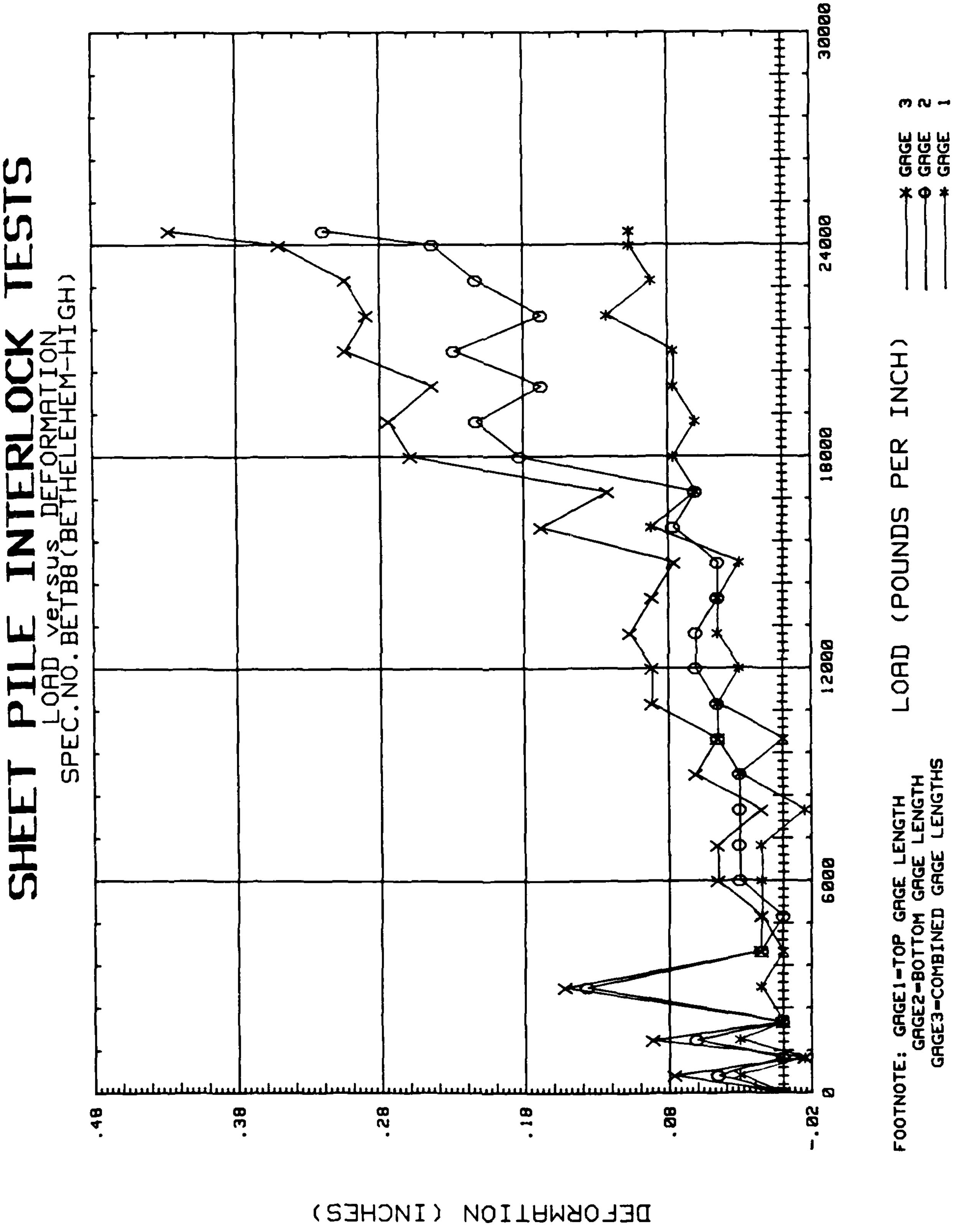

SHEET PILE INTERLOCK TESTS
LOAD versus DEFORMATION
SPEC.NO.BETB8(BETHELEHEM-HIGH)
DEFORMATION (INCHES)
.48
.38
.28
.18
.08
-.02
0
6000
12000
18000
24000
30000
LOAD (POUNDS PER INCH)
GAGE 3
GAGE 2
GAGE 1
FOOTNOTE: GAGE1-TOP GAGE LENGTH
GAGE2-BOTTOM GAGE LENGTH
GAGE3-COMBINED GAGE LENGTHS

FIGURE B8

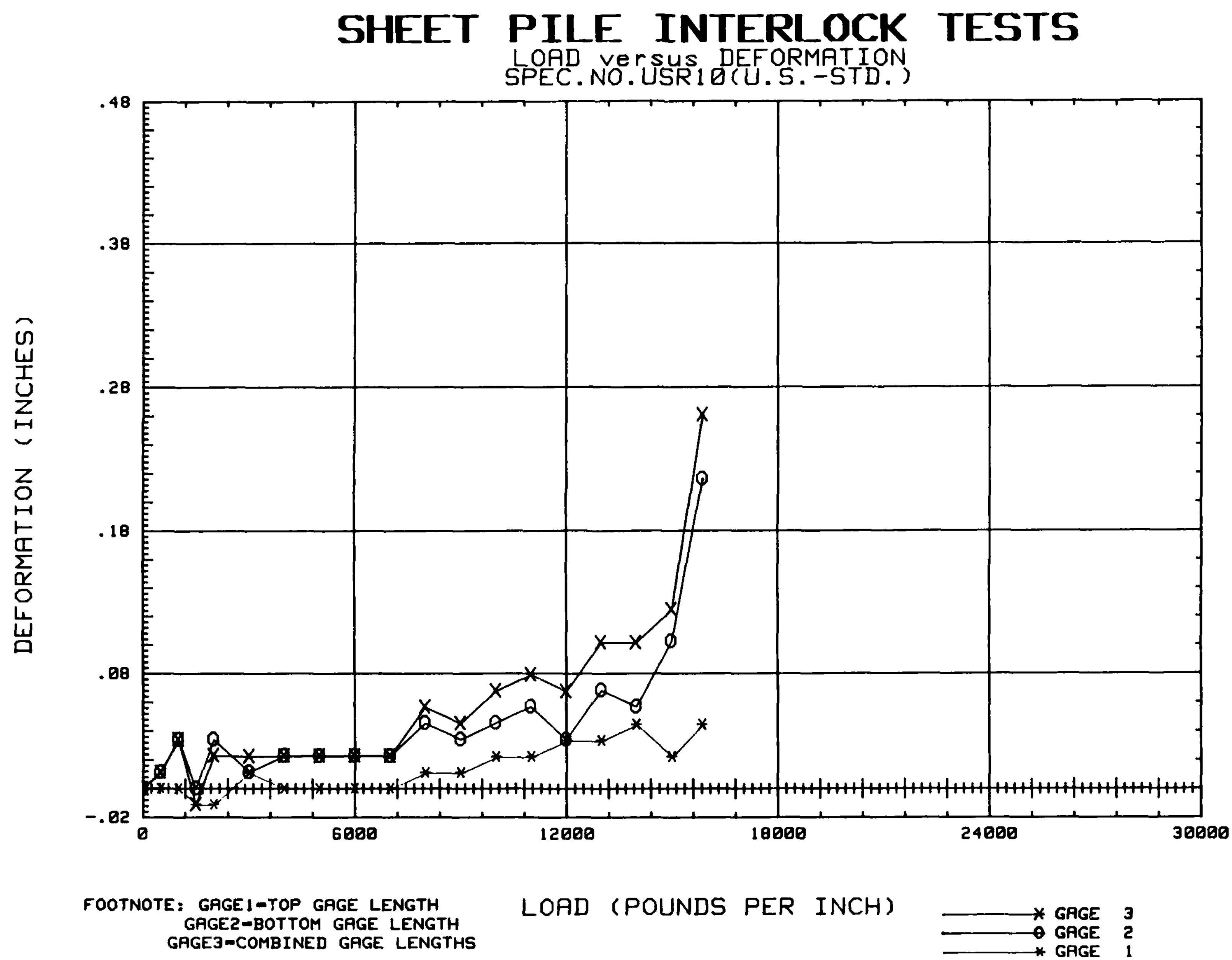

FOOTNOTE: GAGE1=TOP GAGE LENGTH
GAGE2=BOTTOM GAGE LENGTH
GAGE3=COMBINED GAGE LENGTHS

FIGURE B9

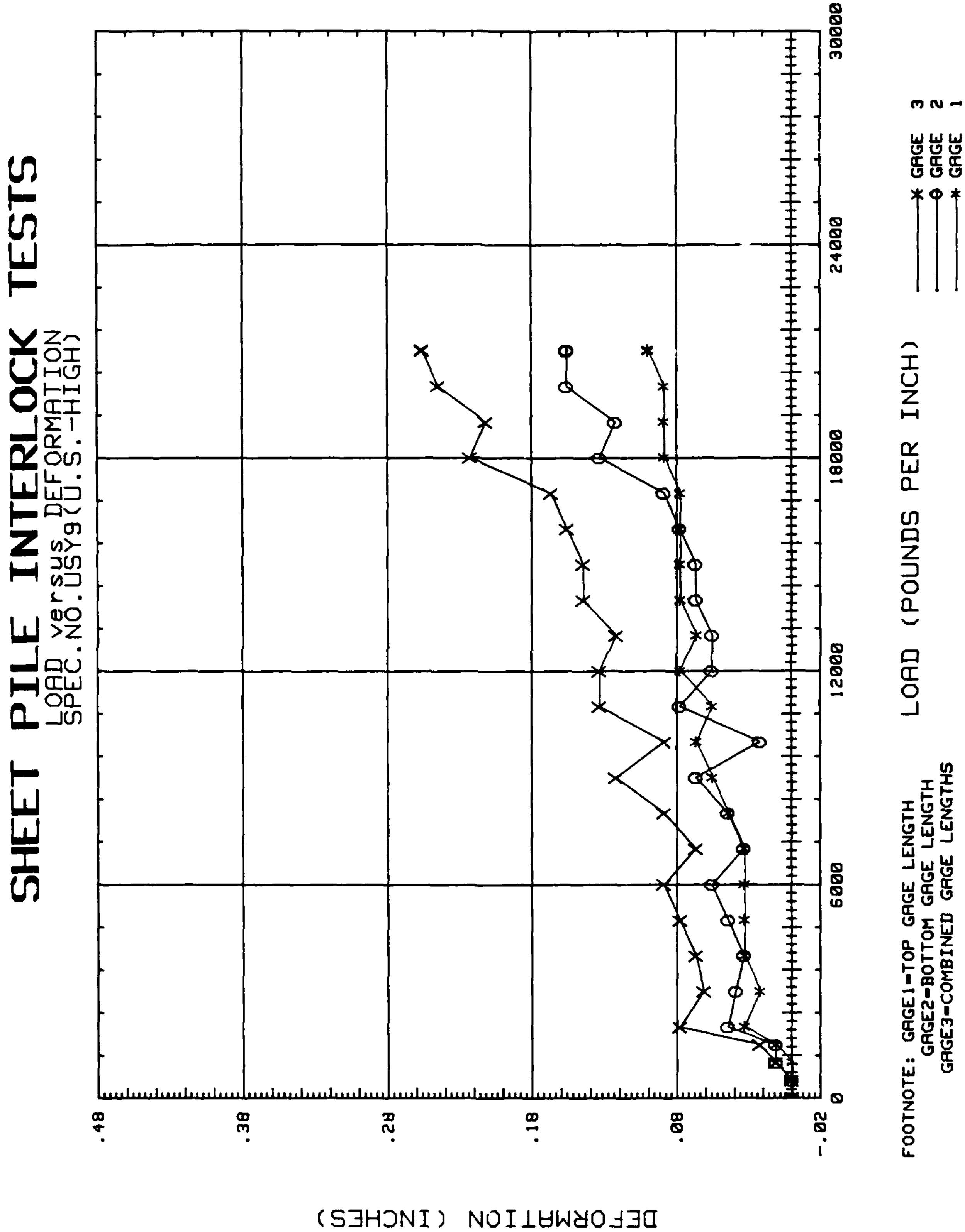

SHEET PILE INTERLOCK TESTS
LOAD versus DEFORMATION
SPEC.NO.USY9(U.S.-HIGH)
DEFORMATION (INCHES)
.48
.38
.28
.18
.08
-.02
0
6000
12000
18000
24000
30000
LOAD (POUNDS PER INCH)
FOOTNOTE: GAGE1-TOP GAGE LENGTH
GAGE2-BOTTOM GAGE LENGTH
GAGE3-COMBINED GAGE LENGTHS
GAGE 3
GAGE 2
GAGE 1

FIGURE B10

Table B1

Sheet Pile Interlock Tests

Load Versus Deformation

Specimen No. BET01 (Bethelehem-Standard)

Average Pile Width = 3.001 in.

Load		Deformation in.	
lb	lb/in.	Top Gage Length	Bottom Gage Length
0	0	0.00000	0.00000
1,500	500	0.03168	0.03188
3,000	1,000	0.04752	0.03188
4,500	1,500	0.01584	0.04782
6,000	2,000	0.01584	0.04782
9,000	2,999	0.03168	0.04782
12,000	3,999	0.03168	0.04782
15,000	4,999	0.06336	0.04782
18,000	5,999	0.03168	0.11158
21,000	6,998	0.04752	0.04782
24,000	7,998	0.06336	0.09564
27,000	8,998	0.06336	0.04782
30,000	9,998	0.06336	0.06376
33,000	10,998	0.04752	0.06376
36,000	11,997	0.06336	0.07970
39,000	12,997	0.07920	0.06376
42,000	13,997	0.07920	0.07970
45,000	14,997	0.08712	0.07970
48,000	15,996	0.09504	0.07970
51,000	16,996	0.14256	0.09564
54,000	17,996	0.11088	0.12752
56,200	18,729	0.14256	0.31880

Table B2

Sheet Pile Interlock Tests

Load Versus Deformation

Specimen No. BET02 (Bethelehem-Standard)

Average Pile Width = 3.003 in.

Load		Deformation in.	
lb	lb/in.	Top Gage Length	Bottom Gage Length
0	0	0.00000	0.00000
1,500	500	-0.01504	-0.01518
3,000	999	-0.01504	0.01518
4,500	1,499	0.00000	0.01518
6,000	1,998	0.00000	0.03036
9,000	2,997	0.00000	0.00000
12,000	3,996	-0.01504	0.04554
15,000	4,995	0.00000	0.03036
18,000	5,994	0.00000	0.06072
21,000	6,993	0.00000	0.03036
24,000	7,992	0.01504	0.06072
27,000	8,991	0.00000	0.03036
30,000	9,990	0.03008	0.07590
33,000	10,989	0.03008	0.06072
36,000	11,988	0.03008	0.04554
39,000	12,987	0.01504	0.06072
42,000	13,986	0.01504	0.04554
45,000	14,985	0.03008	0.06072
48,000	15,984	0.06016	0.06072
51,000	16,983	0.04512	0.06072
54,000	17,982	0.07520	0.07590
56,950	18,964	0.10528	0.16698

Table B3

Sheet Pile Interlock Tests

Load Versus Deformation

Specimen No. BET03 (Bethelehem-Standard)

Average Pile Width = 3.003 in.

Load		Deformation in.	
lb	lb/in.	Top Gage Length	Bottom Gage Length
0	0	0.00000	0.00000
1,500	499	0.03158	0.08035
3,000	999	0.03158	0.03214
4,500	1,498	0.03158	0.03214
6,000	1,998	0.01579	0.03214
9,000	2,997	0.01579	0.03214
12,000	3,996	0.01579	0.04821
15,000	4,994	0.01579	0.03214
18,000	5,993	0.03158	0.08035
21,000	6,992	0.01579	0.04821
24,000	7,991	0.01579	0.01607
27,000	8,990	0.03158	0.03214
30,000	9,989	0.03158	0.04821
33,000	10,988	0.03158	0.06428
36,000	11,987	0.04737	0.04821
39,000	12,986	0.03158	0.08035
42,000	13,984	0.03158	0.06428
45,000	14,983	0.03158	0.04821
48,000	15,982	0.06316	0.06428
51,000	16,981	0.07895	0.08035
54,000	17,980	0.07895	0.08035
57,000	18,979	0.14211	0.12856

Table B4

Sheet Pile Interlock Tests

Load Versus Deformation

Specimen No. BET04 (Bethelehem-Standard)

Average Pile Width = 3.002 in.

Load		Deformation in.	
lb	lb/in.	Top Gage Length	Bottom Gage Length
0	0	0.00000	0.00000
1,500	500	-0.01532	0.01529
3,000	999	-0.03064	0.00000
4,500	1,499	-0.01532	0.00000
6,000	1,999	-0.01532	0.00000
9,000	2,998	-0.01532	0.01529
12,000	3,998	-0.01532	0.00000
15,000	4,997	0.00000	0.00000
18,000	5,997	0.01532	-0.01529
21,000	6,996	0.01532	0.00000
24,000	7,996	0.01532	0.01529
27,000	8,995	0.01532	0.01529
30,000	9,994	0.03064	0.03058
33,000	10,994	0.03064	0.01529
36,000	11,993	0.01532	0.04587
39,000	12,993	0.01532	0.03058
42,000	13,992	0.03064	0.03058
45,000	14,992	0.03064	0.03058
48,000	15,991	0.03064	0.06116
51,000	16,991	0.06128	0.04587
54,000	17,990	0.06128	0.06116
56,400	18,790	0.10724	0.16819

Table B5

Sheet Pile Interlock Tests

Load Versus Deformation

Specimen No. BETB5 (Bethelehem-High)

Average Pile Width = 3.001 in.

Load		Deformation in.	
lb	lb/in.	Top Gage Length	Bottom Gage Length
0	0	0.00000	0.00000
1,500	500	0.01544	0.03188
3,000	1,000	0.06176	0.01594
4,500	1,500	0.04632	0.01594
6,000	2,000	0.03088	0.01594
9,000	2,999	0.01544	0.01594
12,000	3,999	0.01544	0.03188
15,000	4,999	0.01544	0.03188
18,000	5,999	0.07720	0.03188
21,000	6,998	0.06176	0.03188
24,000	7,998	0.06176	0.03188
27,000	8,998	0.06176	0.04782
30,000	9,998	0.04632	0.07970
33,000	10,998	0.12352	0.09564
36,000	11,997	0.04632	0.04782
39,000	12,997	0.10808	0.04782
42,000	13,997	0.12352	0.04782
45,000	14,997	0.09264	0.07970
48,000	15,996	0.10808	0.04782
51,000	16,996	0.12352	0.05579
54,000	17,996	0.10808	0.06376
57,000	18,996	0.12352	0.07970
60,000	19,996	0.12352	0.09564
63,000	20,995	0.13896	0.11158
66,000	21,995	0.13896	0.12752
69,000	22,995	0.16984	0.12752
72,000	23,995	0.15440	0.11158
73,500	24,495	0.18528	0.07970

Table B6

Sheet Pile Interlock Tests

Load Versus Deformation

Specimen No. BETB6 (Bethelehem-High)

Average Pile Width = 3.005 in.

Load		Deformation in.	
lb	lb/in.	Top Gage Length	Bottom Gage Length
0	0	0.00000	0.00000
1,500	499	-0.01513	0.00000
3,000	998	0.00000	-0.01521
4,500	1,498	0.03026	0.01521
6,000	1,997	0.07565	0.01521
9,000	2,995	0.06052	0.03042
12,000	3,993	0.04539	0.01521
15,000	4,992	0.03026	0.04563
18,000	5,990	0.03026	0.06084
21,000	6,988	0.03026	0.06084
24,000	7,987	0.03026	0.03042
27,000	8,985	0.03026	0.10647
30,000	9,983	0.04539	0.04563
33,000	10,982	0.04539	0.09126
36,000	11,980	0.10591	0.03042
39,000	12,978	0.09834	0.07605
42,000	13,977	0.09078	0.03042
45,000	14,975	0.10591	0.12168
48,000	15,973	0.12104	0.07605
51,000	16,972	0.12104	0.12168
54,000	17,970	0.09078	0.10647
57,000	18,968	0.10591	0.06084
60,000	19,967	0.07565	0.10647
63,000	20,965	0.15130	0.06084
66,000	21,963	0.10591	0.04563
69,000	22,962	0.10591	0.06084
72,000	23,960	0.12104	0.10647
75,000	24,958	0.10591	0.09126
78,000	25,957	0.10591	0.08365
80,300	26,722	0.07565	0.08365

Table B7

Sheet Pile Interlock Tests

Load Versus Deformation

Specimen No. BETB7 (Bethelehem-High)

Average Pile Width = 3.002 in.

Load		Deformation in.	
lb	lb/in.	Top Gage Length	Bottom Gage Length
0	0	0.00000	0.00000
0	0	0.00000	0.00000
0	0	0.00000	0.00000
1,500	500	0.00000	0.01530
3,000	999	0.01474	0.00000
4,500	1,499	0.01474	0.01530
6,000	1,999	0.01474	0.01530
9,000	2,998	0.00000	0.00000
12,000	3,997	0.02948	0.04590
15,000	4,997	0.01474	0.04590
18,000	5,996	0.02948	0.04590
21,000	6,995	0.02948	0.03060
24,000	7,995	0.02948	0.04590
27,000	8,994	0.04422	0.07650
30,000	9,993	0.05896	0.04590
33,000	10,993	0.05896	0.07650
36,000	11,992	0.07370	0.12240
39,000	12,991	0.05896	0.04590
42,000	13,991	0.07370	0.07650
45,000	14,990	0.05896	0.12240
48,000	15,989	0.05896	0.10710
51,000	16,989	0.07370	0.10710
54,000	17,988	0.08844	0.12240
57,000	18,987	0.10318	0.07650
60,000	19,987	0.10318	0.10710
63,000	20,986	0.08844	0.12240
66,000	21,985	0.11792	0.12240
69,000	22,985	0.08844	0.10710
72,000	23,984	0.13266	0.13770
75,000	24,983	0.13266	0.18360

Table B8

Sheet Pile Interlock Tests

Load Versus Deformation

Specimen No. BETB8 (Bethelehem-High)

Average Pile Width = 3.002 in.

Load		Deformation in.	
lb	lb/in.	Top Gage Length	Bottom Gage Length
0	0	0.00000	0.00000
1,500	500	0.03048	0.04557
3,000	999	-0.01524	0.00000
4,500	1,499	0.03048	0.06076
6,000	1,999	0.00000	0.00000
9,000	2,998	0.01524	0.13671
12,000	3,997	0.00000	0.01519
15,000	4,997	0.01524	0.00000
18,000	5,996	0.01524	0.03038
21,000	6,995	0.01524	0.03038
24,000	7,995	-0.01524	0.03038
27,000	8,994	0.03048	0.03038
30,000	9,993	0.00000	0.04557
33,000	10,993	0.04572	0.04557
36,000	11,992	0.03048	0.06076
39,000	12,991	0.04572	0.06076
42,000	13,991	0.04572	0.04557
45,000	14,990	0.03048	0.04557
48,000	15,989	0.09144	0.07595
51,000	16,989	0.06096	0.06076
54,000	17,988	0.07620	0.18228
57,000	18,987	0.06096	0.21266
60,000	19,987	0.07620	0.16709
63,000	20,986	0.07620	0.22785
66,000	21,985	0.12192	0.16709
69,000	22,985	0.09144	0.21266
72,000	23,984	0.10668	0.24304
73,200	24,384	0.10668	0.31899

Table B9

Sheet Pile Interlock Tests

Load Versus Deformation

Specimen No. USY9 (US-High)

Average Pile Width = 2.998 in.

Load		Deformation in.	
lb	lb/in.	Top Gage Length	Bottom Gage Length
0	0	0.00000	0.00000
1,500	500	0.00000	0.00000
3,000	1,001	0.00000	0.01112
4,500	1,501	0.01112	0.01112
6,000	2,001	0.03336	0.04448
9,000	3,002	0.02224	0.03892
12,000	4,002	0.03336	0.03336
15,000	5,003	0.03336	0.04448
18,000	6,003	0.03336	0.05560
21,000	7,004	0.03336	0.03336
24,000	8,004	0.04448	0.04448
27,000	9,005	0.05560	0.06672
30,000	10,006	0.06672	0.02224
33,000	11,006	0.05560	0.07784
36,000	12,007	0.07784	0.05560
39,000	13,007	0.06672	0.05560
42,000	14,008	0.07784	0.06672
45,000	15,008	0.07784	0.06672
48,000	16,009	0.07784	0.07784
51,000	17,009	0.07784	0.08896
54,000	18,010	0.08896	0.13344
57,000	19,011	0.08896	0.12232
60,000	20,011	0.08896	0.15568
63,000	21,012	0.10008	0.15568
63,100	21,045	0.10008	0.15568

Table B10

Sheet Pile Interlock Tests

Load Versus Deformation

Specimen No. USR10 (US-Standard)

Average Pile Width = 3.002 in.

Load		Deformation in.	
lb	lb/in.	Top Gage Length	Bottom Gage Length
0	0	0.00000	0.00000
1,500	500	0.00000	0.01137
3,000	999	0.00000	0.03411
4,500	1,499	-0.01113	0.00000
6,000	1,999	-0.01113	0.03411
9,000	2,998	0.01113	0.01137
12,000	3,998	0.00000	0.02274
15,000	4,997	0.00000	0.02274
18,000	5,997	0.00000	0.02274
21,000	6,996	0.00000	0.02274
24,000	7,996	0.01113	0.04548
27,000	8,995	0.01113	0.03411
30,000	9,994	0.02226	0.04548
33,000	10,994	0.02226	0.05685
36,000	11,993	0.03339	0.03411
39,000	12,993	0.03339	0.06822
42,000	13,992	0.04452	0.05685
45,000	14,992	0.02226	0.10233
47,600	15,858	0.04452	0.21603

APPENDIX C: PLOTS AND DATA TABLES OF LOAD VERSUS BENDING STRAIN

Plots of load versus bending strain are given in Figures C1 through C10 with three curves for each test of PS31 standard- and high-strength, PS32 standard-strength and PSX32 high-strength piles. The individual, calculated bending strain and load data for the tests are given in Tables C1 through C10.

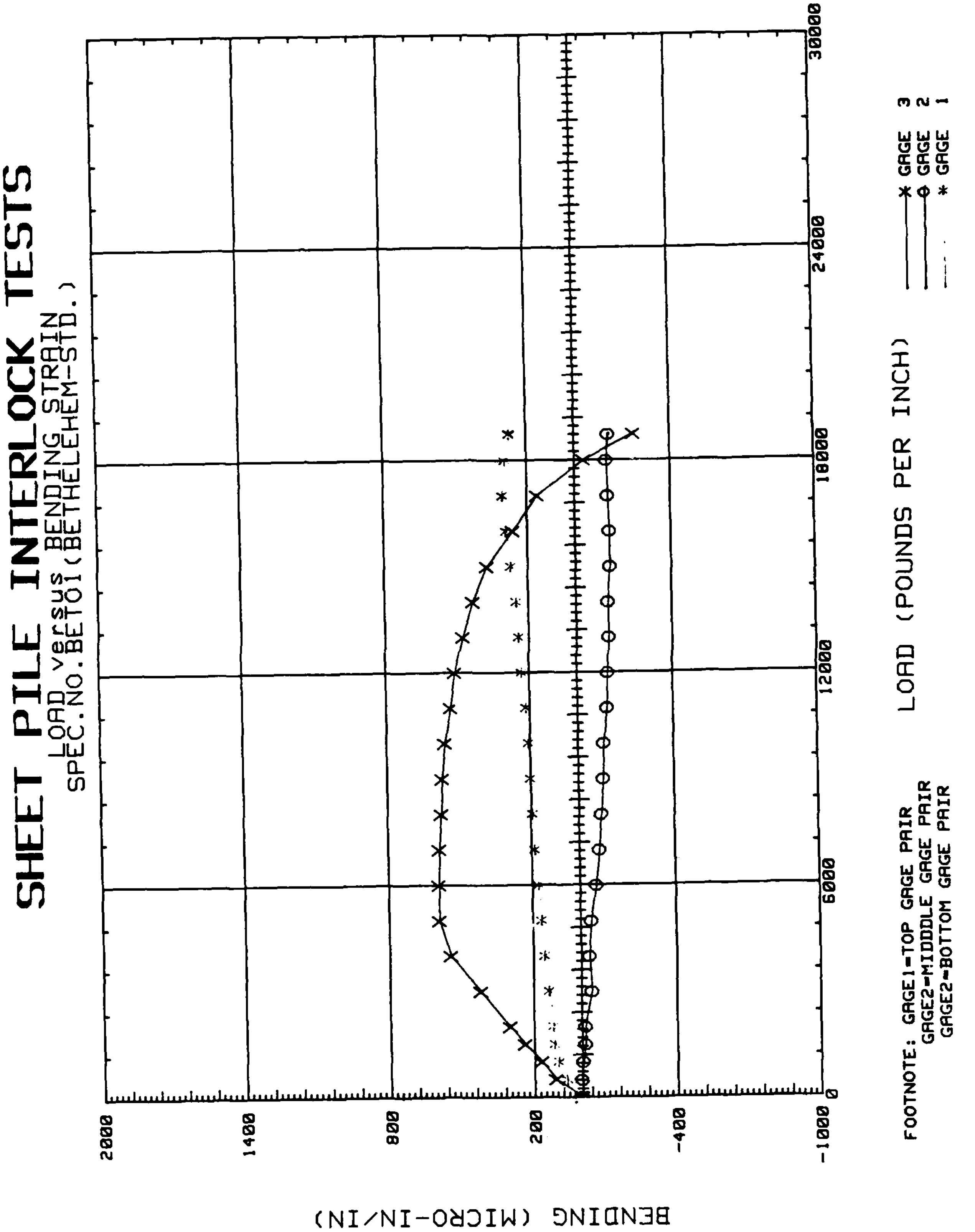
SHEET PILE INTERLOCK TESTS
LOAD versus BENDING STRAIN
SPEC.NO.BET01(BETHELEHEM-STD.)
LOAD (POUNDS PER INCH)
0
6000
12000
18000
24000
30000
BENDING (MICRO-IN/IN)
2000
1400
800
200
-400
-1000
GAGE 3
GAGE 2
GAGE 1
FOOTNOTE: GAGE1-TOP GAGE PAIR
GAGE2-MIDDLE GAGE PAIR
GAGE2-BOTTOM GAGE PAIR

FIGURE C1

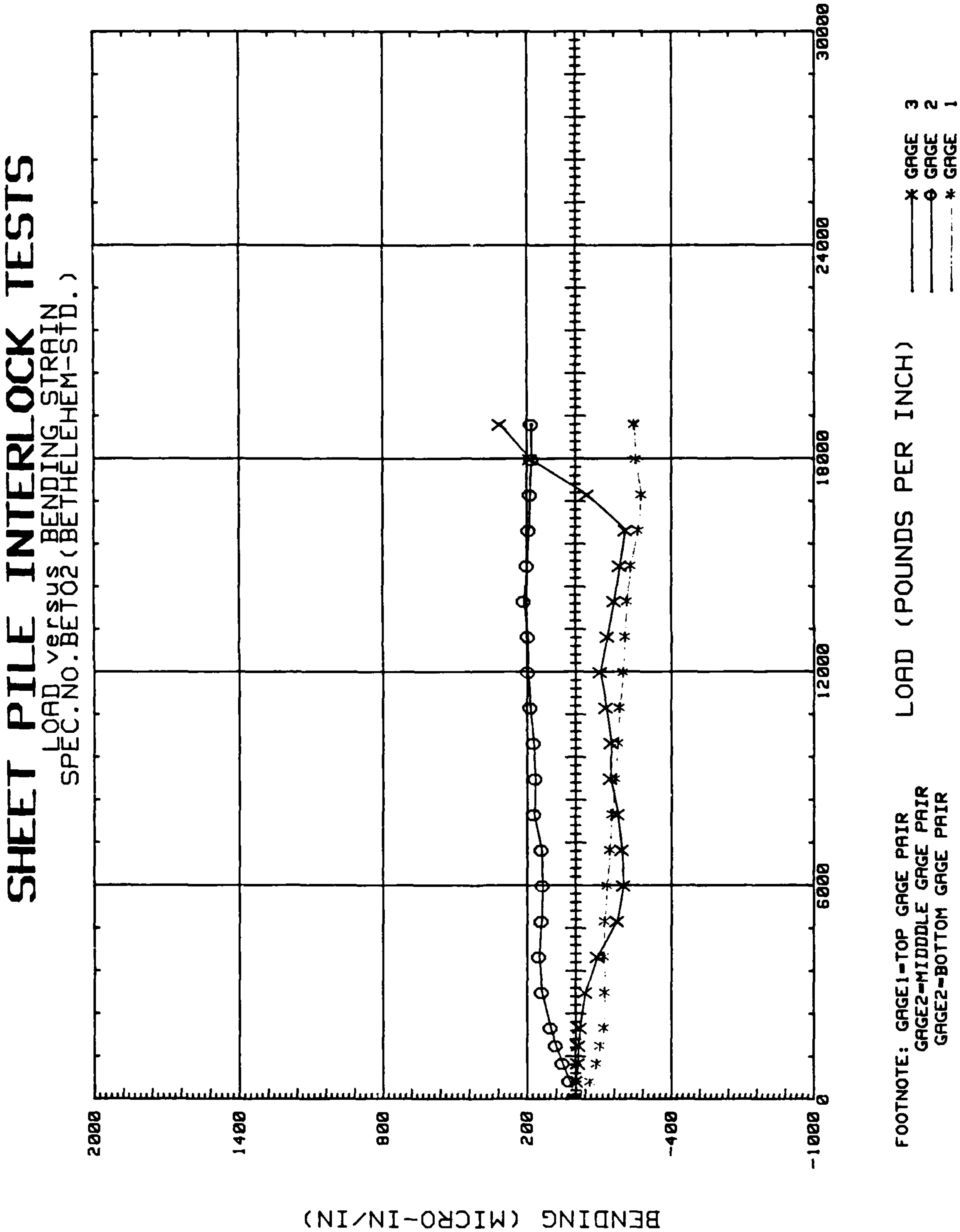
SHEET PILE INTERLOCK TESTS
LOAD versus BENDING STRAIN
SPEC.NO.BETO2(BETHELEHEM-STD.)
LOAD (POUNDS PER INCH)
BENDING (MICRO-IN/IN)
0
6000
12000
18000
24000
30000
2000
1400
800
200
-400
-1000
FOOTNOTE: GAGE1=TOP GAGE PAIR
GAGE2=MIDDDLE GAGE PAIR
GAGE2=BOTTOM GAGE PAIR
GAGE 3
GAGE 2
GAGE 1

FIGURE C2

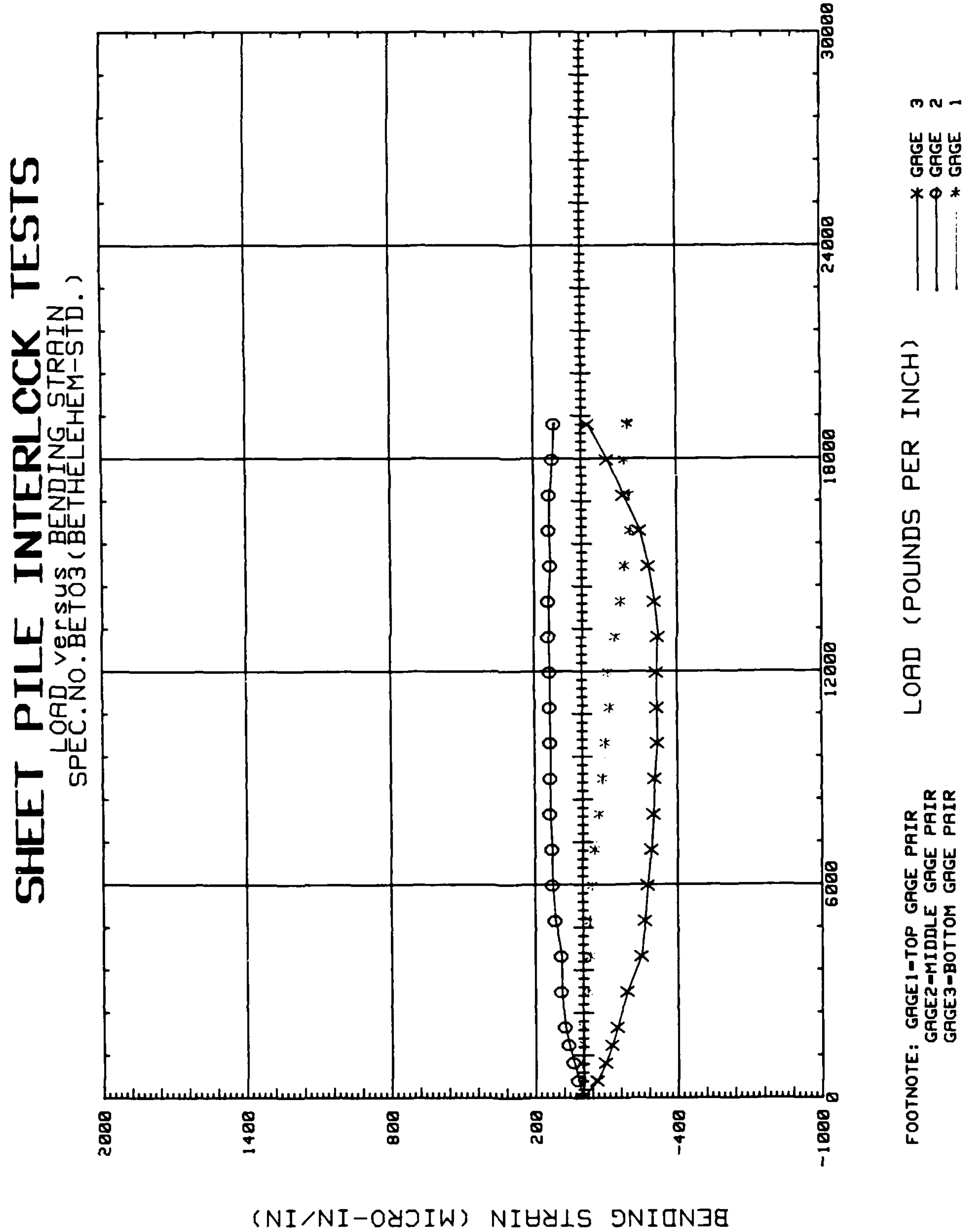
SHEET PILE INTERLOCK TESTS
LOAD versus BENDING STRAIN
SPEC.NO.BET03(BETHELEHEM-STD.)
BENDING STRAIN (MICRO-IN/IN)
2000
1400
800
200
-400
-1000
0
6000
12000
18000
24000
30000
LOAD (POUNDS PER INCH)
FOOTNOTE: GAGE1-TOP GAGE PAIR
GAGE2-MIDDLE GAGE PAIR
GAGE3-BOTTOM GAGE PAIR
GAGE 3
GAGE 2
GAGE 1

FIGURE C3

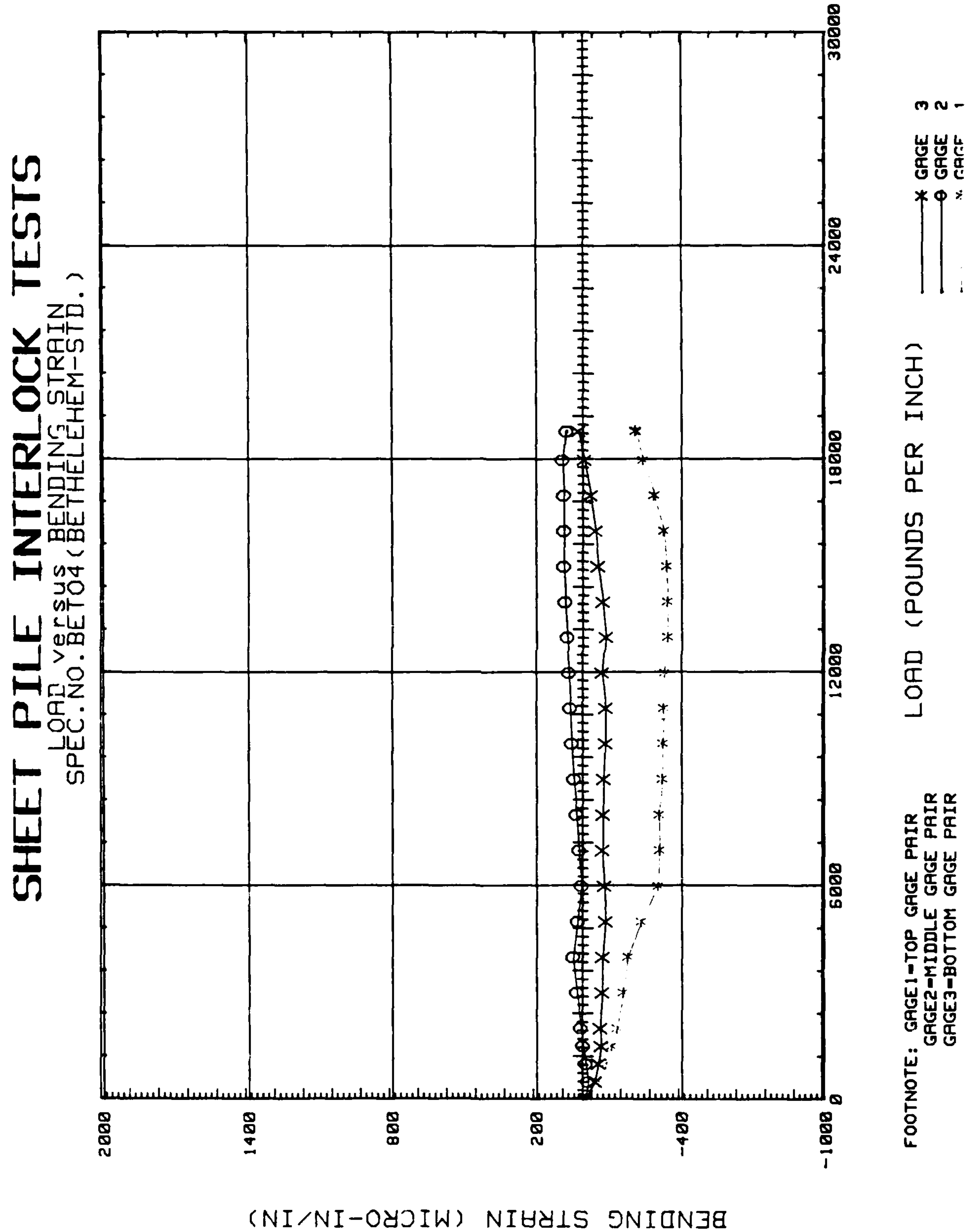
SHEET PILE INTERLOCK TESTS
LOAD versus BENDING STRAIN
SPEC.NO.BET04(BETHELEHEM-STD.)
2000
1400
800
200
-400
-1000
BENDING STRAIN (MICRO-IN/IN)
0
6000
12000
18000
24000
30000
LOAD (POUNDS PER INCH)
FOOTNOTE: GAGE1-TOP GAGE PAIR
GAGE2-MIDDLE GAGE PAIR
GAGE3-BOTTOM GAGE PAIR
GAGE 3
GAGE 2
GAGE 1

FIGURE C4

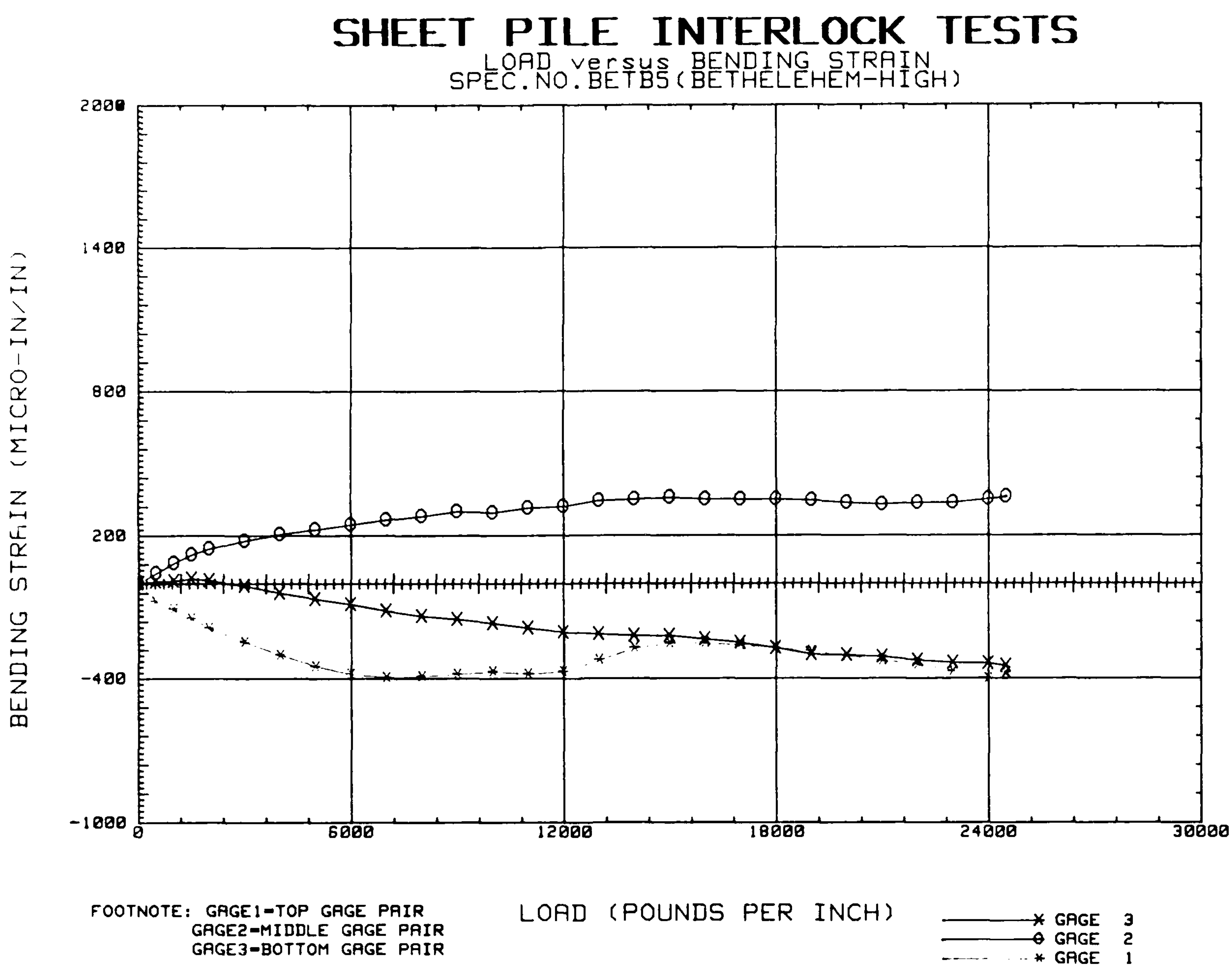
SHEET PILE INTERLOCK TESTS
LOAD versus BENDING STRAIN
SPEC.NO.BETB5(BETHELEHEM-HIGH)
BENDING STRAIN (MICRO-IN/IN)
2000
1400
800
200
-400
-1000
0
6000
12000
18000
24000
30000
LOAD (POUNDS PER INCH)
FOOTNOTE: GAGE1=TOP GAGE PAIR
GAGE2=MIDDLE GAGE PAIR
GAGE3=BOTTOM GAGE PAIR
GAGE 3
GAGE 2
GAGE 1

FIGURE C5

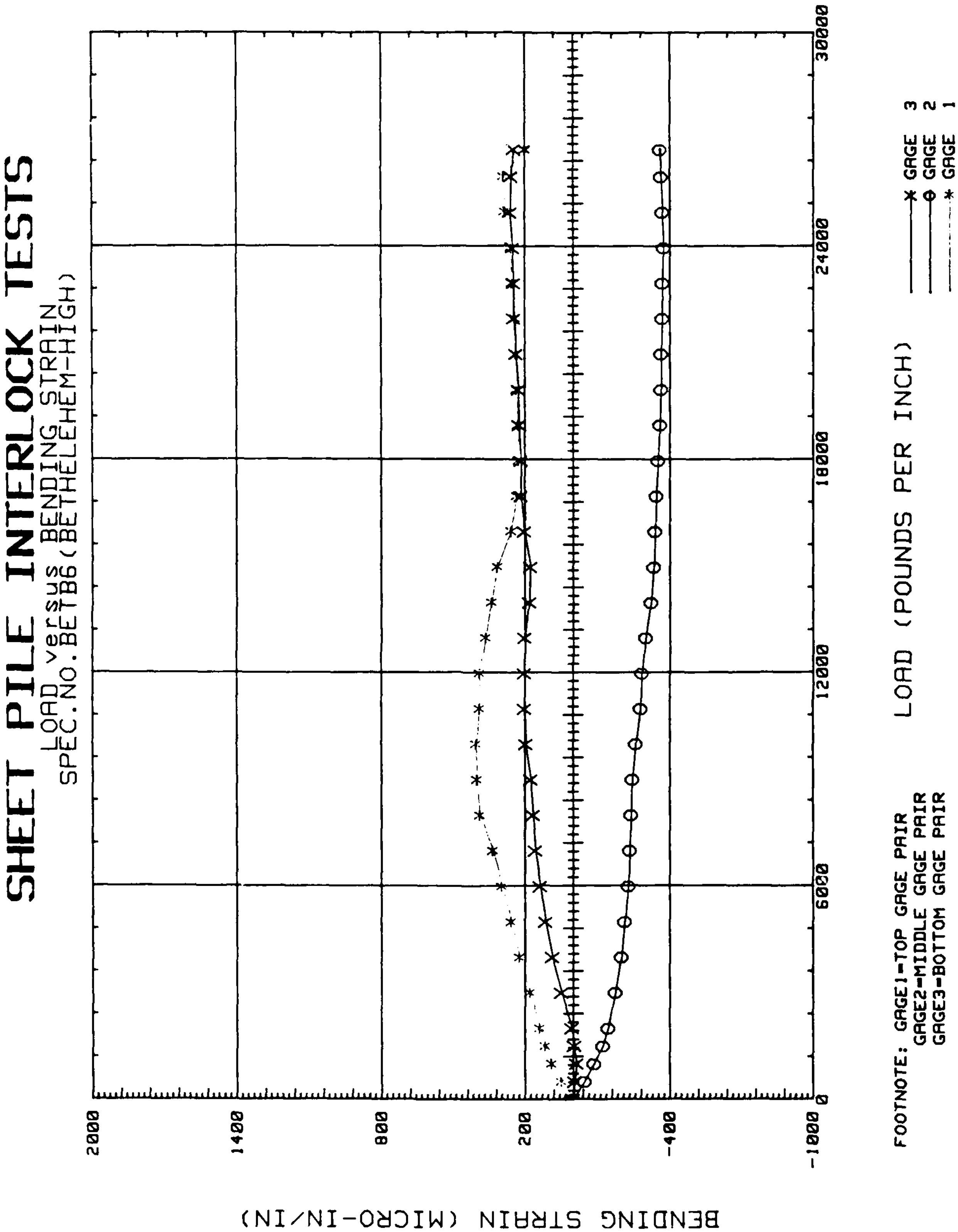

SHEET PILE INTERLOCK TESTS
LOAD versus BENDING STRAIN
SPEC.NO.BETB6(BETHELEHEM-HIGH)
BENDING STRAIN (MICRO-IN/IN)
2000
1400
800
200
-400
-1000
0
6000
12000
18000
24000
30000
LOAD (POUNDS PER INCH)
FOOTNOTE: GAGE1-TOP GAGE PAIR
GAGE2-MIDDLE GAGE PAIR
GAGE3-BOTTOM GAGE PAIR
GAGE 3
GAGE 2
GAGE 1

FIGURE C6

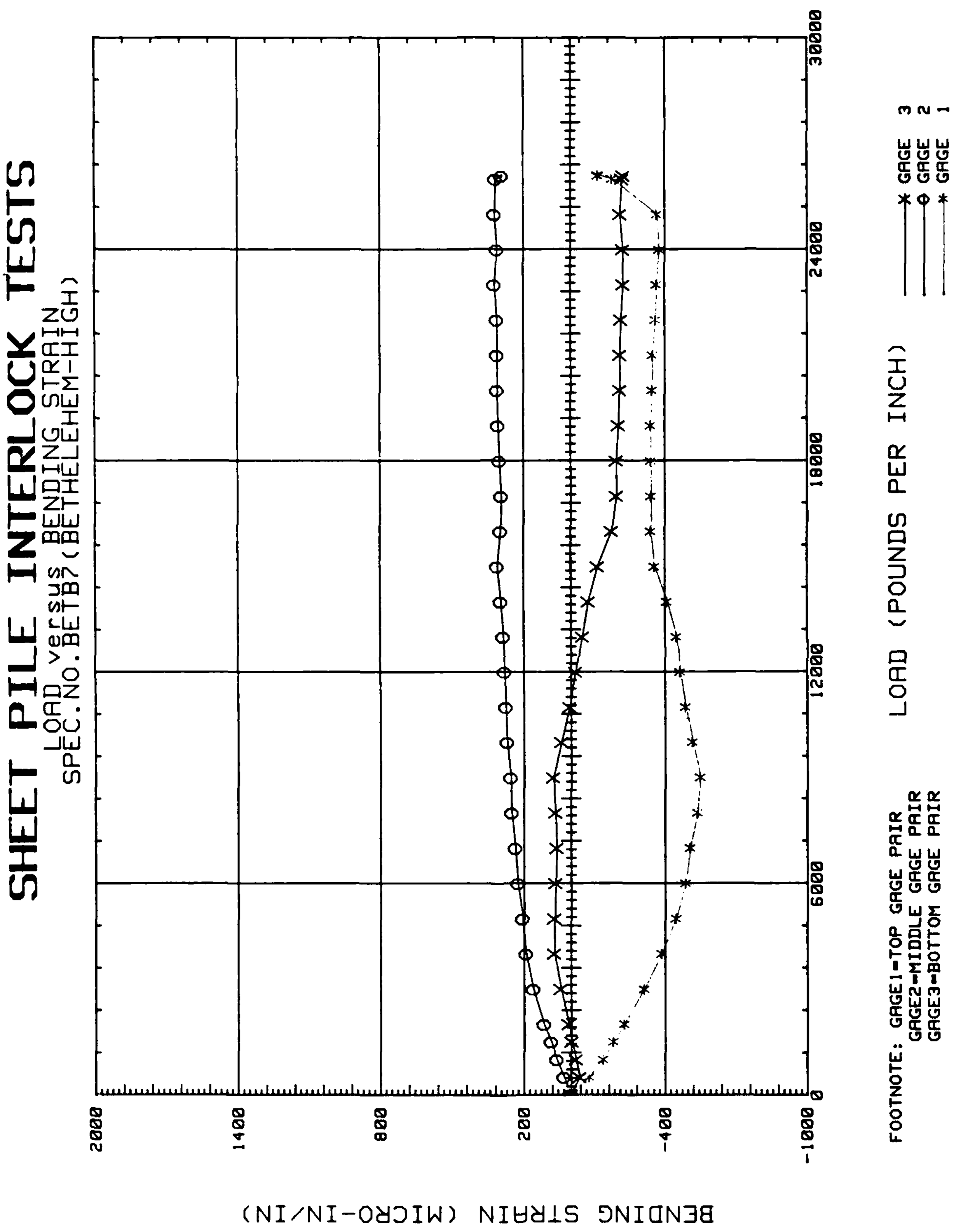
SHEET PILE INTERLOCK TESTS
LOAD versus BENDING STRAIN
SPEC.NO.BETB7 (BETHELEHEM-HIGH)
BENDING STRAIN (MICRO-IN/IN)
2000
1400
800
200
-400
-1000
0
6000
12000
18000
24000
30000
LOAD (POUNDS PER INCH)
FOOTNOTE: GAGE1-TOP GAGE PAIR
GAGE2-MIDDLE GAGE PAIR
GAGE3-BOTTOM GAGE PAIR
GAGE 3
GAGE 2
GAGE 1

FIGURE C7

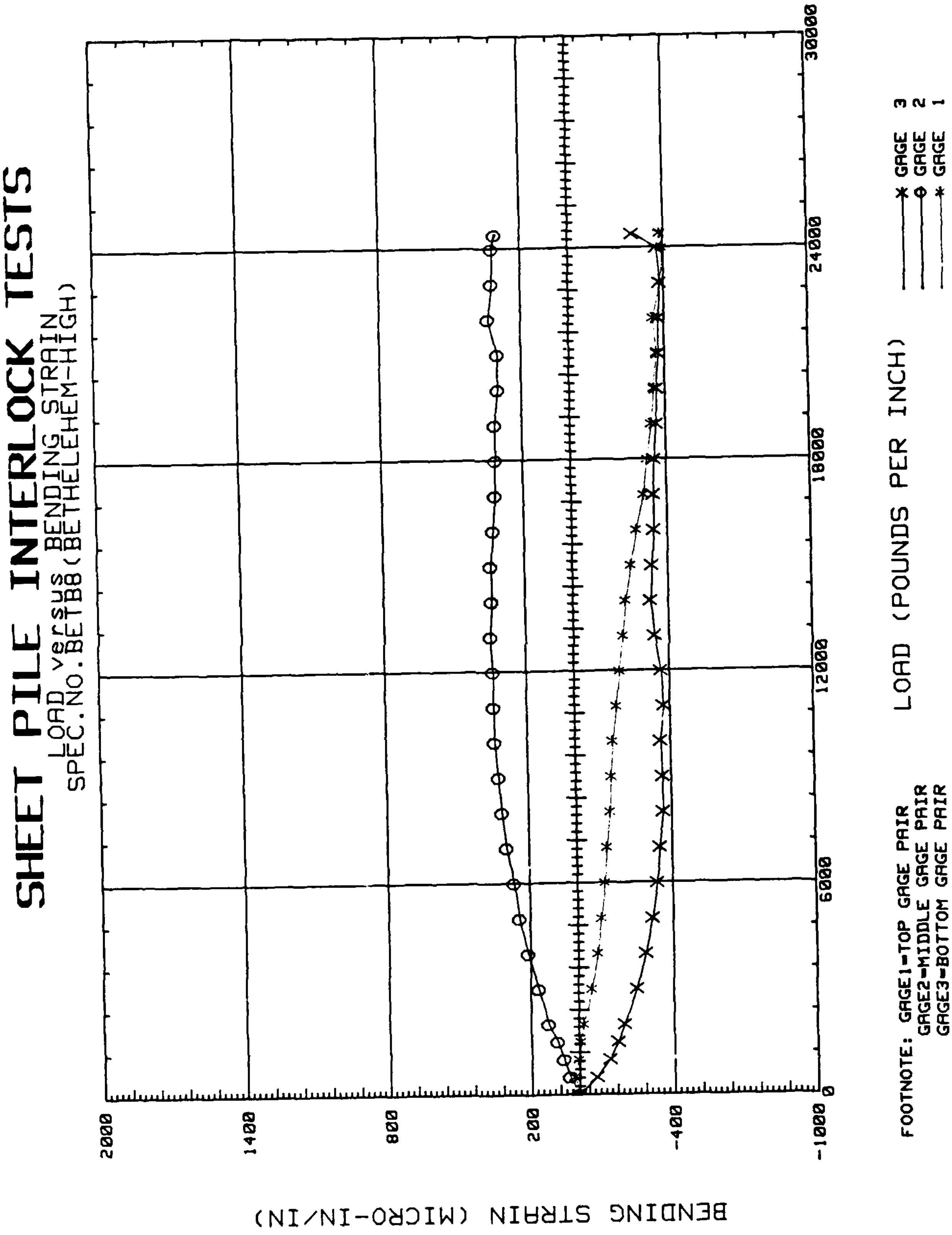
SHEET PILE INTERLOCK TESTS
LOAD versus BENDING STRAIN
SPEC.NO.BETB8(BETHELEHEM-HIGH)
LOAD (POUNDS PER INCH)
BENDING STRAIN (MICRO-IN/IN)
0
6000
12000
18000
24000
30000
2000
1400
800
200
-400
-1000
GAGE 3
GAGE 2
GAGE 1
FOOTNOTE: GAGE1-TOP GAGE PAIR
GAGE2-MIDDLE GAGE PAIR
GAGE3-BOTTOM GAGE PAIR

FIGURE C8

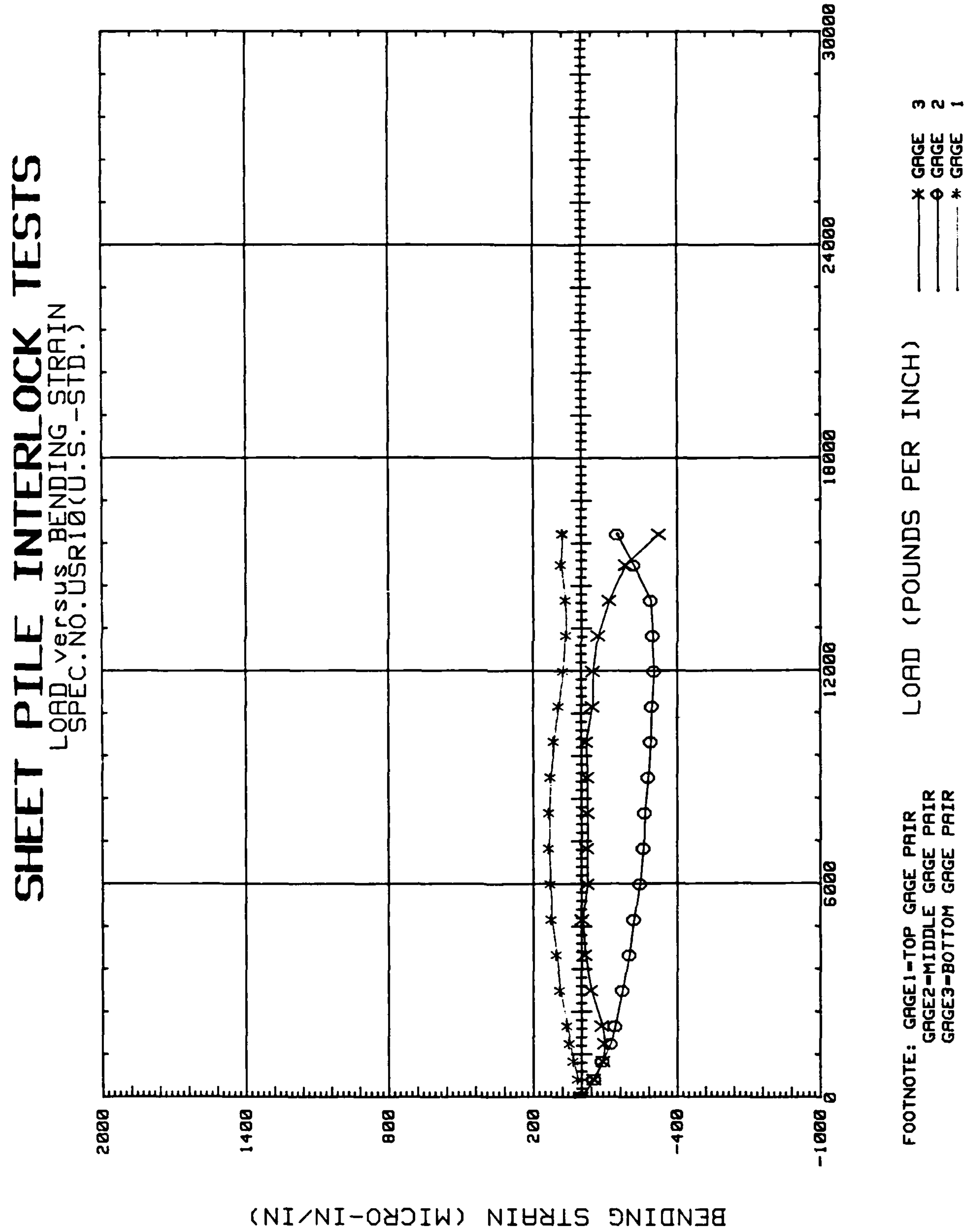
SHEET PILE INTERLOCK TESTS
LOAD versus BENDING STRAIN
SPEC.NO.USR10(U.S.-STD.)
BENDING STRAIN (MICRO-IN/IN)
2000
1400
800
200
-400
-1000
0
6000
12000
18000
24000
30000
LOAD (POUNDS PER INCH)
FOOTNOTE: GAGE1-TOP GAGE PAIR
GAGE2-MIDDLE GAGE PAIR
GAGE3-BOTTOM GAGE PAIR
GAGE 3
GAGE 2
GAGE 1

FIGURE C9

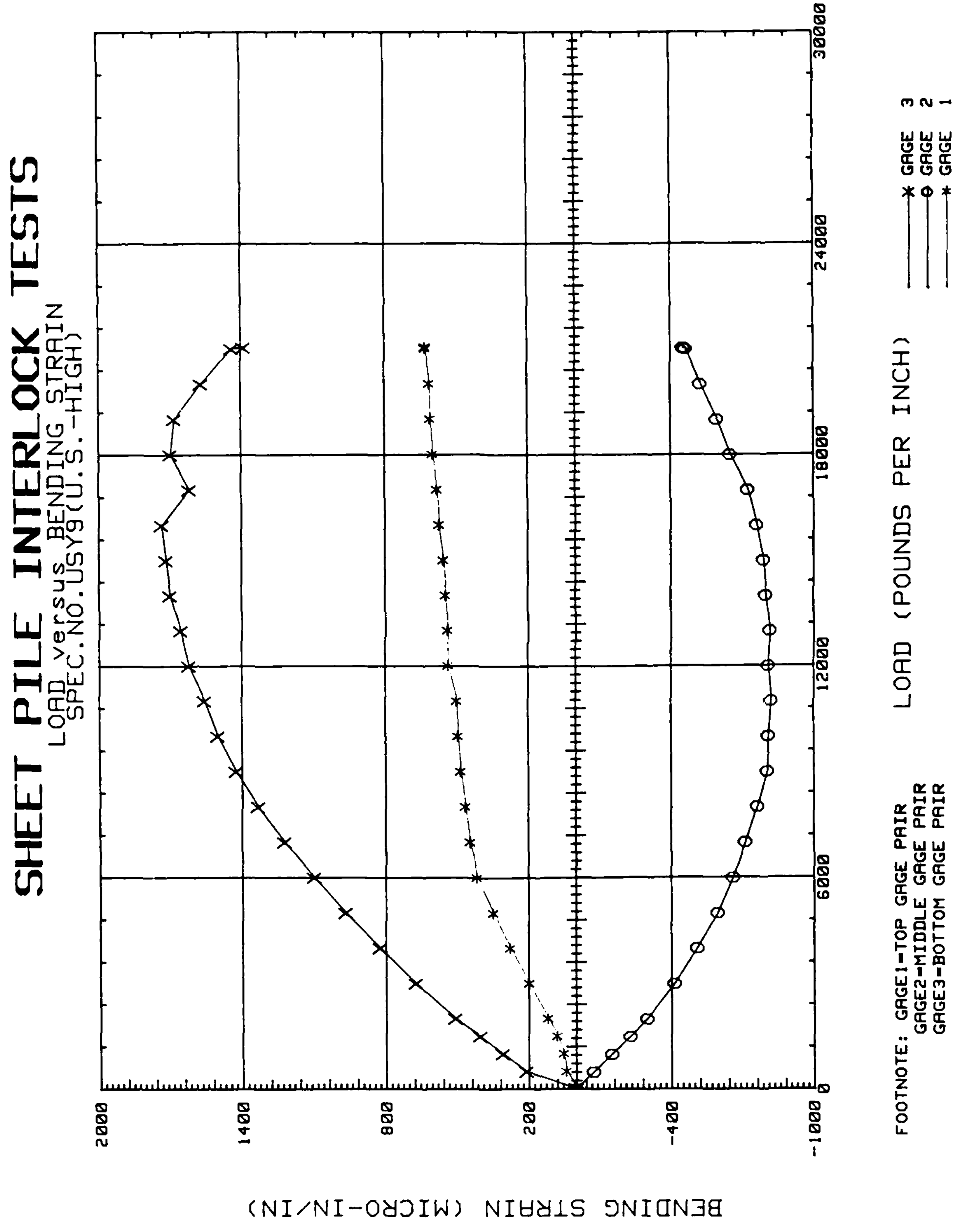
SHEET PILE INTERLOCK TESTS
LOAD versus BENDING STRAIN
SPEC.NO.USY9(U.S.-HIGH)
BENDING STRAIN (MICRO-IN/IN)
2000
1400
800
200
-400
-1000
LOAD (POUNDS PER INCH)
0
6000
12000
18000
24000
30000
GAGE 3
GAGE 2
GAGE 1
FOOTNOTE: GAGE1-TOP GAGE PAIR
GAGE2-MIDDLE GAGE PAIR
GAGE3-BOTTOM GAGE PAIR

Figure C10

Table C1

Sheet Pile Interlock Tests

Load Versus Bending Strain

Specimen No. BET01 (Bethelehem-Standard)

Average Pile Width = 3.001 in.

Load		Bending Strain μin./in.		
lb	lb/in.	Top Gage Pairs	Middle Gage Pairs	Bottom Gage Pairs
0	0	0	0	0
1,500	500	63	0	110
3,000	1,000	97	-5	170
4,500	1,500	115	-15	238
6,000	2,000	120	-15	300
9,000	2,999	135	-45	420
12,000	3,999	152	-35	545
15,000	4,999	163	-45	590
18,000	5,999	173	-68	590
21,000	6,998	185	-85	585
24,000	7,998	193	-95	575
27,000	8,998	200	-105	570
30,000	9,998	205	-110	555
33,000	10,998	215	-125	530
36,000	11,997	230	-130	510
39,000	12,997	242	-135	475
42,000	13,997	250	-135	430
45,000	14,997	270	-145	370
48,000	15,996	288	-145	260
51,000	16,996	300	-140	155
54,000	17,996	290	-135	-40
56,200	18,729	270	-145	-250

Table C2

Sheet Pile Interlock Tests

Load Versus Bending Strain

Specimen No. BET02 (Bethelehem-Standard)

Average Pile Width = 3.003 in.

Load		Bending Strain μin./in.		
lb	lb/in.	Top Gage Pairs	Middle Gage Pairs	Bottom Gage Pairs
0	0	0	0	0
1,500	500	-58	25	0
3,000	999	-85	53	-10
4,500	1,499	-100	80	-13
6,000	1,998	-115	103	-18
9,000	2,997	-120	138	-40
12,000	3,996	-115	150	-90
15,000	4,995	-118	140	-173
18,000	5,994	-130	135	-200
21,000	6,993	-140	140	-193
24,000	7,992	-150	170	-175
27,000	8,991	-165	165	-145
30,000	9,990	-175	173	-147
33,000	10,989	-182	185	-128
36,000	11,988	-198	195	-103
39,000	12,987	-205	195	-133
42,000	13,986	-215	210	-163
45,000	14,985	-230	198	-185
48,000	15,984	-263	190	-210
51,000	16,983	-275	185	-49
54,000	17,982	-250	180	186
56,950	18,964	-245	180	311

Table C3

Sheet Pile Interlock Tests

Load Versus Bending Strain

Specimen No. BETO3 (Bethelehem-Standard)

Average Pile Width = 3.003 in.

Load		Bending Strain µin./in.		
lb	lb/in.	Top Gage Pairs	Middle Gage Pairs	Bottom Gage Pairs
0	0	0	0	0
1,500	499	-5	20	-60
3,000	999	5	40	-95
4,500	1,498	-5	60	-122
6,000	1,998	-3	75	-145
9,000	2,997	-20	90	-188
12,000	3,996	-30	90	-247
15,000	4,994	-30	115	-263
18,000	5,993	-40	125	-275
21,000	6,992	-50	128	-290
24,000	7,991	-70	135	-300
27,000	8,990	-85	133	-305
30,000	9,989	-97	133	-318
33,000	10,988	-115	135	-315
36,000	11,987	-110	133	-315
39,000	12,986	-140	138	-320
42,000	13,984	-163	140	-305
45,000	14,983	-180	130	-280
48,000	15,982	-205	135	-245
51,000	16,981	-203	133	-177
54,000	17,980	-182	118	-110
57,000	18,979	-198	110	-30

Table C4

Sheet Pile Interlock Tests

Load Versus Bending Strain

Specimen No. BET04 (Bethelehem-Standard)

Average Pile Width = 3.002 in.

Load		Bending Strain µin./in.		
lb	lb/in.	Top Gage Pairs	Middle Gage Pairs	Bottom Gage Pairs
0	0	0	0	0
1,500	500	-55	-13	-40
3,000	999	-85	-3	-55
4,500	1,499	-107	10	-65
6,000	1,999	-130	18	-63
9,000	2,998	-155	35	-70
12,000	3,998	-175	50	-72
15,000	4,997	-230	30	-85
18,000	5,997	-300	15	-80
21,000	6,996	-305	25	-72
24,000	7,996	-305	35	-75
27,000	8,995	-318	45	-78
30,000	9,994	-320	55	-85
33,000	10,994	-325	60	-88
36,000	11,993	-330	65	-72
39,000	12,993	-340	72	-88
42,000	13,992	-340	80	-75
45,000	14,992	-338	85	-55
48,000	15,991	-325	85	-45
51,000	16,991	-285	85	-25
54,000	17,990	-240	90	0
56,400	18,790	-208	75	25

Table C5

Sheet Pile Interlock Tests

Load Versus Bending Strain

Specimen No. BETB5 (Bethelehem-High)

Average Pile Width = 3.001 in.

Load		Bending Strain μin./in.		
lb	lb/in.	Top Gage Pairs	Middle Gage Pairs	Bottom Gage Pairs
0	0	0	0	0
1,500	500	-72	42	8
3,000	1,000	-105	85	10
4,500	1,500	-145	120	20
6,000	2,000	-185	145	13
9,000	2,999	-245	177	-10
12,000	3,999	-300	205	-40
15,000	4,999	-348	225	-65
18,000	5,999	-380	245	-88
21,000	6,998	-395	265	-115
24,000	7,998	-390	280	-138
27,000	8,998	-380	300	-150
30,000	9,998	-370	295	-168
33,000	10,998	-380	315	-188
36,000	11,997	-370	320	-205
39,000	12,997	-320	345	-212
42,000	13,997	-270	350	-220
45,000	14,997	-250	357	-220
48,000	15,996	-250	350	-235
51,000	16,996	-260	350	-250
54,000	17,996	-270	350	-273
57,000	18,996	-285	345	-300
60,000	19,996	-305	335	-302
63,000	20,995	-325	328	-310
66,000	21,995	-340	335	-325
69,000	22,995	-370	335	-335
72,000	23,995	-400	350	-338
73,500	24,495	-375	360	-348

Table C6

Sheet Pile Interlock Tests

Load Versus Bending Strain

Specimen No. BETB6 (Bethelehem-High)

Average Pile Width = 3.005 in.

Load		Bending Strain µin./in.		
lb	lb/in.	Top Gage Pairs	Middle Gage Pairs	Bottom Gage Pairs
0	0	0	0	0
1,500	499	50	-48	-8
3,000	998	90	-88	-15
4,500	1,498	118	-122	-5
6,000	1,997	140	-145	5
9,000	2,995	180	-175	48
12,000	3,993	225	-200	85
15,000	4,992	258	-215	113
18,000	5,990	297	-230	135
21,000	6,988	335	-235	155
24,000	7,987	390	-240	165
27,000	8,985	403	-245	175
30,000	9,983	405	-260	195
33,000	10,982	390	-280	200
36,000	11,980	390	-285	200
39,000	12,978	365	-300	200
42,000	13,977	340	-323	180
45,000	14,975	315	-335	175
48,000	15,973	258	-340	200
51,000	16,972	235	-345	215
54,000	17,970	228	-352	215
57,000	18,968	230	-360	223
60,000	19,967	235	-365	225
63,000	20,965	238	-365	235
66,000	21,963	240	-370	245
69,000	22,962	255	-370	245
72,000	23,960	260	-375	250
75,000	24,958	285	-370	260
78,000	25,957	290	-365	255
80,300	26,722	200	-360	245

Table C7

Sheet Pile Interlock Tests

Load Versus Bending Strain

Specimen No. BETB7 (Bethelehem-High)

Average Pile Width = 3.002 in.

Load		Bending Strain µin./in.		
lb	lb/in.	Top Gage Pairs	Middle Gage Pairs	Bottom Gage Pairs
0	0	0	0	0
1,500	500	-75	30	-38
3,000	999	-135	60	-23
4,500	1,499	-177	85	-3
6,000	1,999	-225	115	10
9,000	2,998	-310	160	42
12,000	3,997	-385	190	70
15,000	4,997	-445	205	70
18,000	5,996	-485	225	65
21,000	6,995	-505	235	60
24,000	7,995	-537	250	65
27,000	8,994	-547	255	75
30,000	9,993	-515	270	40
33,000	10,993	-485	275	5
36,000	11,992	-463	280	-20
39,000	12,991	-448	285	-50
42,000	13,991	-408	295	-75
45,000	14,990	-355	310	-115
48,000	15,989	-340	295	-175
51,000	16,989	-340	292	-195
54,000	17,988	-340	300	-195
57,000	18,987	-340	305	-205
60,000	19,987	-345	310	-210
63,000	20,986	-348	310	-210
66,000	21,985	-360	310	-215
69,000	22,985	-365	320	-225
72,000	23,984	-375	310	-223
75,000	24,983	-365	320	-210
78,000	25,983	-175	315	-220
78,300	26,083	-115	290	-225

Table C8

Sheet Pile Interlock Tests

Load Versus Bending Strain

Specimen No. BETB8 (Bethelehem-High)

Average Pile Width = 3.002 in.

Load		Bending Strain µin./in.		
lb	lb/in.	Top Gage Pairs	Middle Gage Pairs	Bottom Gage Pairs
0	0	0	0	0
1,500	500	23	40	-75
3,000	999	5	65	-130
4,500	1,499	-5	90	-165
6,000	1,999	-20	125	-195
9,000	2,998	-55	165	-247
12,000	3,997	-80	210	-285
15,000	4,997	-97	245	-315
18,000	5,996	-115	265	-338
21,000	6,995	-125	295	-350
24,000	7,995	-140	313	-365
27,000	8,994	-147	325	-365
30,000	9,993	-158	338	-360
33,000	10,993	-175	340	-375
36,000	11,992	-190	340	-365
39,000	12,991	-205	350	-340
42,000	13,991	-220	340	-328
45,000	14,990	-245	343	-335
48,000	15,989	-270	330	-345
51,000	16,989	-302	320	-345
54,000	17,988	-320	315	-350
57,000	18,987	-340	315	-362
60,000	19,987	-352	300	-365
63,000	20,986	-365	300	-375
66,000	21,985	-352	338	-378
69,000	22,985	-385	320	-385
72,000	23,984	-395	320	-370
73,200	24,384	-385	305	-273

AD-A201 285 LOCK AND DAM NUMBER 26 (REPLACEMENT) COFFERDAM EXPERIMENTAL AND ANALYTICA (U) ARMY ENGINEER WATERWAYS EXPERIMENT STATION VICKSBURG MS INFOR 2/2

UNCLASSIFIED E F O'NEIL ET AL SEP 88 WES/TR/ITL-88-3-5 F/G 13/3 NL

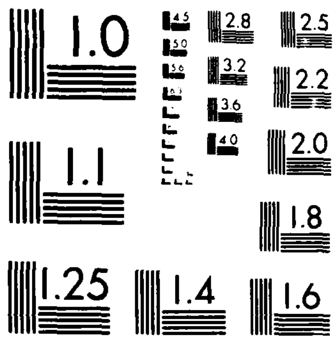

MICROCOPY RESOLUTION TEST CHART
NATIONAL BUREAU OF STANDARDS 1963-A

Table C9

Sheet Pile Interlock Tests

Load Versus Bending Strain

Specimen No. USY9 (US-High)

Average Pile Width = 2.998 in.

Load		Bending Strain μin./in.		
lb	lb/in.	Top Gage Pairs	Middle Gage Pairs	Bottom Gage Pairs
0	0	0	0	0
1,500	500	42	-75	210
3,000	1,001	53	-152	310
4,500	1,501	80	-230	405
6,000	2,001	120	-300	510
9,000	3,002	198	-415	675
12,000	4,002	278	-510	825
15,000	5,003	350	-595	970
18,000	6,003	417	-660	1,100
21,000	7,004	445	-713	1,223
24,000	8,004	465	-763	1,333
27,000	9,005	485	-805	1,425
30,000	10,006	495	-810	1,500
33,000	11,006	500	-823	1,555
36,000	12,007	535	-810	1,620
39,000	13,007	540	-815	1,655
42,000	14,008	545	-800	1,698
45,000	15,008	555	-790	1,715
48,000	16,009	573	-760	1,733
51,000	17,009	580	-725	1,615
54,000	18,010	598	-650	1,695
57,000	19,011	608	-595	1,678
60,000	20,011	610	-527	1,565
63,000	21,012	628	-465	1,438
63,100	21,045	628	-455	1,388

Table C10

Sheet Pile Interlock Tests

Load Versus Bending Strain

Specimen No. USR10 (US Standard)

Average Pile Width = 3.002 in.

Load		Bending Strain μin./in.		
lb	lb/in.	Top Gage Pairs	Middle Gage Pairs	Bottom Gage Pairs
0	0	0	0	0
1,500	500	18	-53	-53
3,000	999	35	-88	-90
4,500	1,499	50	-122	-97
6,000	1,999	61	-140	-85
9,000	2,998	90	-173	-40
12,000	3,998	105	-200	-15
15,000	4,997	125	-220	-5
18,000	5,997	130	-245	-25
21,000	6,996	135	-260	-25
24,000	7,996	135	-265	-25
27,000	8,995	128	-280	-25
30,000	9,994	115	-290	-20
33,000	10,994	95	-295	-48
36,000	11,993	75	-305	-50
39,000	12,993	65	-297	-70
42,000	13,992	65	-290	-118
45,000	14,992	85	-217	-185
47,600	15,858	78	-150	-325

APPENDIX D: PLOTS AND DATA TABLES OF WEB STRAIN VERSUS GROSS STRAIN

Plots of web strain versus gross strain for tests of PS31 standard- and high-strength, PS32 standard-strength, and PSX32 high-strength piles are given in Figures D1 through D10. Tabular data for each test are given in Tables D1 through D10.

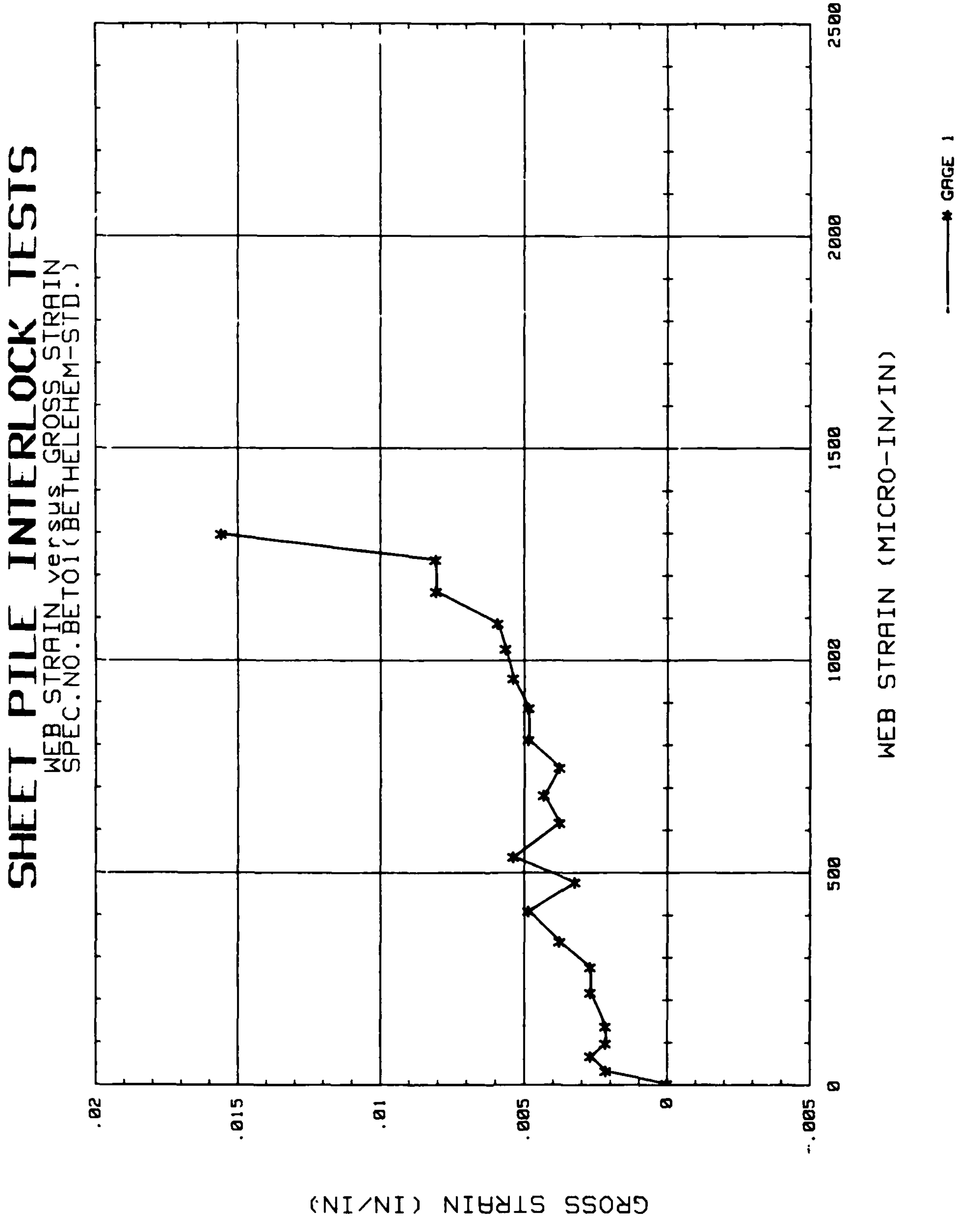
SHEET PILE INTERLOCK TESTS
WEB STRAIN versus GROSS STRAIN
SPEC.NO.BET01(BETHELEHEM-STD.)
WEB STRAIN (MICRO-IN/IN)
GROSS STRAIN (IN/IN)
GAGE 1
0
500
1000
1500
2000
2500
-.005
0
.005
.01
.015
.02

FIGURE D1

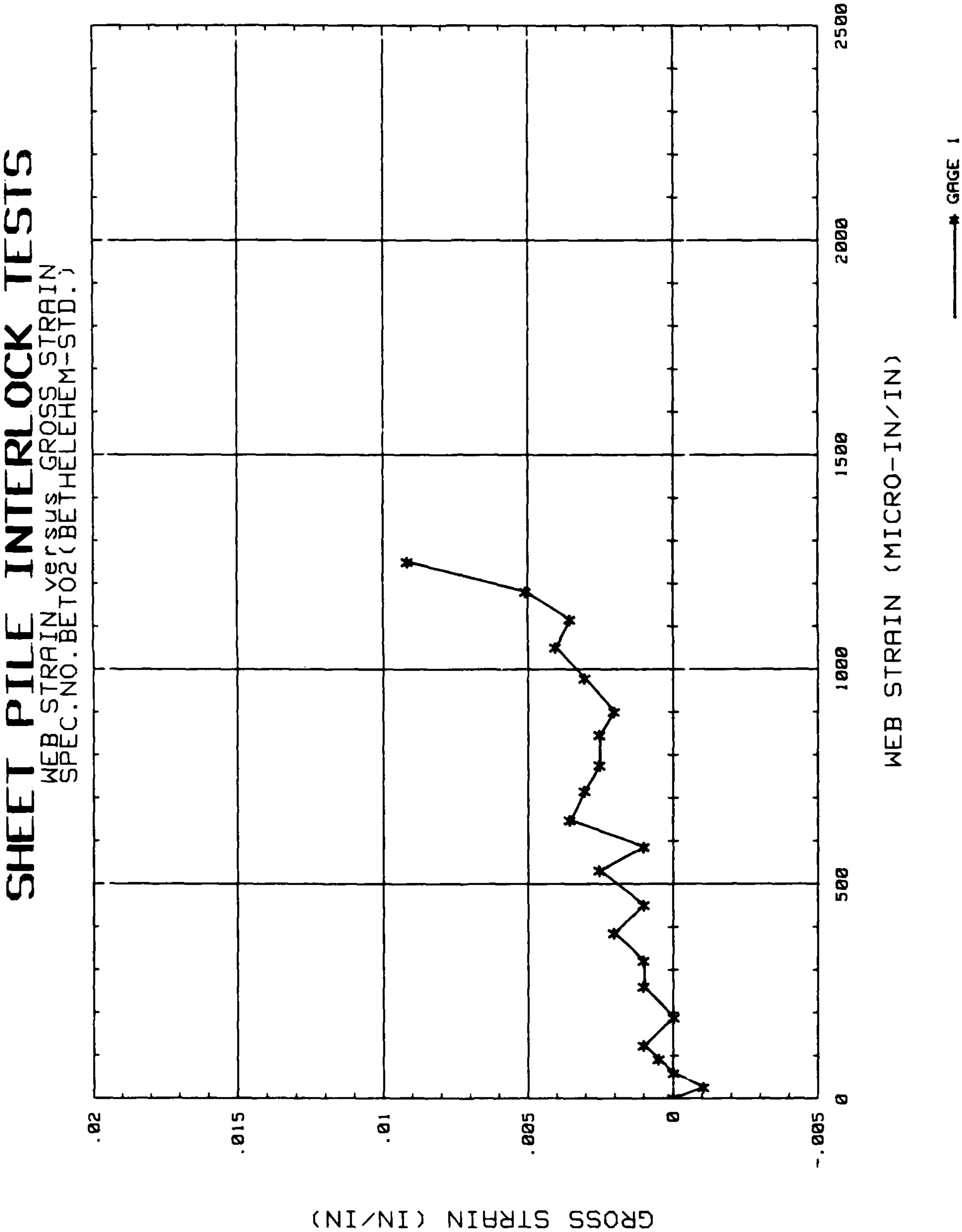

SHEET PILE INTERLOCK TESTS
WEB STRAIN versus GROSS STRAIN
SPEC.NO.BETO2(BETHELEHEM-STD.)
WEB STRAIN (MICRO-IN/IN)
GROSS STRAIN (IN/IN)
GAGE 1
0
500
1000
1500
2000
2500
.02
.015
.01
.005
0
-.005

FIGURE D2

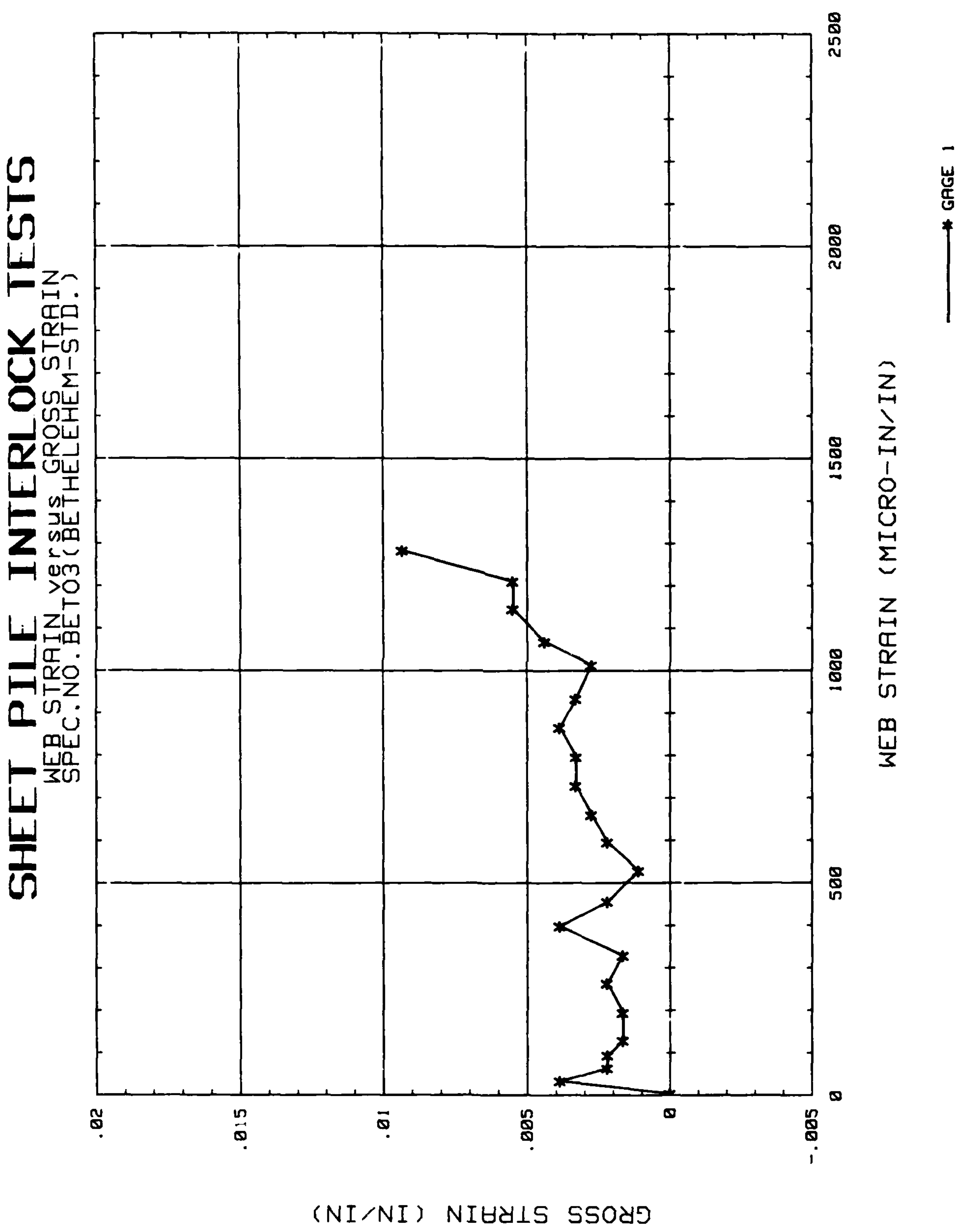
SHEET PILE INTERLOCK TESTS
WEB STRAIN versus GROSS STRAIN
SPEC.NO.BET03(BETHELEHEM-STD.)
.02
.015
.01
.005
0
-.005
GROSS STRAIN (IN/IN)
0
500
1000
1500
2000
2500
WEB STRAIN (MICRO-IN/IN)
GAGE 1

FIGURE D3

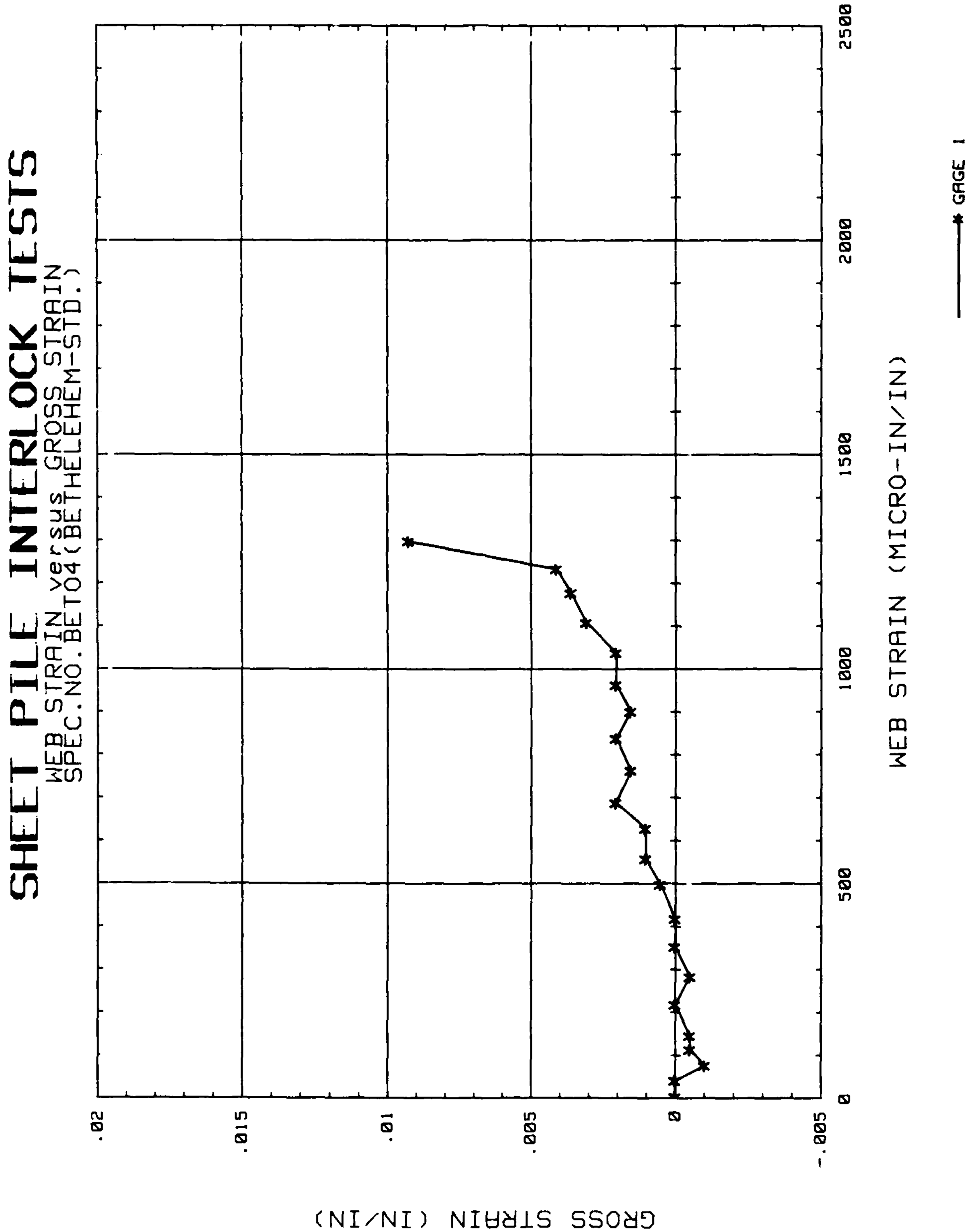
SHEET PILE INTERLOCK TESTS
WEB STRAIN versus GROSS STRAIN
SPEC.NO.BET04(BETHELEHEM-STD.)
GROSS STRAIN (IN/IN)
.02
.015
.01
.005
0
-.005
WEB STRAIN (MICRO-IN/IN)
0
500
1000
1500
2000
2500
GAGE 1

FIGURE D4

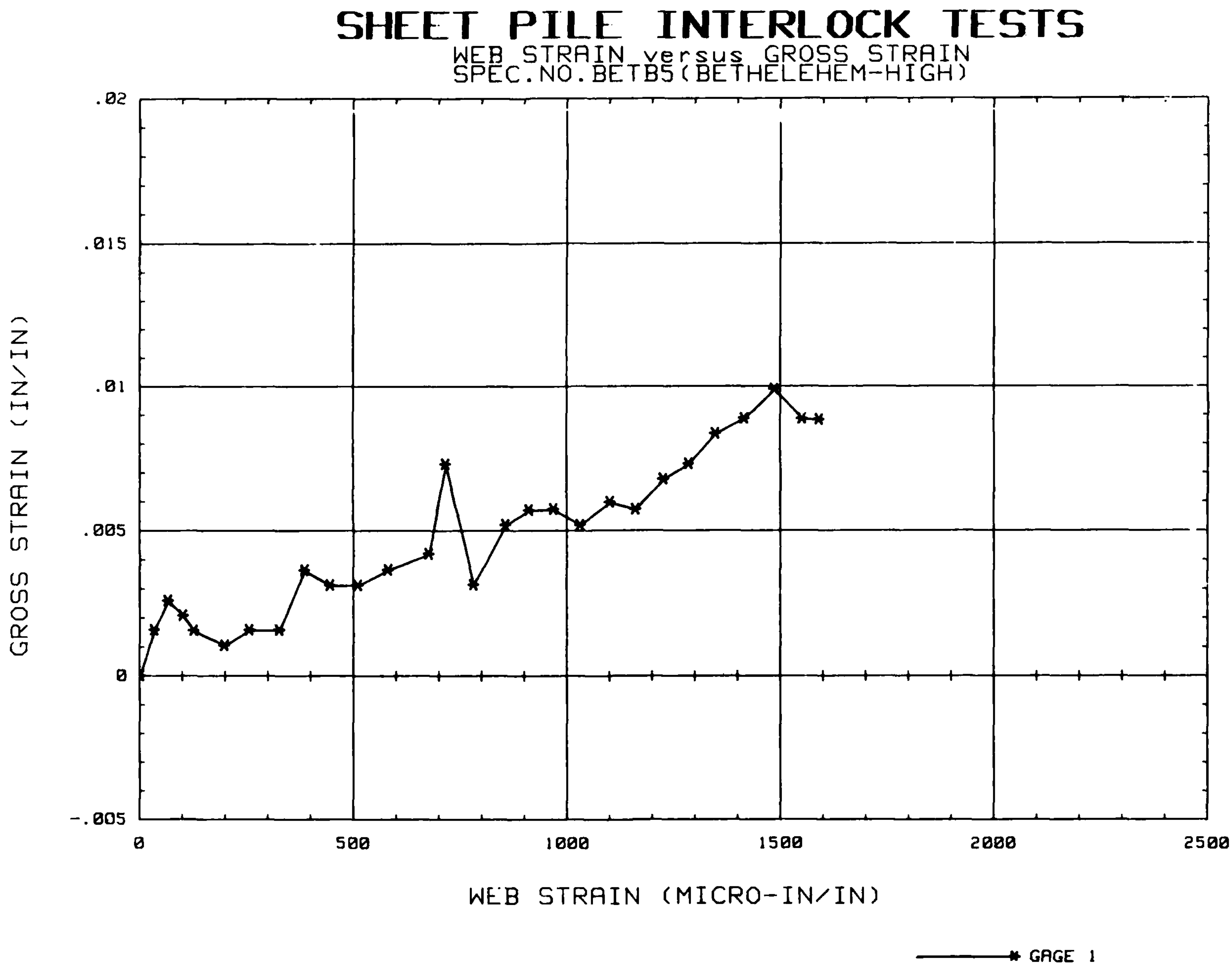

SHEET PILE INTERLOCK TESTS
WEB STRAIN versus GROSS STRAIN
SPEC.NO.BETB5(BETHELEHEM-HIGH)
.02
.015
.01
.005
0
-.005
0
500
1000
1500
2000
2500
GROSS STRAIN (IN/IN)
WEB STRAIN (MICRO-IN/IN)
GAGE 1

FIGURE D5

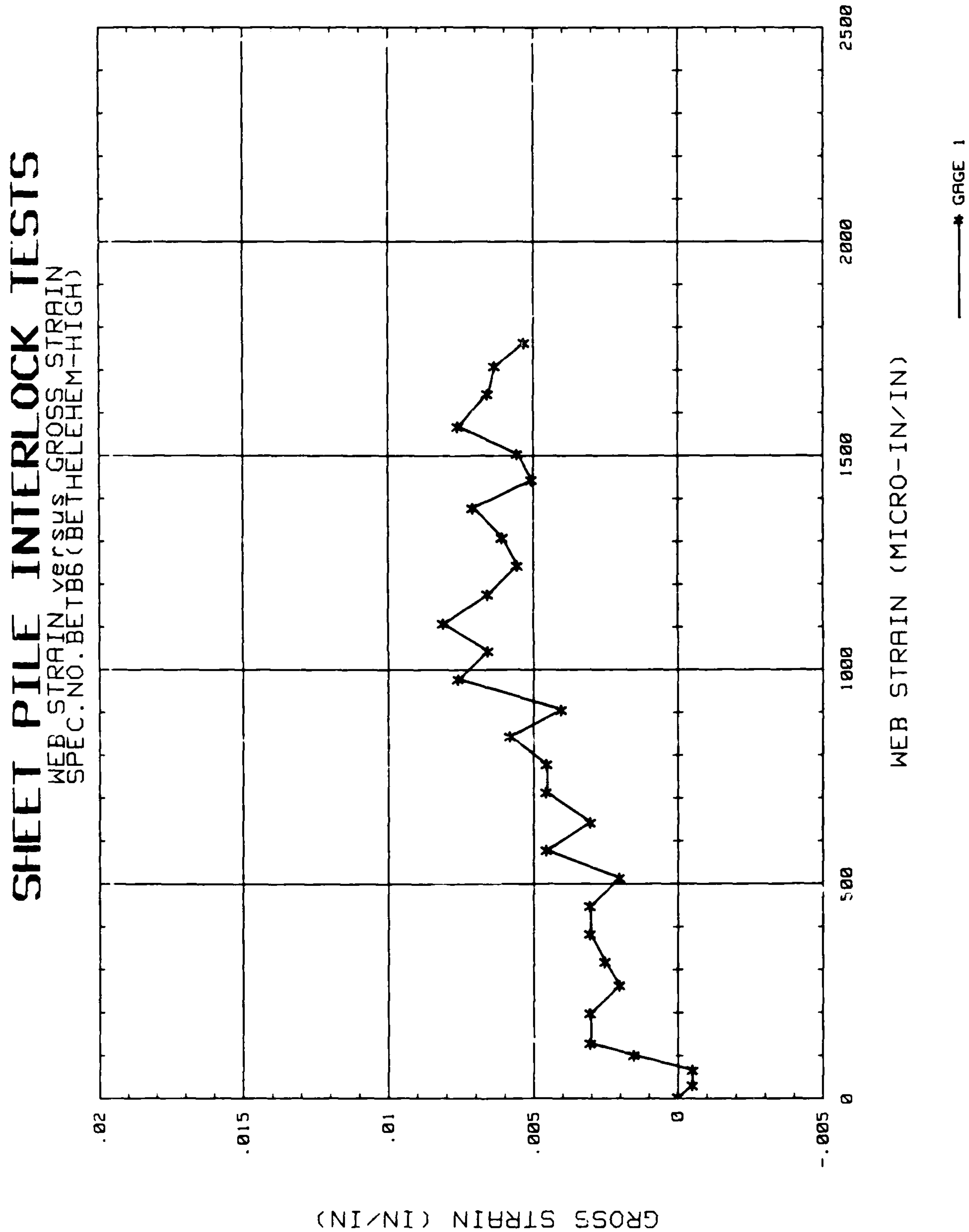
SHEET PILE INTERLOCK TESTS
WEB STRAIN versus GROSS STRAIN
SPEC.NO.BETB6(BETHELEHEM-HIGH)
WEB STRAIN (MICRO-IN/IN)
GROSS STRAIN (IN/IN)
GAGE 1
0
500
1000
1500
2000
2500
.02
.015
.01
.005
0
-.005

FIGURE D6

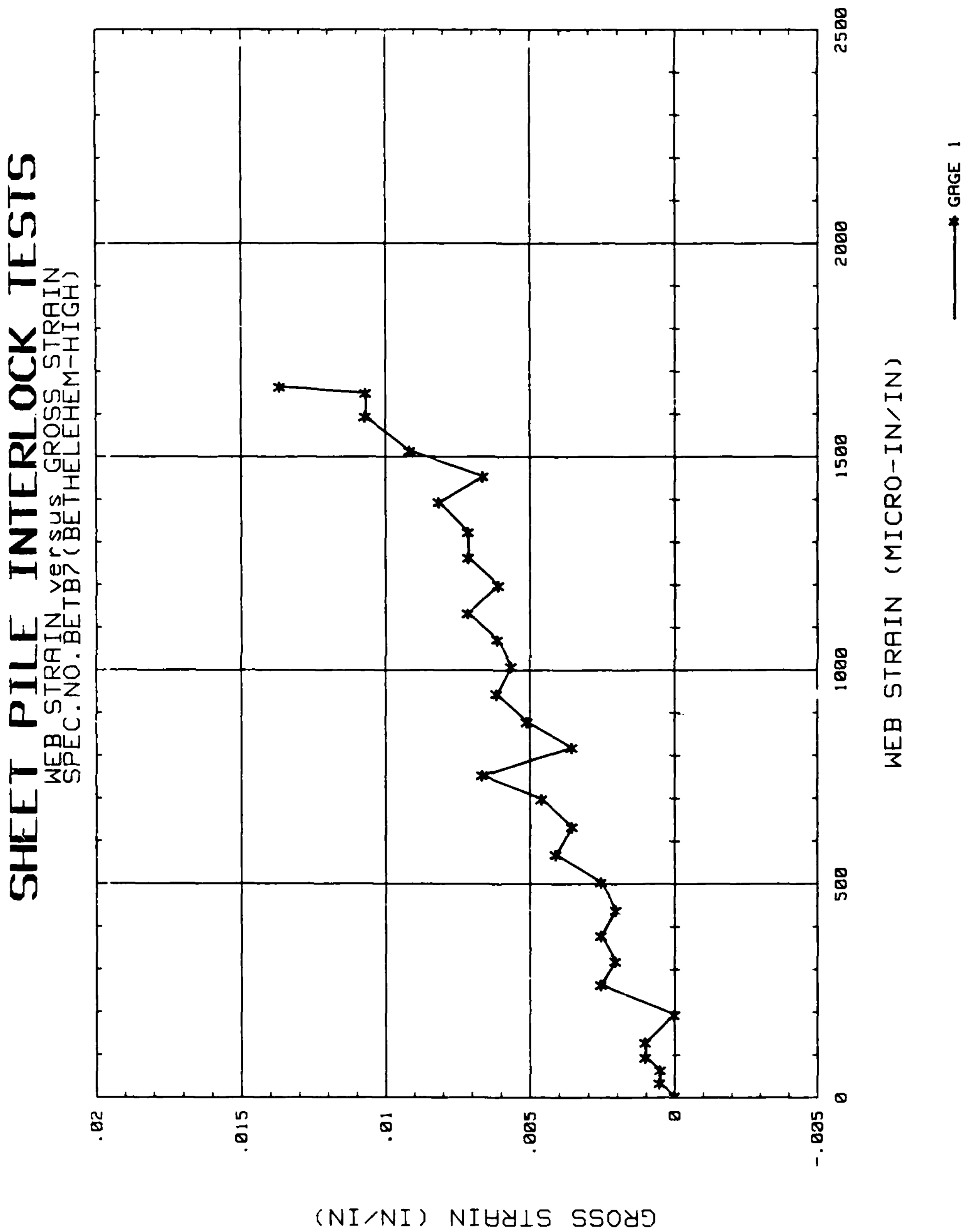
SHEET PILE INTERLOCK TESTS
WEB STRAIN versus GROSS STRAIN
SPEC.NO.BETB7(BETHELEHEM-HIGH)
WEB STRAIN (MICRO-IN/IN)
GROSS STRAIN (IN/IN)
0
500
1000
1500
2000
2500
.02
.015
.01
.005
0
-.005
GAGE 1

FIGURE C7

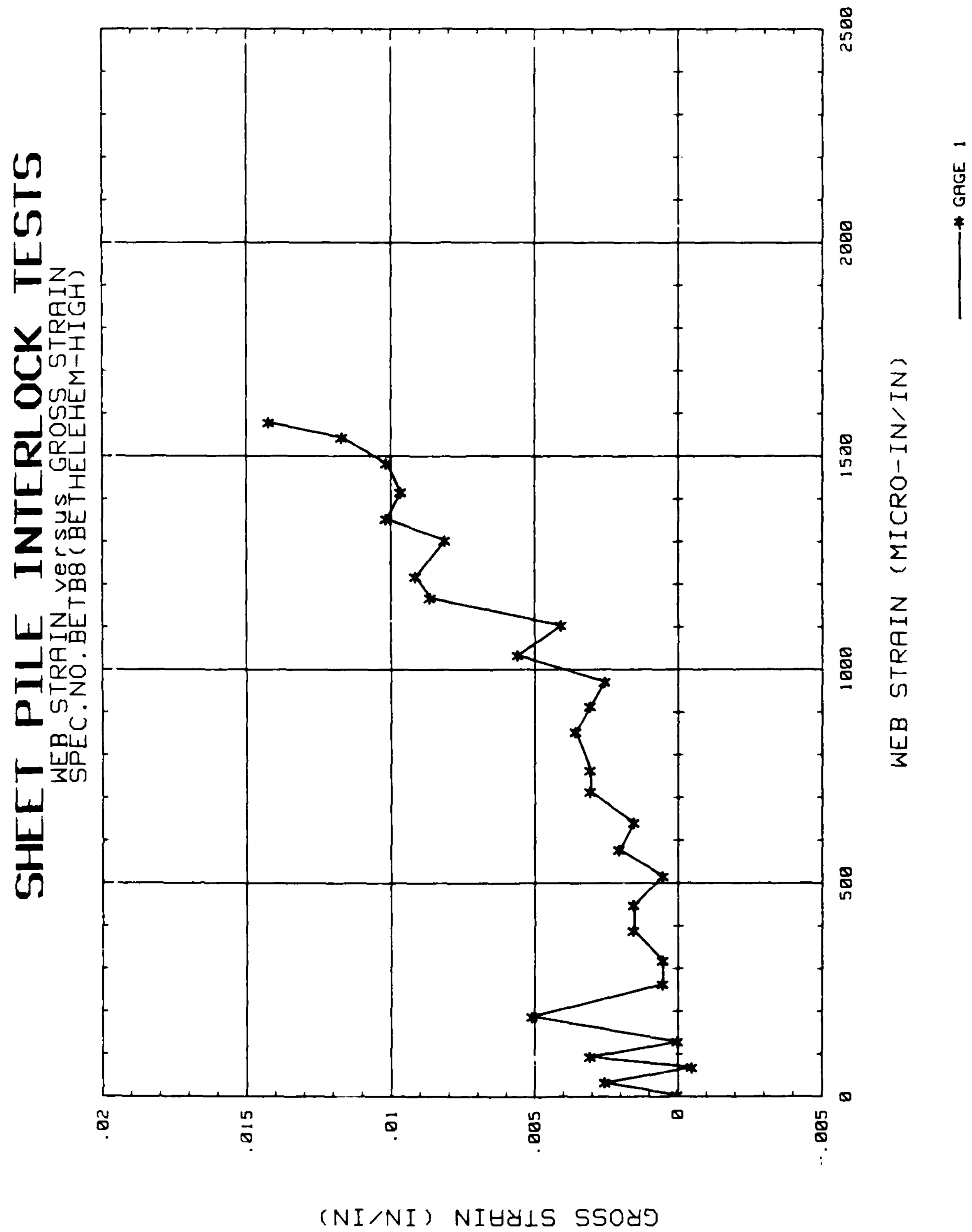

SHEET PILE INTERLOCK TESTS
WEB STRAIN versus GROSS STRAIN
SPEC.NO.BETB8(BETHELEHEM-HIGH)
WEB STRAIN (MICRO-IN/IN)
GROSS STRAIN (IN/IN)
0
500
1000
1500
2000
2500
.02
.015
.01
.005
0
-.005
GAGE 1

FIGURE D8

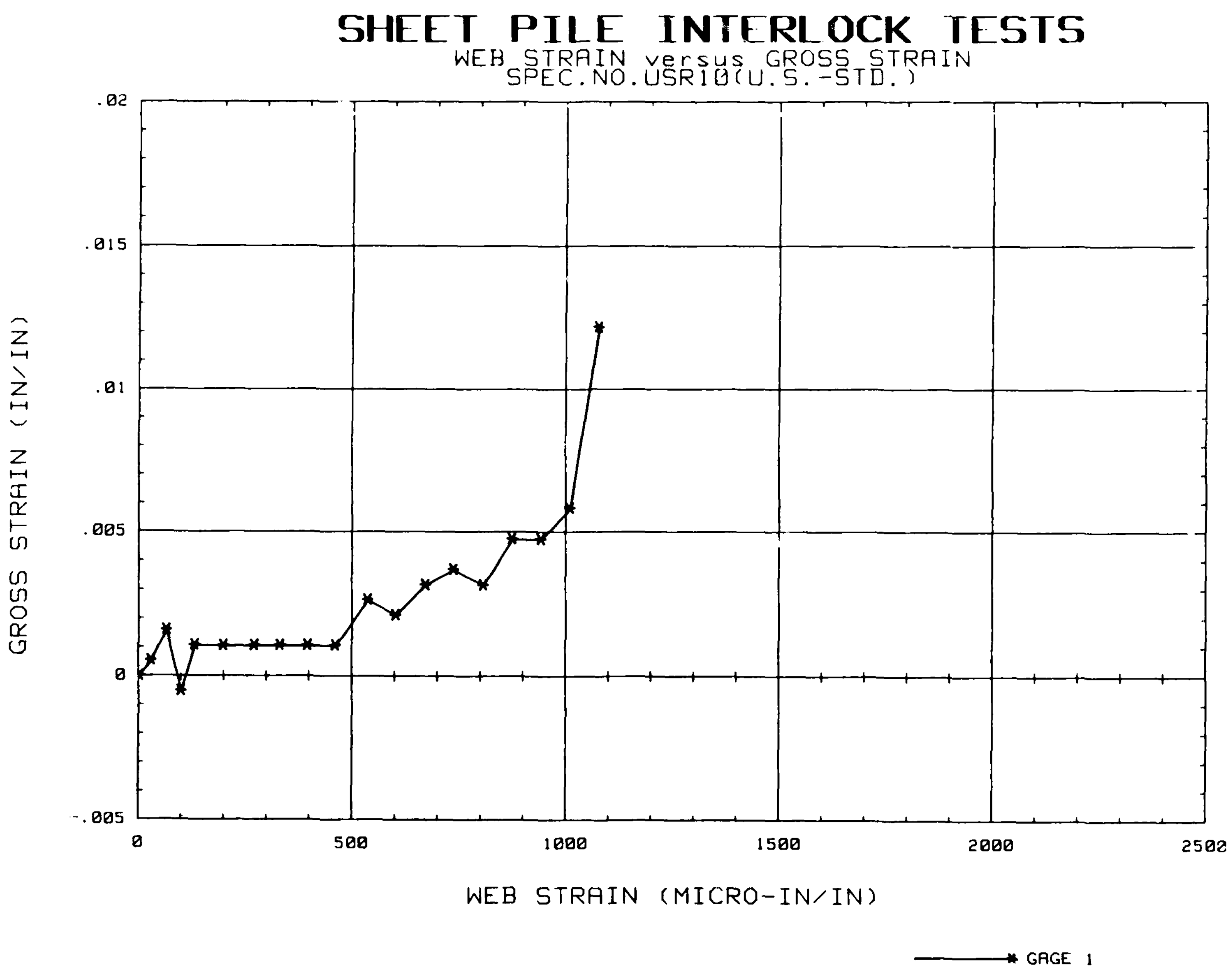
SHEET PILE INTERLOCK TESTS
WEB STRAIN versus GROSS STRAIN
SPEC.NO.USR10(U.S.-STD.)
GROSS STRAIN (IN/IN)
.02
.015
.01
.005
0
-.005
0
500
1000
1500
2000
2502
WEB STRAIN (MICRO-IN/IN)
GAGE 1

FIGURE D9

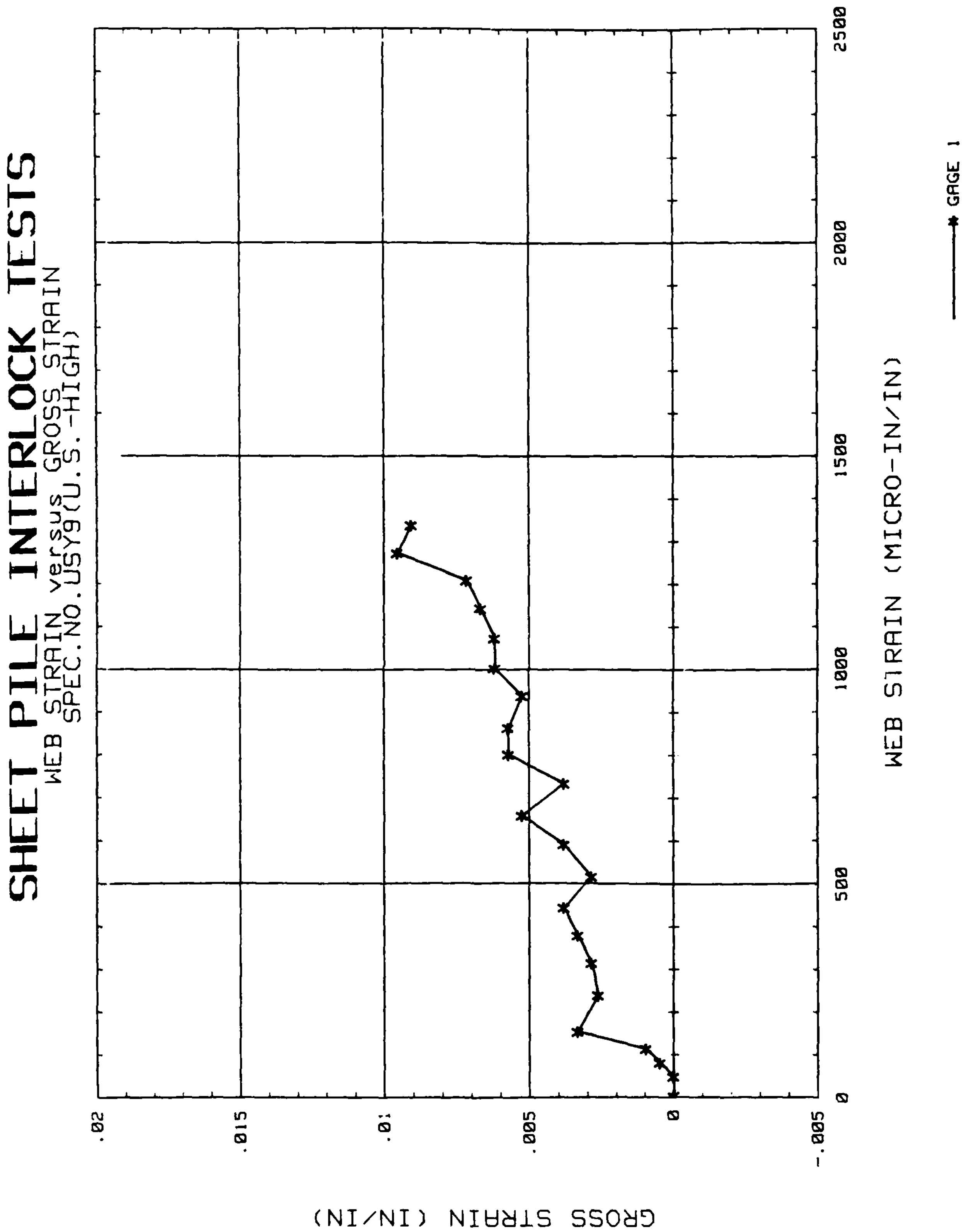
SHEET PILE INTERLOCK TESTS
WEB STRAIN versus GROSS STRAIN
SPEC.NO.USY9(U.S.-HIGH)
GROSS STRAIN (IN/IN)
.02
.015
.01
.005
0
-.005
WEB STRAIN (MICRO-IN/IN)
0
500
1000
1500
2000
2500
GAGE 1

FIGURE D10

Table D1

Sheet Pile Interlock Tests

Average Web Strain Versus Gross Strain

Specimen No. BET01 (Bethelehem-Standard)

Average Pile Width = 3.001 in.

Average Web Strain μin./in.	Gross Strain in./in.
0	0.000000
30	0.002144
65	0.002678
95	0.002147
135	0.002147
215	0.002681
275	0.002681
335	0.003750
408	0.004832
475	0.003216
535	0.005363
615	0.003750
680	0.004288
745	0.003753
810	0.004825
885	0.004822
955	0.005359
1,025	0.005627
1,085	0.005894
1,160	0.008034
1,235	0.008041
1,295	0.015561

Table D2

Sheet Pile Interlock Tests

Average Web Strain Versus Gross Strain

Specimen No. BET02 (Bethelehem-Standard)

Average Pile Width = 3.003 in.

Average Web Strain μin./in.	Gross Strain in./in.
0	0.000000
25	-0.001018
58	0.000005
90	0.000512
122	0.001023
188	0.000000
260	0.001028
320	0.001023
385	0.002046
450	0.001023
530	0.002553
585	0.001023
647	0.003571
715	0.003060
775	0.002548
845	0.002553
900	0.002041
978	0.003060
1,050	0.004073
1,115	0.003567
1,180	0.005092
1,250	0.009174

Table D3

Sheet Pile Interlock Tests

Average Web Strain Versus Gross Strain

Specimen No. BET03 (Bethelehem-Standard)

Average Pile Width = 3.003 in.

Average Web Strain μin./in.	Gross Strain in./in.
0	0.000000
30	0.003856
60	0.002195
90	0.002195
125	0.001651
190	0.001651
260	0.002205
325	0.001651
395	0.003856
453	0.002205
525	0.001098
593	0.002195
657	0.002749
725	0.003302
792	0.003293
863	0.003856
930	0.003302
1,010	0.002749
1,065	0.004390
1,143	0.005488
1,208	0.005488
1,280	0.009324

Table D4

Sheet Pile Interlock Tests

Average Web Strain Versus Gross Strain

Specimen No. BETO4 (Bethelehem-Standard)

Average Pile Width = 3.002 in.

Average Web Strain μin./in.	Gross Strain in./in.
0	0.000000
38	-0.000001
72	-0.001029
110	-0.000515
143	-0.000515
215	-0.000001
280	-0.000515
350	0.000000
415	0.000001
495	0.000515
555	0.001028
625	0.001028
685	0.002057
760	0.001543
835	0.002056
897	0.001542
960	0.002057
1,035	0.002057
1,105	0.003048
1,175	0.003600
1,230	0.004113
1,295	0.009253

Table D5

Sheet Pile Interlock Tests

Average Web Strain Versus Gross Strain

Specimen No. BETB5 (Bethelehem-High)

Average Pile Width = 3.001 in.

Average Web Strain μin./in.	Gross Strain in./in.
0	0.000000
33	0.001574
65	0.002584
100	0.002071
125	0.001557
198	0.001044
255	0.001574
325	0.001574
385	0.003628
445	0.003114
510	0.003114
580	0.003645
675	0.004191
715	0.007289
780	0.003131
855	0.005185
910	0.005699
968	0.005732
1,030	0.005185
1,100	0.005964
1,160	0.005715
1,225	0.006759
1,285	0.007289
1,348	0.008333
1,415	0.008863
1,485	0.009890
1,550	0.008847
1,590	0.008813

Table D6

Sheet Pile Interlock Tests

Average Web Strain Versus Gross Strain

Specimen No. BETB6 (Bethelehem-High)

Average Pile Width = 3.005 in.

Average Web Strain μin./in.	Gross Strain in./in.
0	0.000000
28	-0.000504
63	-0.000507
97	0.001515
125	0.003028
195	0.003031
260	0.002020
315	0.002529
380	0.003036
445	0.003036
510	0.002022
575	0.004557
640	0.003034
710	0.004554
775	0.004544
840	0.005812
902	0.004040
975	0.007585
1,040	0.006569
1,105	0.008090
1,173	0.006574
1,240	0.005558
1,305	0.006070
1,375	0.007070
1,440	0.005051
1,500	0.005558
1,565	0.007583
1,640	0.006572
1,705	0.006318
1,760	0.005310

Table D7

Sheet Pile Interlock Tests

Average Web Strain Versus Gross Strain

Specimen No. BETB7 (Bethelehem-High)

Average Pile Width = 3.002 in.

Average Web Strain μin./in.	Gross Strain in./in.
0	0.000000
30	0.000517
60	0.000498
90	0.001015
125	0.001015
190	0.000000
260	0.002546
315	0.002048
375	0.002546
435	0.002030
500	0.002546
565	0.004078
630	0.003542
695	0.004576
750	0.006624
815	0.003542
875	0.005074
940	0.006127
1,005	0.005610
1,068	0.006108
1,130	0.007122
1,195	0.006070
1,260	0.007104
1,320	0.007122
1,390	0.008118
1,450	0.006606
1,510	0.009133
1,590	0.010684
1,645	0.010665
1,660	0.013652

Table D8

Sheet Pile Interlock Tests

Average Web Strain Versus Gross Strain

Specimen No. BETB8 (Bethelehem-High)

Average Pile Width = 3.002 in.

Average Web Strain μin./in.	Gross Strain in./in.
0	0.000000
30	0.002536
65	-0.000508
90	0.003043
125	0.000000
185	0.005067
260	0.000507
315	0.000508
385	0.001521
445	0.001521
512	0.000505
575	0.002030
638	0.001520
710	0.003044
760	0.003043
850	0.003551
910	0.003044
968	0.002536
1,030	0.005582
1,100	0.004059
1,165	0.008620
1,215	0.009124
1,300	0.008113
1,350	0.010139
1,413	0.009638
1,480	0.010141
1,540	0.011662
1,575	0.014195

Table D9

Sheet Pile Interlock Tests

Average Web Strain Versus Gross Strain

Specimen No. USY9 (US-High)

Average Pile Width = 2.998 in.

Average Web Strain μin./in.	Gross Strain in./in.
0	0.000000
45	0.000000
78	0.000476
110	0.000953
150	0.003335
235	0.002620
310	0.002859
375	0.003335
440	0.003811
512	0.002859
588	0.003811
655	0.005241
730	0.003811
797	0.005717
860	0.005717
935	0.005241
1,000	0.006193
1,070	0.006193
1,140	0.006670
1,205	0.007146
1,270	0.009528
1,335	0.009052
1,403	0.010481
1,465	0.010958
1,475	0.010958

Table D10

Sheet Pile Interlock Tests

Average Web Strain Versus Gross Strain

Specimen No. USR10 (US-Standard)

Average Pile Width = 3.002 in.

Average Web Strain μin./in.	Gross Strain in./in.
0	0.000000
28	0.000531
63	0.001593
97	-0.000520
130	0.001073
198	0.001051
270	0.001062
330	0.001062
395	0.001062
460	0.001062
535	0.002643
600	0.002112
670	0.003163
735	0.003694
805	0.003152
873	0.004744
940	0.004733
1,008	0.005817
1,075	0.012165

APPENDIX E: REGRESSION ANALYSES

Approach

1. The data used in the regression analyses were taken from the photographs of the tests. These data were grouped as discussed in the main text in paragraphs 73 through 75, and the coefficients for the two types of curves which best fit the data were reported. The data were fit to linear, exponential, power, two common log functions, one natural log function, three polynomial functions, and a hyperbolic function. The curves used in the regressions are listed in Table E1.

Table E1

Regression Equations

Type	Equation
Linear	Y = A* X + B
Exponential	Y = A* EXP [B*(X + X1)] - Y1
Power	Y = A*(X + X1)**B - Y1
Common log (log 1)	Y = A1 + A2* LOG (X + X1) + A3* [LOG (X + X1)]**2
Common log (log 2)	Y = A1 + A2*(X + X1) + A3* LOG (X + X1)
Natural log (ln 1)	Y = A + B* LN (X + X1)
Poly 1	Y = A1 + A2*(X + X1)
Poly 2	Y = A1 + A2*(X + X1) + A3*(X + X1)**2
Poly 3	Y = A1 + A2*(X + X1) + A3*(X + X1)**2 + A4*(X + X1)**3
Hyperbolic	$Y = \frac{A + B}{X + X1}$

2. For all equations, the program calculated the coefficients A , B , A1 , A2 , A3 , X1 . The dependent variable Y is the calculated deformation, and the independent variable X is the load, P/W .

Failure End Equations

3. The sum of the squares regression analysis yielded two curves with close correlation coefficients for the failure interlock, PS31 standard-strength tests. The correlation coefficient for an exponential fit of the data was 0.7301086, and for a third-order polynomial was 0.7793327. The seven

remaining curve types had coefficients below these two. The index of "best fit of the data," the sum of the squares of the residuals, for these two curves were 0.10748 and 0.08237, respectively. These two equations are given in Table E2.

Table E2

Best Fit Equations for Failure Interlock, PS31 Standard-Strength Tests

---

Exponential: Y = A* EXP [B*(X + X1)] - Y1

A = 0.21291898E - 01	Correlation coefficient	0.7301086
B = 0.89231699E - 04	Sum squares residual	0.10748
X1 = 0.40000000E - 03		
Y1 = 0.15690000E - 01		

Third-order polynomial: Y = A1 + A2*(X + X1) + A3*(X + X1)**2 + A4*(X + X1)**3

A1 = -0.15127122E - 03	Correlation coefficient	0.7793327
A2 = 0.16882784E - 04	Sum squares residual	0.08237
A3 = -0.23313819E - 08		
A4 = 0.98255684E - 13		
X1 = 0.40000000E - 03		

---

4. The plots of the equations as fit to the data are given in Figures E1 (exponential) and E2 (polynomial). Both plots show the data and the graph of the best fit curve. The dotted lines represent the bounds of two standard deviations. The best fit of the data is obtained by the third-order polynomial, and the correlation coefficient is closer to 1. This suggests that the polynomial equation is the most appropriate fit of the data: however, observation of both curves leads one to choose the exponential curve as more appropriate in this case since the polynomial curve has a decrease in deformation with an increase of load.

5. Figures E3 and E4 give the regression analysis curves for the failure end, PS31 high-strength data. The correlation coefficient for an exponential fit of the data was 0.8373474, and for a third-order polynomial was 0.8137031. The sum of the squares of the residuals, for these two curves

were 0.18042 and 0.15586, respectively. These two equations are given below in Table E3.

Table E3

Best Fit Equations for Failure Interlock, PS31 High-Strength Tests

---

Exponential: Y = A* EXP [B*(X + X1)] - Y1

A = 0.26617088E - 01	Correlation coefficient 0.8373474
B = 0.8115506E - 04	Sum squares residual 0.18042
X1 = 0.40000000E - 03	
Y1 = 0.15530000E - 01	

Third-order polynomial: Y = A1 + A2*(X + X1) + A3*(X + X1)**2 + A4*(X + X1)**3

A1 = 0.21735091E - 01	Correlation coefficient 0.8137031
A2 = -0.97147149E - 06	Sum squares residual 0.15586
A3 = 0.55094809E - 09	
A4 = -0.11730516E - 13	
X1 = 0.40000000E - 03	

---

6. The correlation coefficient for both curves is essentially the same, and the fact that the residual for the third-order polynomial is smaller again suggests that the third-order polynomial equation is a better representation of the data. In this case the shape of the polynomial equation is more characteristic of the typical load-deformation curve.

7. Figures E5 through E8 give the best fit curves for the failure end of the PS32 and the PSX32 piles, respectively. For the PS32 test, the correlation coefficient for the third-order polynomial was 0.9086438, and for an exponential fit was 0.8818037. The sum of the squares residual for this test was 0.00734 for the polynomial, and 0.01005 for the exponential curve. For the PSX32 test, the correlation coefficient for the third-order polynomial was 0.9298335, and for an exponential fit was 0.9158804. The sum of the squares residual for this test was 0.00729 for the polynomial, and 0.01558 for the exponential curve. Table E4 gives these curves and their constants.

8. For both the PS32 and the PSX32 piles the third-order polynomial equations provide better correlation coefficients and smaller residual terms,

Table E4

Best Fit Equations for Failure Interlock, PS32 Standard-Strength Test and PSX32 High-Strength Test

---

PS32 Standard-Strength Test

Exponential: Y = A* EXP [B*(X + X1)] - Y1

A = 0.48243025E - 02	Correlation coefficient 0.8818037
B = 0.21710544E - 03	Sum squares residual 0.01005
X1 = 0.40000000E - 03	
Y1 = 0.40000000E - 03	

Third-order polynomial: Y = A1 + A2*(X + X1) + A3*(X + X1)**2 + A4*(X + X1)**3

A1 = -0.12936242E - 02	Correlation coefficient 0.9086438
A2 = 0.18953044E - 04	Sum squares residual 0.00734
A3 = -0.34558245E - 08	
A4 = 0.18579483E - 12	
X1 = 0.40000000E - 03	

PSX32 High-Strength Test

Exponential: Y = A* EXP [B*(X + X1)] - Y1

A = 0.72185959E - 02	Correlation coefficient 0.9158804
B = 0.15558178E - 03	Sum squares residual 0.01558
X1 = 0.40000000E - 03	
Y1 = 0.40000000E - 03	

Third-order polynomial: Y = A1 + A2*(X + X1) + A3*(X + X1)**2 + A4*(X + X1)**3

A1 = 0.14280751E - 02	Correlation coefficient 0.9298335
A2 = 0.15382750E - 04	Sum squares residual 0.00729
A3 = -0.16899397E - 08	
A4 = 0.63426079E - 13	
X1 = 0.40000000E - 03	

---

indicating that the polynomial better represents the data. These equations are less statistically accurate due to the limited number of data points (only one deformation point per load point), but the same type of equation emerged as the best fit of the data as did the group tests where there were four pieces of deformation data for each load point. The polynomial equation for the PS32 standard-strength test again has an area where there is decreasing deformation for increasing load and is perhaps a less appropriate choice of curve than the exponential.

Nonfailure End Equations

9. It was decided, that to separate the data into data groups of failure and nonfailure end would be useful in observing whether or not the two groups behaved differently. The following tables show that the types of equations which best fit the data from the two groups are the same (exponential and third-order polynomial), and that the coefficients and constants are very nearly the same from failure to nonfailure end. From this, it can be said that since the equations are nearly the same, the behavior of each end is similar, indicating that both failure and nonfailure interlocks deformed in a similar manner under load, up until near failure.

10. The regression analysis for the PS31 standard-strength tests at the nonfailure end yielded best fit curves of exponential and third-order polynomial types. The correlation coefficient for the exponential equation was 0.8712457 and for the polynomial 0.8496959. The sum of the squares residuals for the exponential curve was 0.06116 and for the polynomial it was 0.05531. Table E5 presents these two equations.

11. The correlation coefficients and the residuals are enough alike that either curve can give approximately the same results. Relating the data to Figures E9 (exponential) and E10 (polynomial), it appears that the polynomial equation behaves more like the pile group.

12. The regression analysis for the nonfailure ends of the PS31 high-strength tests are given in Table E6. The curve fitting analysis again gave both the exponential and the third-order polynomial as the curves which best fit the data. The exponential equation had a correlation coefficient of 0.8573806, while the polynomial equation gave 0.8379552. The sum of the squares of the residuals was lower for the polynomial equation at 0.07426 where the exponential fit returned 0.10307.

13. These graphs are shown in Figures E11 (exponential) and E12 (polynomial). The analysis data are so close together that either curve supports the data to approximately the same degree. The polynomial equation is

Table E5

Best Fit Equations for Nonfailure Interlock,

PS31 Standard-Strength Tests

Exponential: Y = A* EXP [B*(X + X1)] - Y1

A = 0.27895231E - 01	Correlation coefficient	0.8712457
B = 0.78867657E - 04	Sum squares residual	0.06116
X1 = 0.40000000E - 03		
Y1 = 0.31040000E - 01		

Third-order polynomial: Y = A1 + A2*(X + X1) + A3*(X + X1)**2 + A4*(X + X1)**3

A1 = 0.26003733E - 02	Correlation coefficient	0.8496959
A2 = 0.68947035E - 05	Sum squares residual	0.05531
A3 = -0.72784819E - 09		
A4 = 0.34383144E - 13		
X1 = 0.40000000E - 03		

Table E6

Best Fit Equations for Nonfailure Interlock,

PS31 High-Strength Tests

Exponential: Y = A* EXP [B*(X + X1)] - Y1

A = 0.20954190E - 01	Correlation coefficient	0.8573806
B = 0.81356070E - 04	Sum squares residual	0.10307
X1 = 0.40000000E - 03		
Y1 = 0.15640000E - 01		

Third-order polynomial: Y = A1 + A2*(X + X1) + A3*(X + X1)**2 + A4*(X + X1)**3

A1 = 0.30684487E - 02	Correlation coefficient	0.8379552
A2 = 0.59711107E - 05	Sum squares residual	0.07426
A3 = -0.14478910E - 09		
A4 = 0.34965232E - 14		
X1 = 0.40000000E - 03		

probably the better descriptor of the data since its sum square residual is smaller, and hence the data points closer to the fitted curve.

14. Figures E13 (exponential) and E14 (third-order polynomial) present the two best fitting curves for the nonfailure end of the PS32 standard-strength test; and Figure E15 (exponential) and E16 (third-order polynomial) give the best fits for the PSX32 high-strength test. These data are compared in Table E7. For the PS32 standard-strength test, the third-order polynomial produced a higher correlation coefficient of 0.9479090 compared to the exponential coefficient of 0.9308143. The polynomial equation also gave a better fit of the data with a residual value of 0.00081 where the exponential equation fit with 0.00165. Both equations fit the data well, with the polynomial giving the best fit; however, the shape of the exponential curve better describes the behavior of the pile test.

15. While these data fit well, the raw data are suspected of being in error. Both curves begin with dependent variables in the negative range, indicating that the piles were compressing under tensile load. This is not possible, and suggests that the photographic data, or the accuracy in reading it were unsatisfactory.

16. The regression data for the nonfailure end of the PSX32 test for the exponential curve (Figure E15) and the third-order polynomial (Figure E16) are also given in Table E7. The third-order polynomial curve had a higher correlation coefficient of 0.8996070 compared to the exponential value of 0.8348795. Additionally, the polynomial residual value was less at 0.00475 compared with 0.03485 for the exponential equation.

17. In the case of the PSX32 test, the polynomial regression analysis appears to fit the data the best. It also depicts the load-deformation history better than the exponential curve in the higher load ranges.

18. From these regression analyses, it can be said that the fit of the raw data are adequate to be described by both third-order polynomial and exponential curves. On the whole, the third-order polynomials represent the data more closely. Only where the polynomial exhibits decreasing deformation with increasing load does the polynomial curve become inappropriate.

Table E7

Best Fit Equations for Nonfailure Interlock, PS32 Standard-Strength Test and PSX32 High-Strength Test

PS32 Standard-Strength Test

Exponential: Y = A* EXP [B*(X + X1)] - Y1

A = 0.38954459E - 02	Correlation coefficient 0.9308143
B = 0.18165513E - 03	Sum squares residual 0.00165
X1 = 0.40000000E - 03	
Y1 = 0.11530000E - 01	

Third-order polynomial: Y = A1 + A2*(X + X1) + A3*(X + X1)**2 + A4*(X + X1)**3

A1 = 0.32667966E - 03	Correlation coefficient 0.9479090
A2 = -0.37739669E - 05	Sum squares residual 0.00081
A3 = 0.87745854E - 09	
A4 = -0.30605953E - 13	
X1 = 0.40000000E - 03	

PSX32 High-Strength Test

Exponential: Y = A* EXP [B*(X + X1)] - Y1

A = 0.45266855E - 02	Correlation coefficient 0.8348795
B = 0.17717333E - 03	Sum squares residual 0.03485
X1 = 0.40000000E - 03	
Y1 = 0.40000000E - 03	

Third-order polynomial: Y = A1 + A2*(X + X1) + A3*(X + X1)**2 + A4*(X + X1)**3

A1 = -0.20189486E - 02	Correlation coefficient 0.8996070
A2 = 0.10584459E - 04	Sum squares residual 0.00475
A3 = -0.69015804E - 09	
A4 = 0.19828361E - 13	
X1 = 0.40000000E - 03	

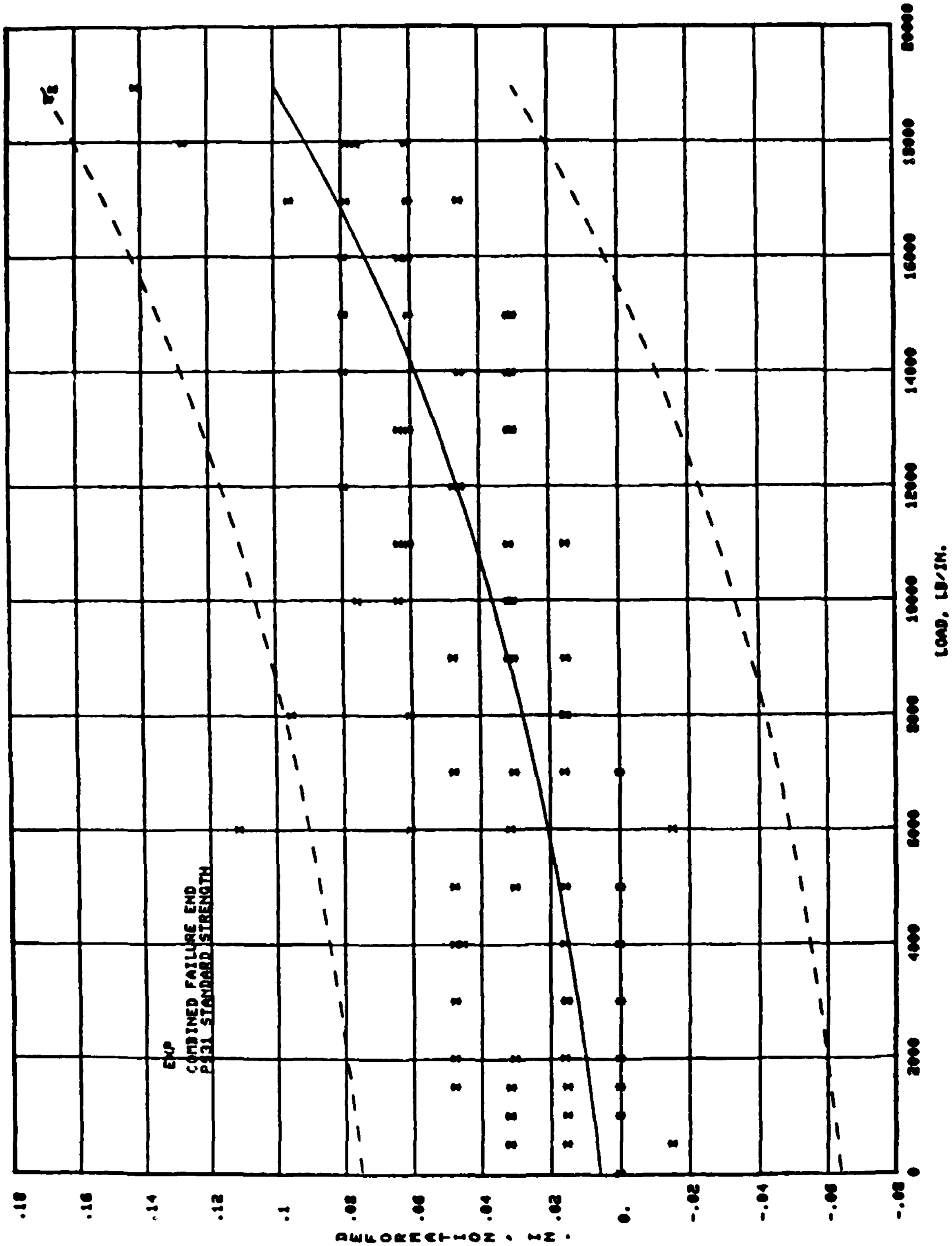

EXP
COMBINED FAILURE END
PS31 STANDARD STRENGTH
LOAD, LB/IN.
DEFORMATION, IN.

FIGURE E1

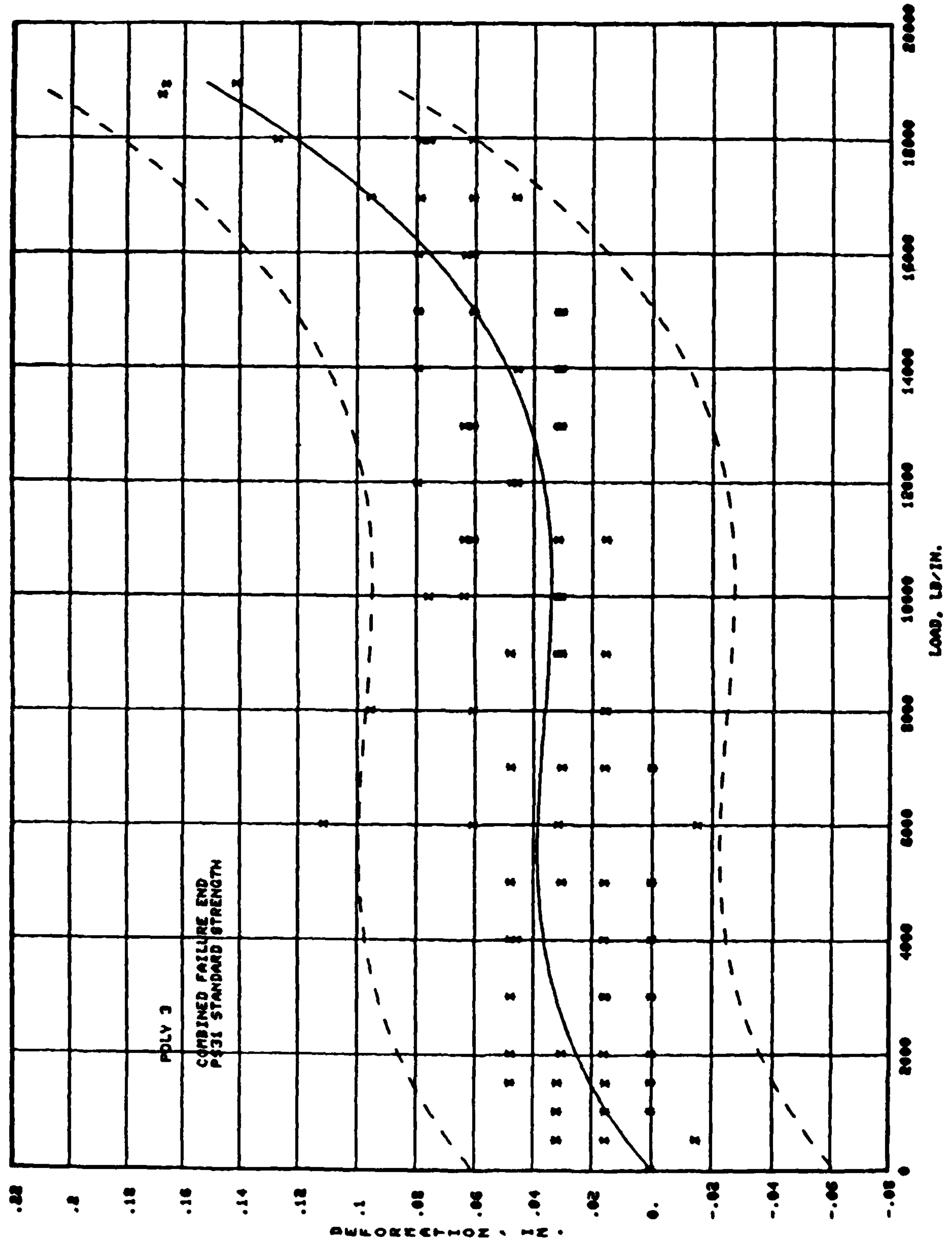
POLY 3
COMBINED FAILURE END
PS31 STANDARD STRENGTH
LOAD, LB/IN.

FIGURE E2

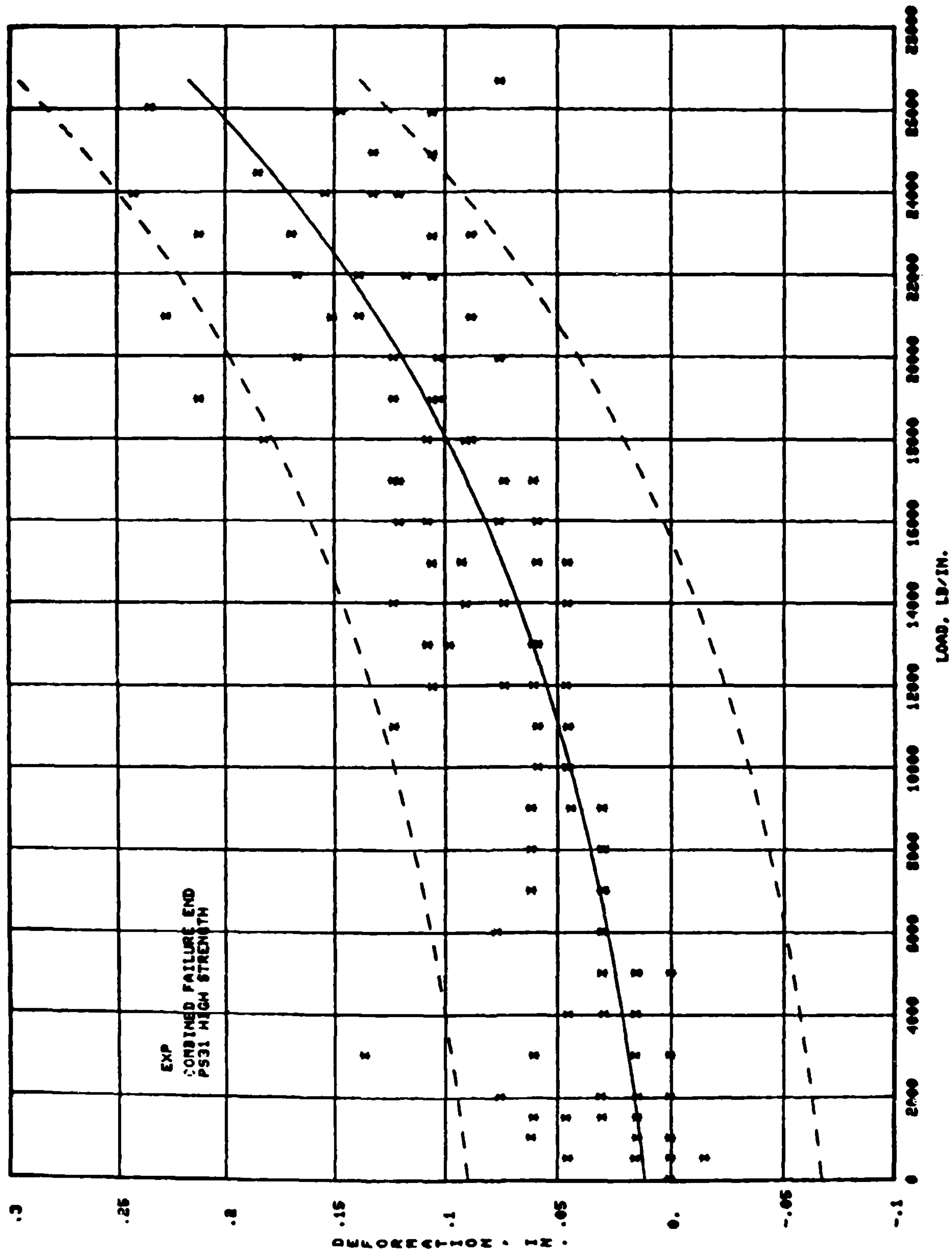

FIGURE E3

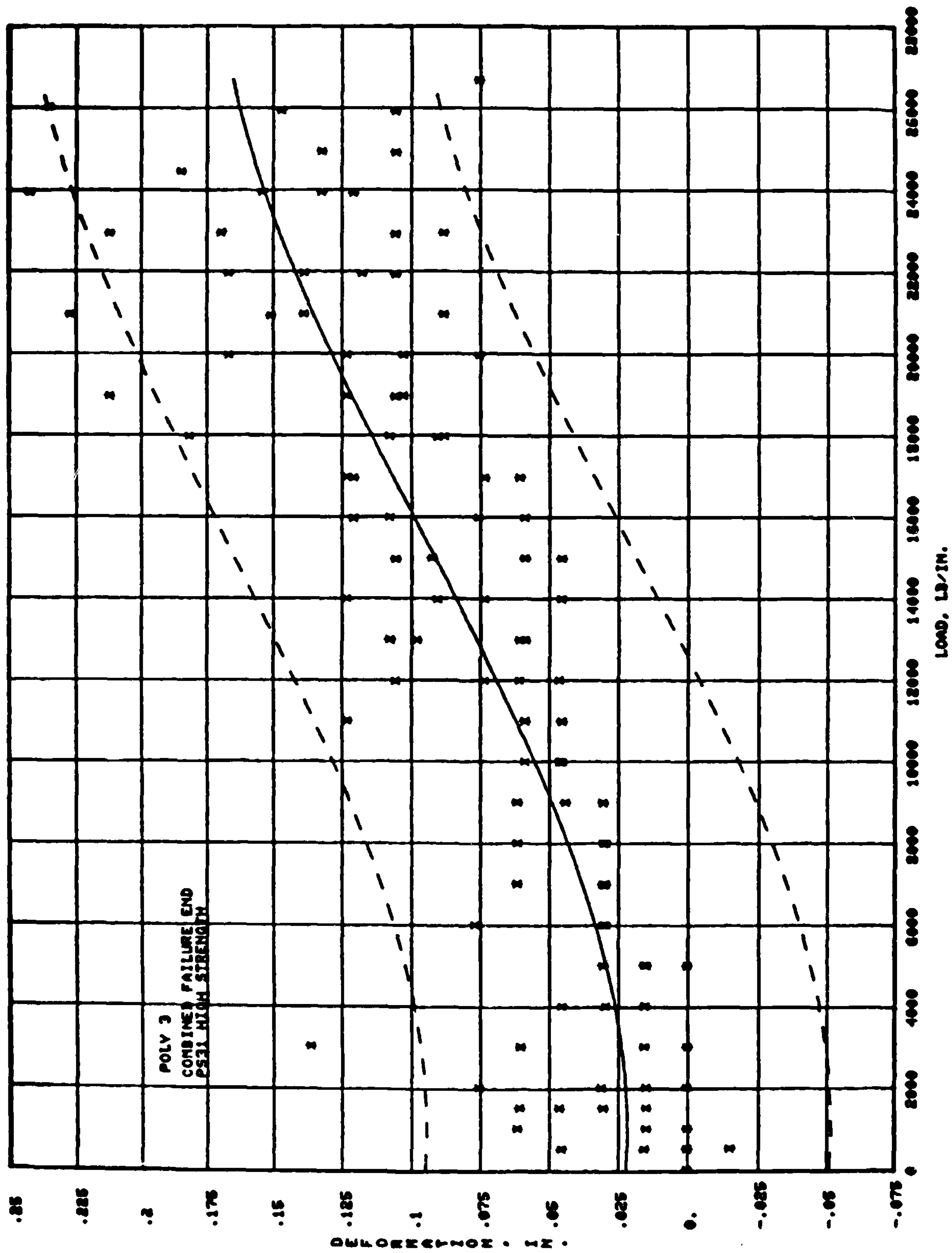

FIGURE E4

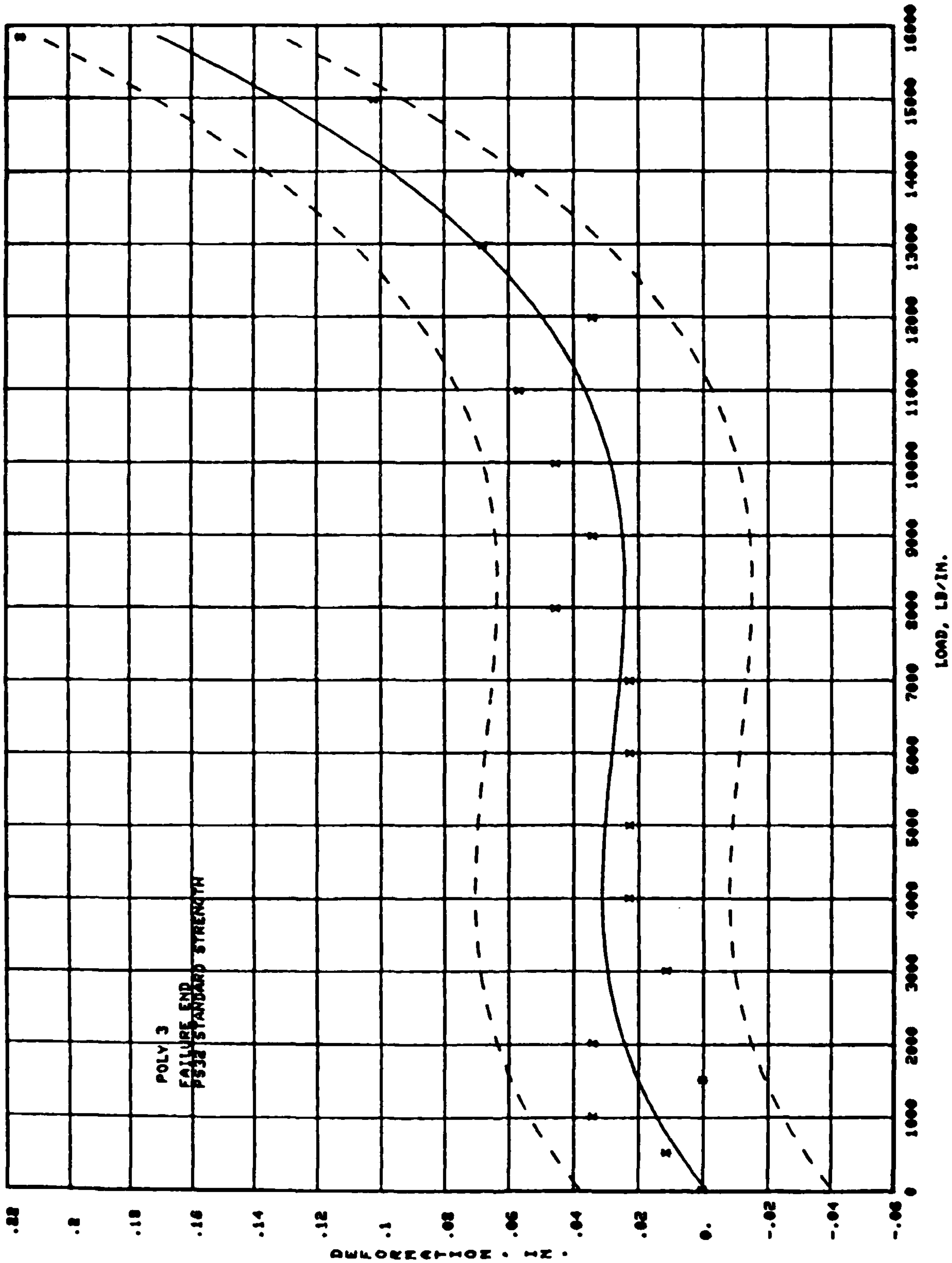

POLY 3
FAILURE END
FS32 STANDARD STRENGTH
LOAD, LB/IN.
0
1000
2000
3000
4000
5000
6000
7000
8000
9000
10000
11000
12000
13000
14000
15000
16000
.22
.2
.18
.16
.14
.12
.1
.08
.06
.04
.02
0.
-.02
-.04
-.06

FIGURE E5

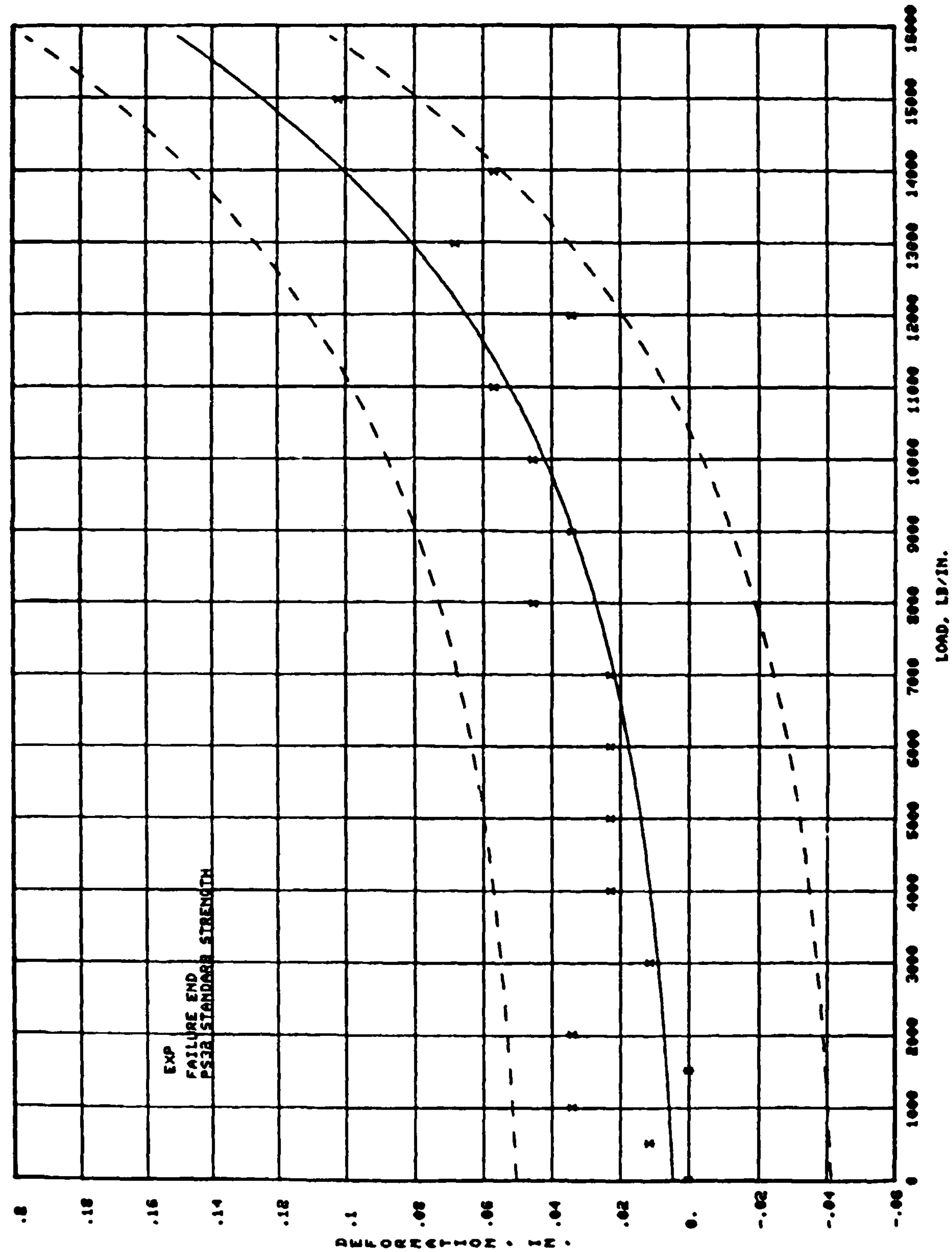
EXP
FAILURE END
PS32 STANDARD STRENGTH
LOAD, LB/IN.
0
1000
2000
3000
4000
5000
6000
7000
8000
9000
10000
11000
12000
13000
14000
15000
16000
.8
.18
.16
.14
.12
.1
.08
.06
.04
.02
0.
-.02
-.04
-.06

FIGURE E6

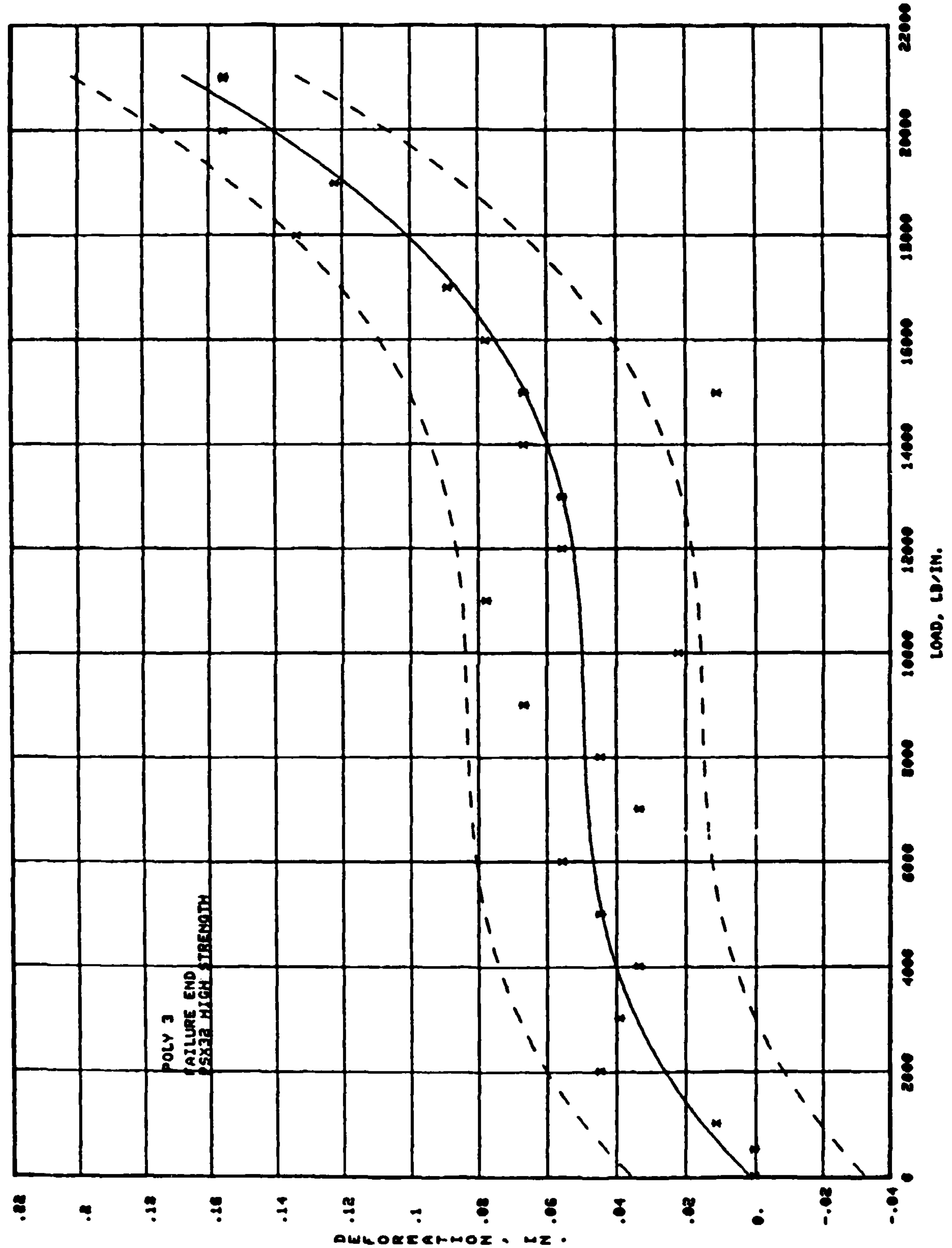

FIGURE E7

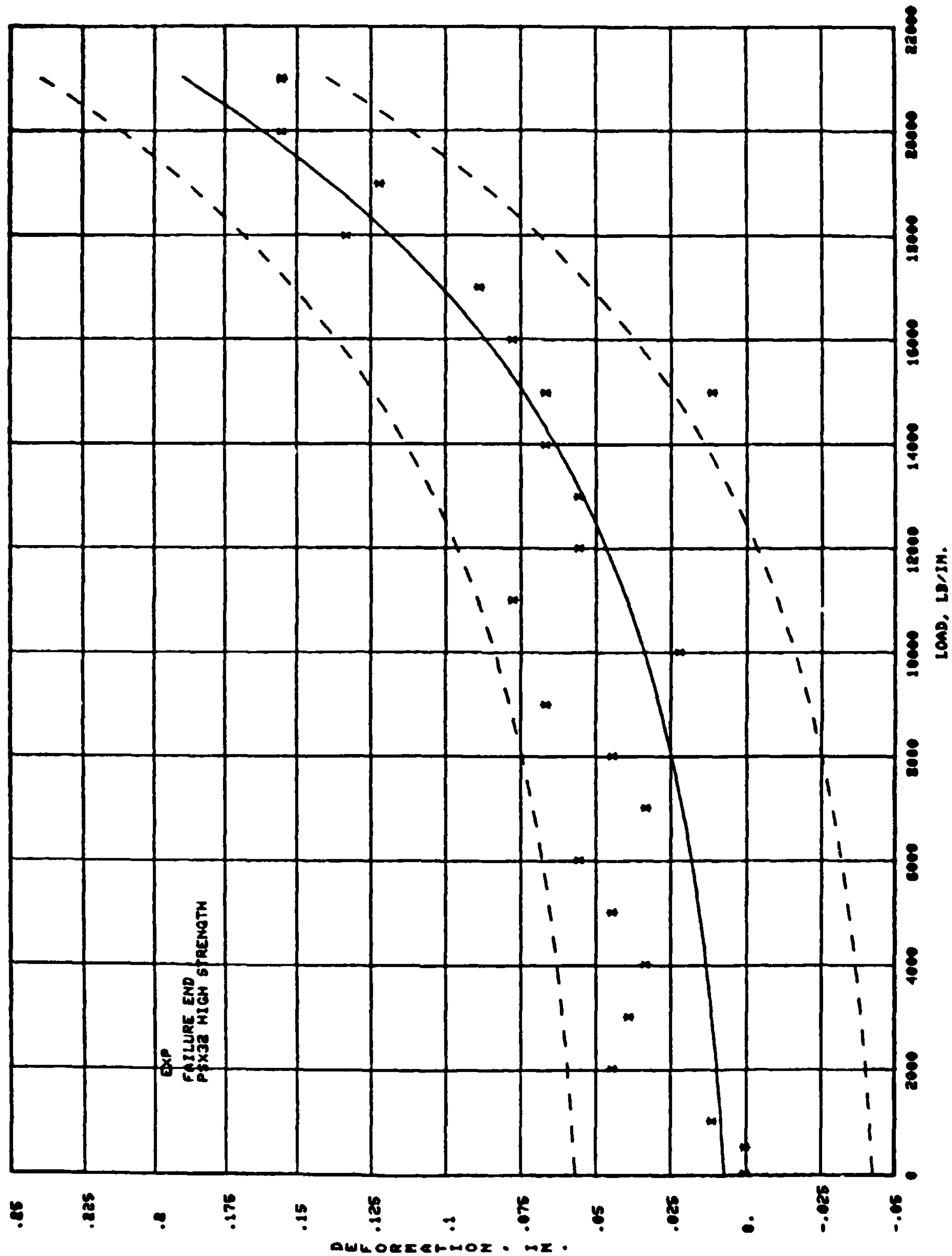
EXP
FAILURE END
PSX32 HIGH STRENGTH
LOAD, LB/IN.
DEFLECTION, IN.
0
2000
4000
6000
8000
10000
12000
14000
16000
18000
20000
22000
.25
.225
.2
.175
.15
.125
.1
.075
.05
.025
0.
-.025
-.05

FIGURE E8

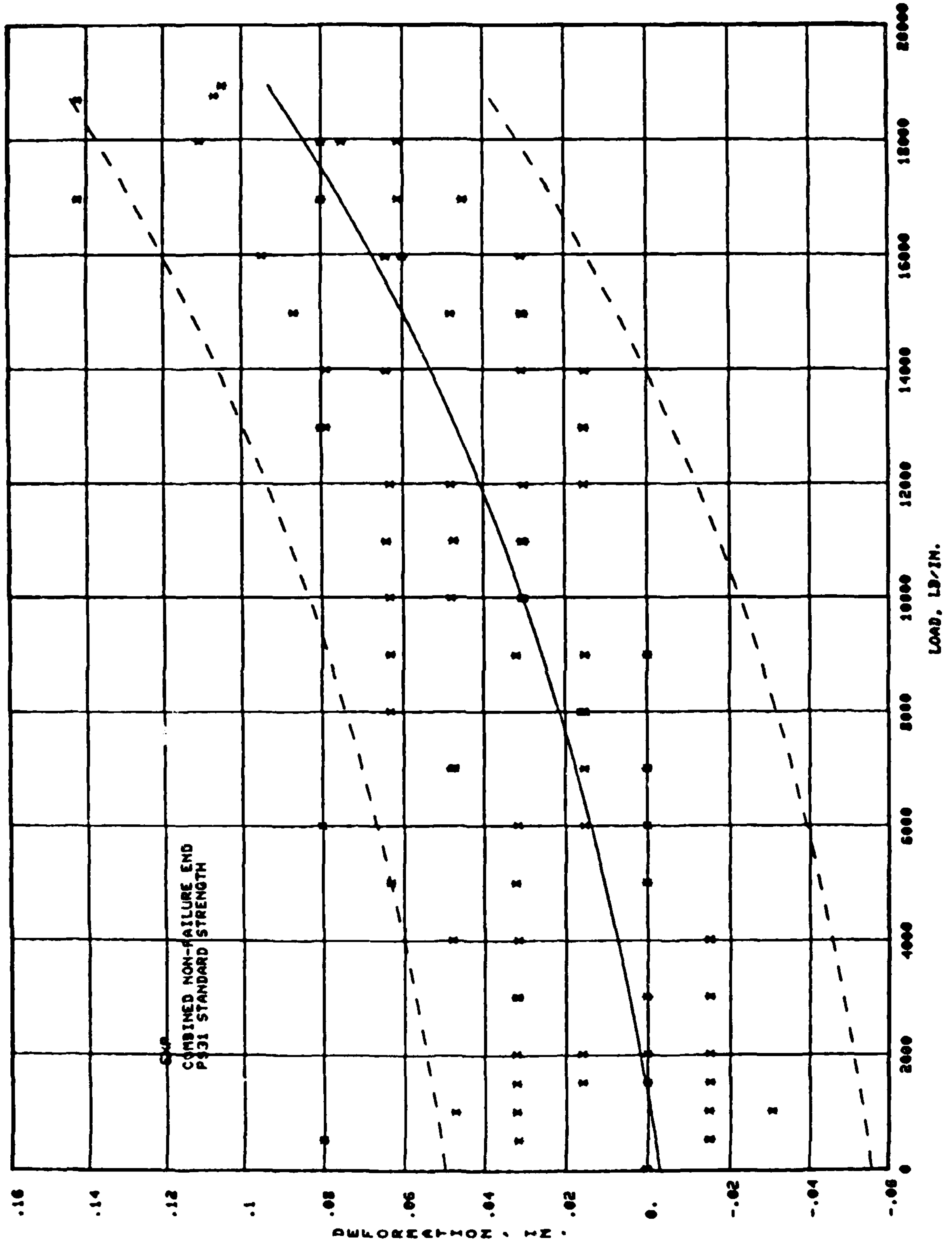
COMBINED NON-FAILURE END
PS31 STANDARD STRENGTH
LOAD, LB/IN.
0
2000
4000
6000
8000
10000
12000
14000
16000
18000
20000
.16
.14
.12
.1
.08
.06
.04
.02
0.
-.02
-.04
-.06

FIGURE E9

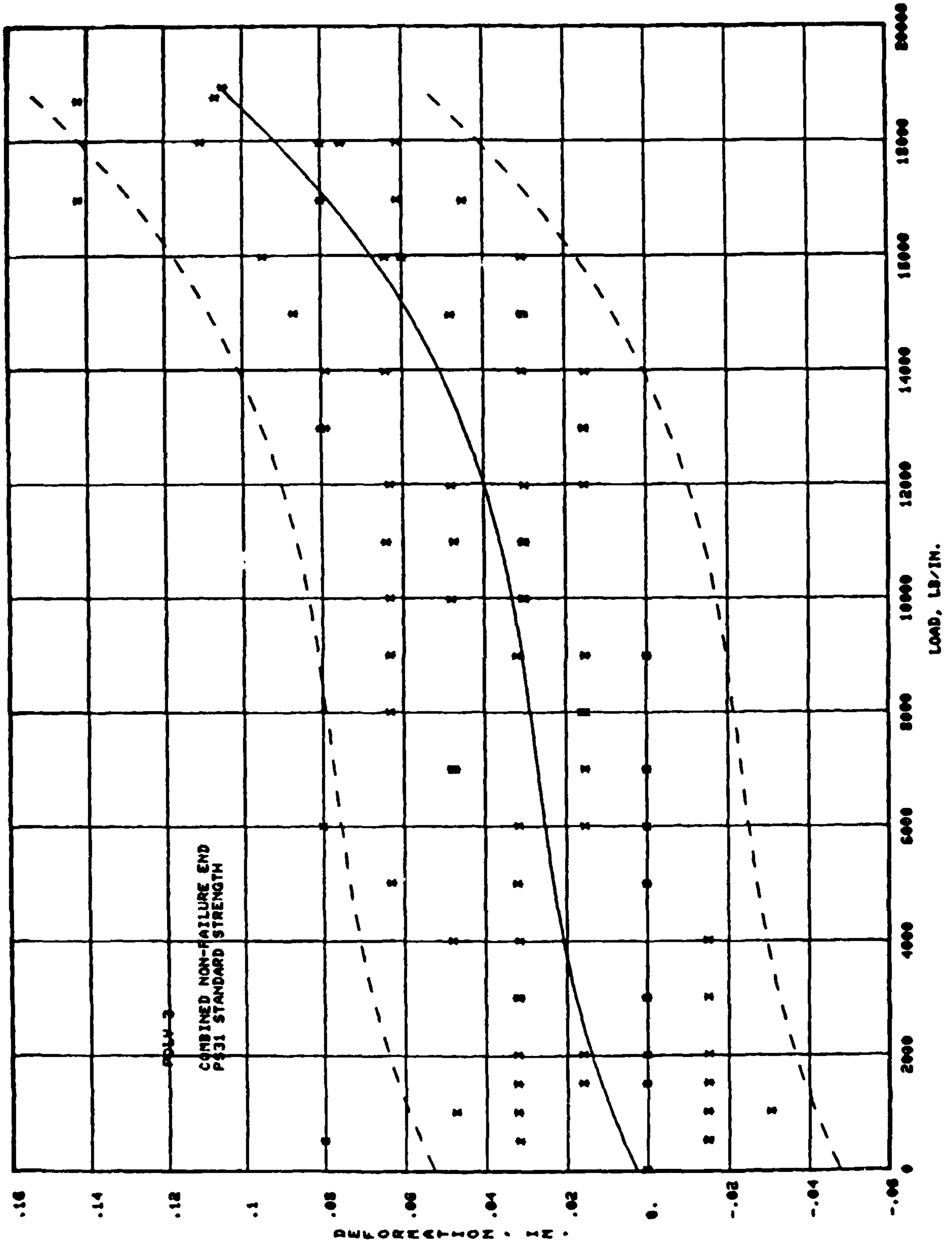

FIGURE E10

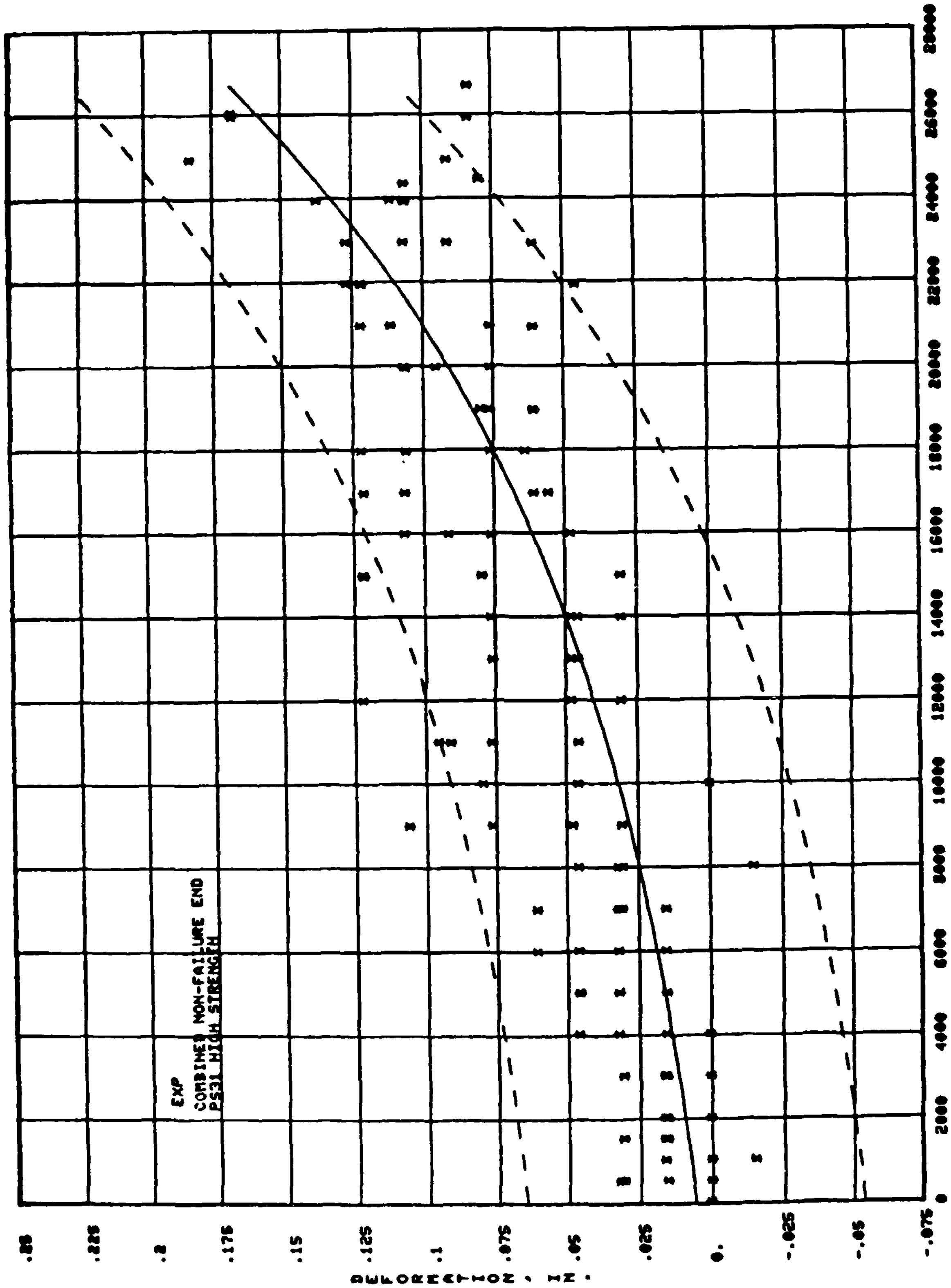

FIGURE E11

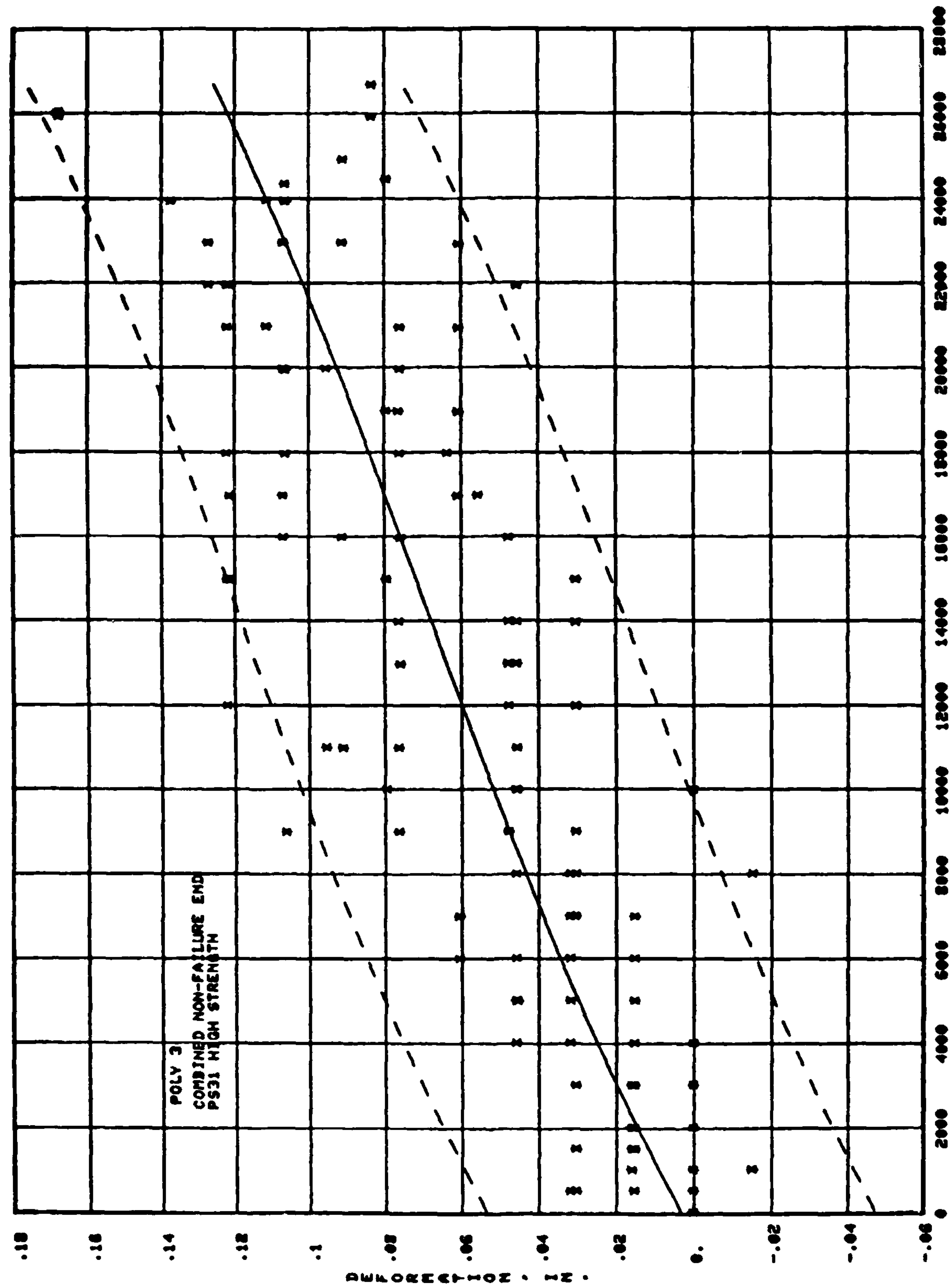

POLY 3
COMBINED NON-FAILURE END
PS31 HIGH STRENGTH
LOAD, LB/IN.
0
2000
4000
6000
8000
10000
12000
14000
16000
18000
20000
22000
24000
26000
28000
.18
.16
.14
.12
.1
.08
.06
.04
.02
0.
-.02
-.04
-.06

FIGURE E12

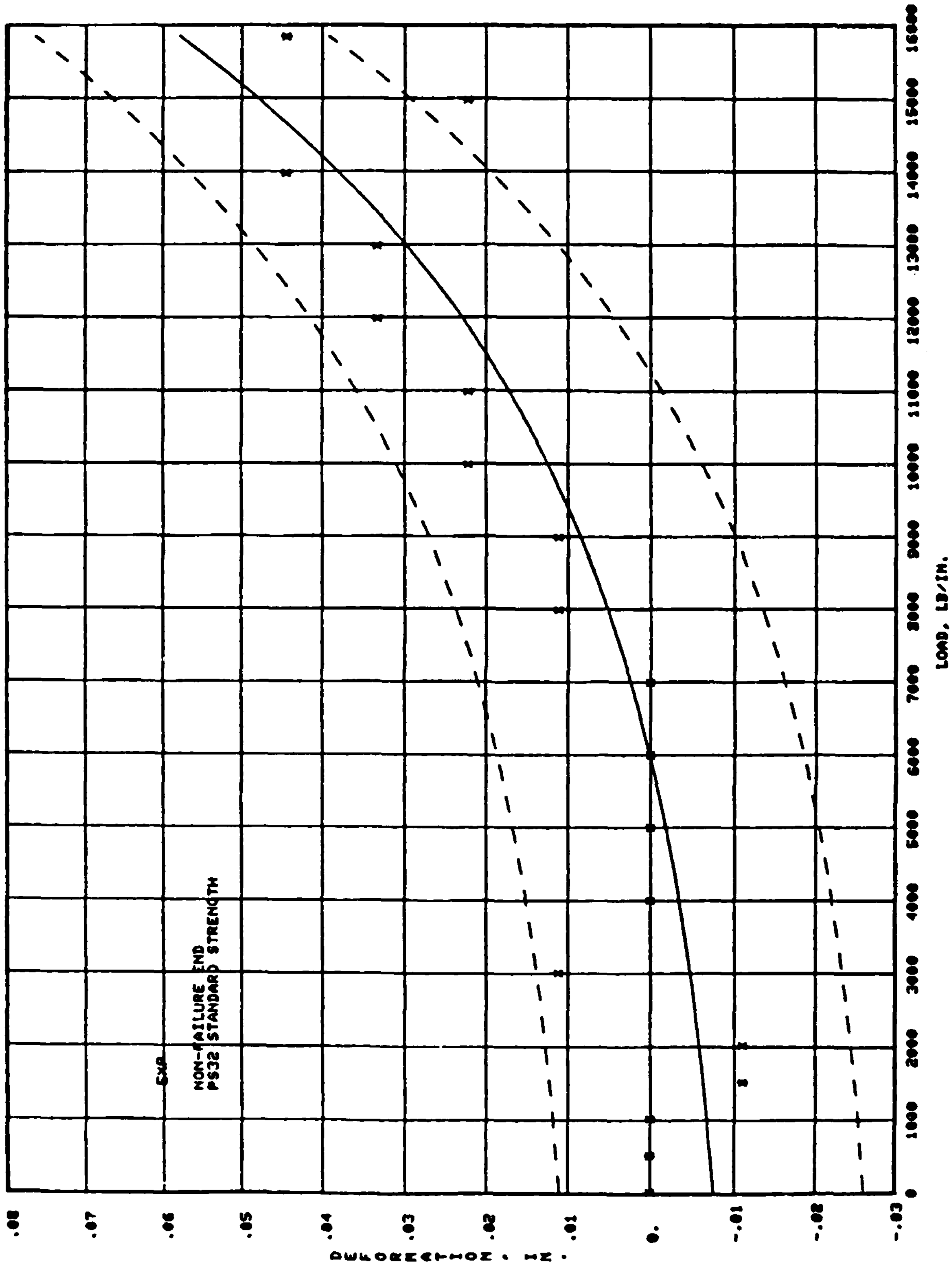
NON-FAILURE END
PS32 STANDARD STRENGTH
EXP
LOAD, LB/IN.
0
1000
2000
3000
4000
5000
6000
7000
8000
9000
10000
11000
12000
13000
14000
15000
16000
.08
.07
.06
.05
.04
.03
.02
.01
0.
-.01
-.02
-.03

FIGURE E13

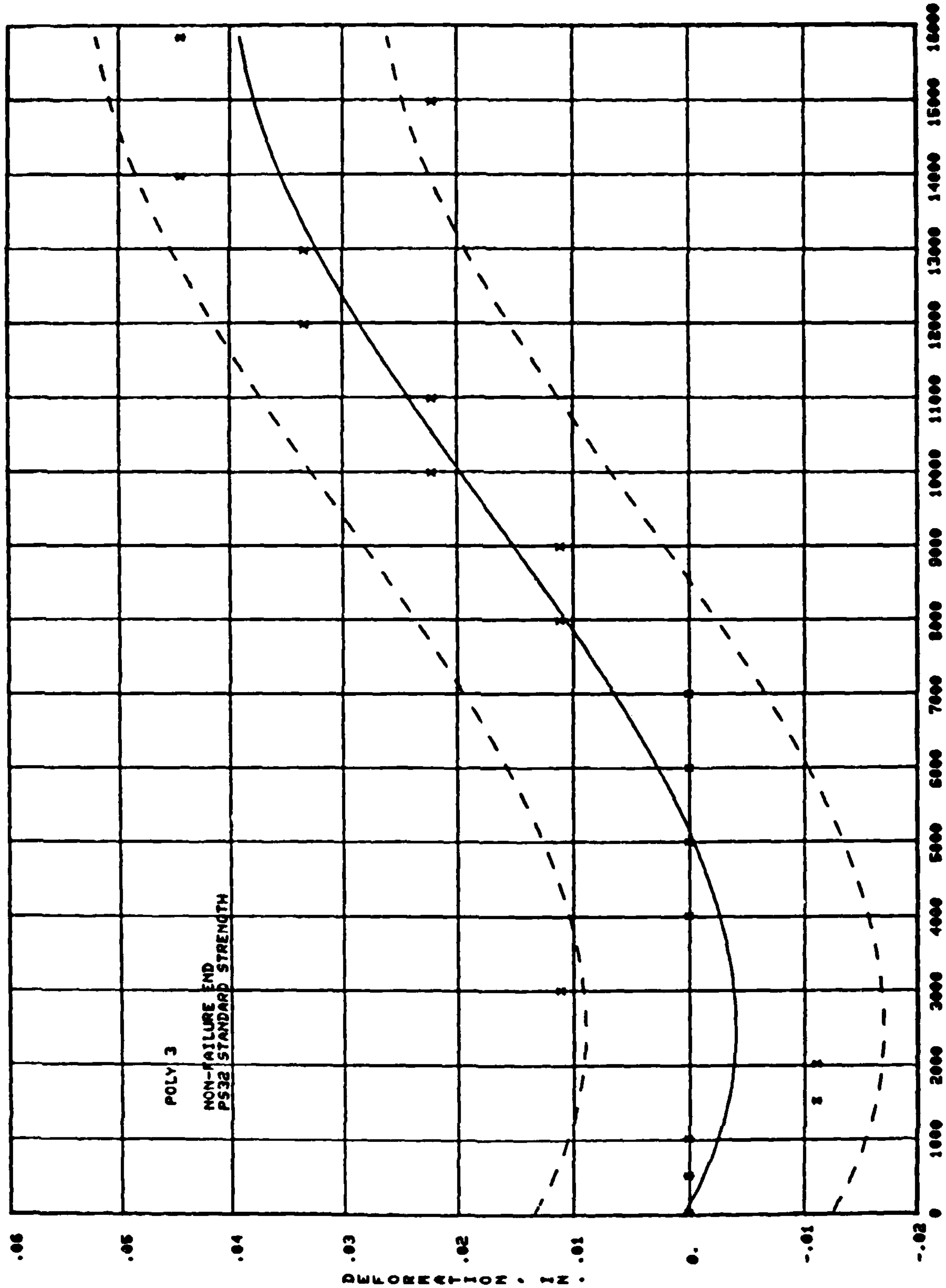
POLY 3
NON-FAILURE END
PS32 STANDARD STRENGTH
LOAD, LB/IN.
0
1000
2000
3000
4000
5000
6000
7000
8000
9000
10000
11000
12000
13000
14000
15000
16000
.06
.05
.04
.03
.02
.01
0.
-.01
-.02

FIGURE E14

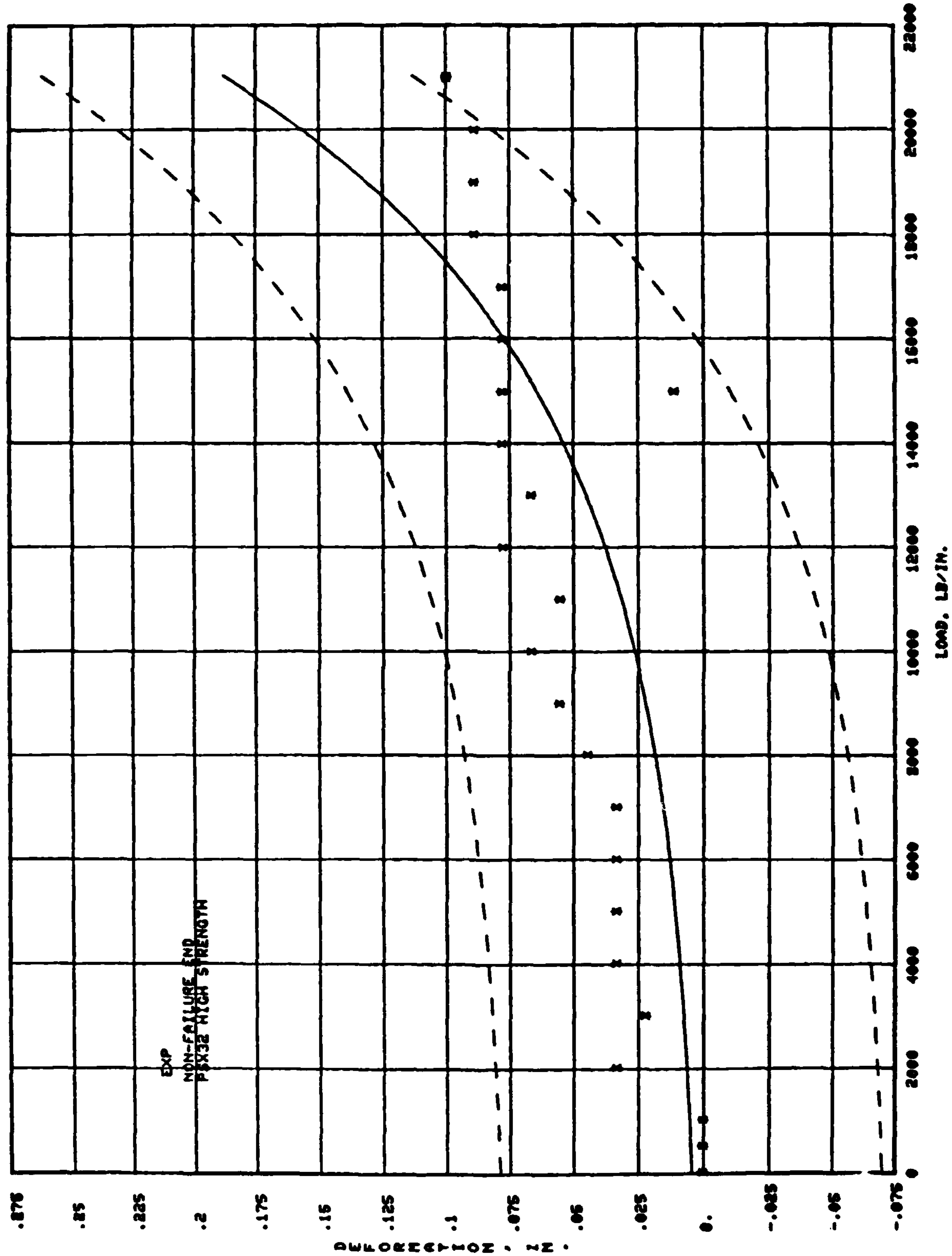
EXP
NON-FAILURE END
P3X32 HIGH STRENGTH
LOAD, LB/IN.
0
2000
4000
6000
8000
10000
12000
14000
16000
18000
20000
22000
.275
.25
.225
.2
.175
.15
.125
.1
.075
.05
.025
0.
-.025
-.05
-.075

FIGURE E15

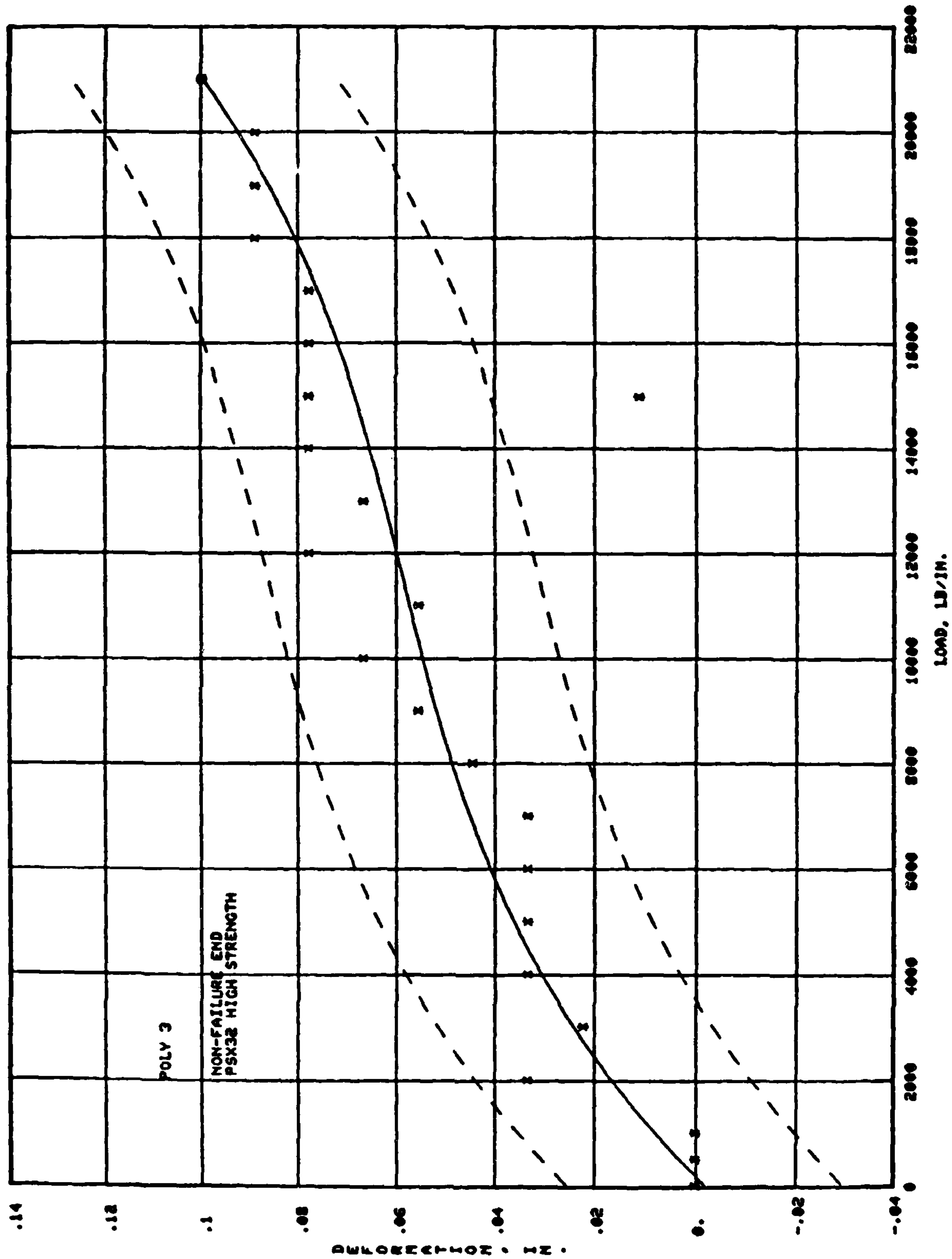
POLY 3
NON-FAILURE END
PSX32 HIGH STRENGTH
LOAD, LB/IN.
0
2000
4000
6000
8000
10000
12000
14000
16000
18000
20000
22000
.14
.12
.1
.08
.06
.04
.02
0.
-.02
-.04

FIGURE E16

APPENDIX F: PLOTS OF STRESS VERSUS GROSS STRAIN

Plots of stress versus gross strain were generated for tests of PS31 standard- and high-strength, PS32 standard-strength, and PSX32 high-strength piles and are shown in Figures F1 through F10.

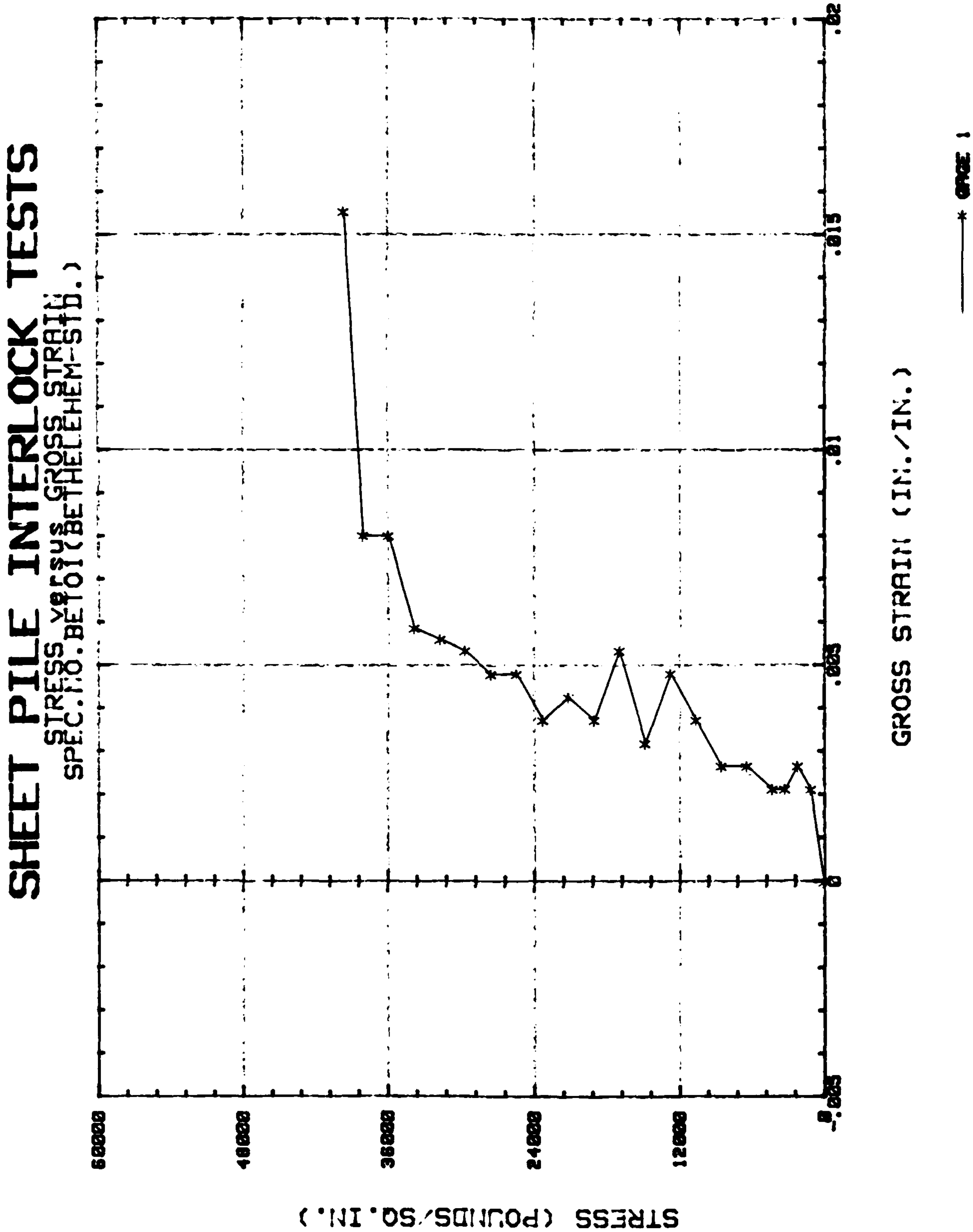

SHEET PILE INTERLOCK TESTS
STRESS versus GROSS STRAIN
SPEC.NO.BETO1(BETHELEHEM-STD.)
STRESS (POUNDS/SQ.IN.)
60000
48000
36000
24000
12000
0
GROSS STRAIN (IN./IN.)
-.005
0
.005
.01
.015
.02
GAGE 1

FIGURE F1

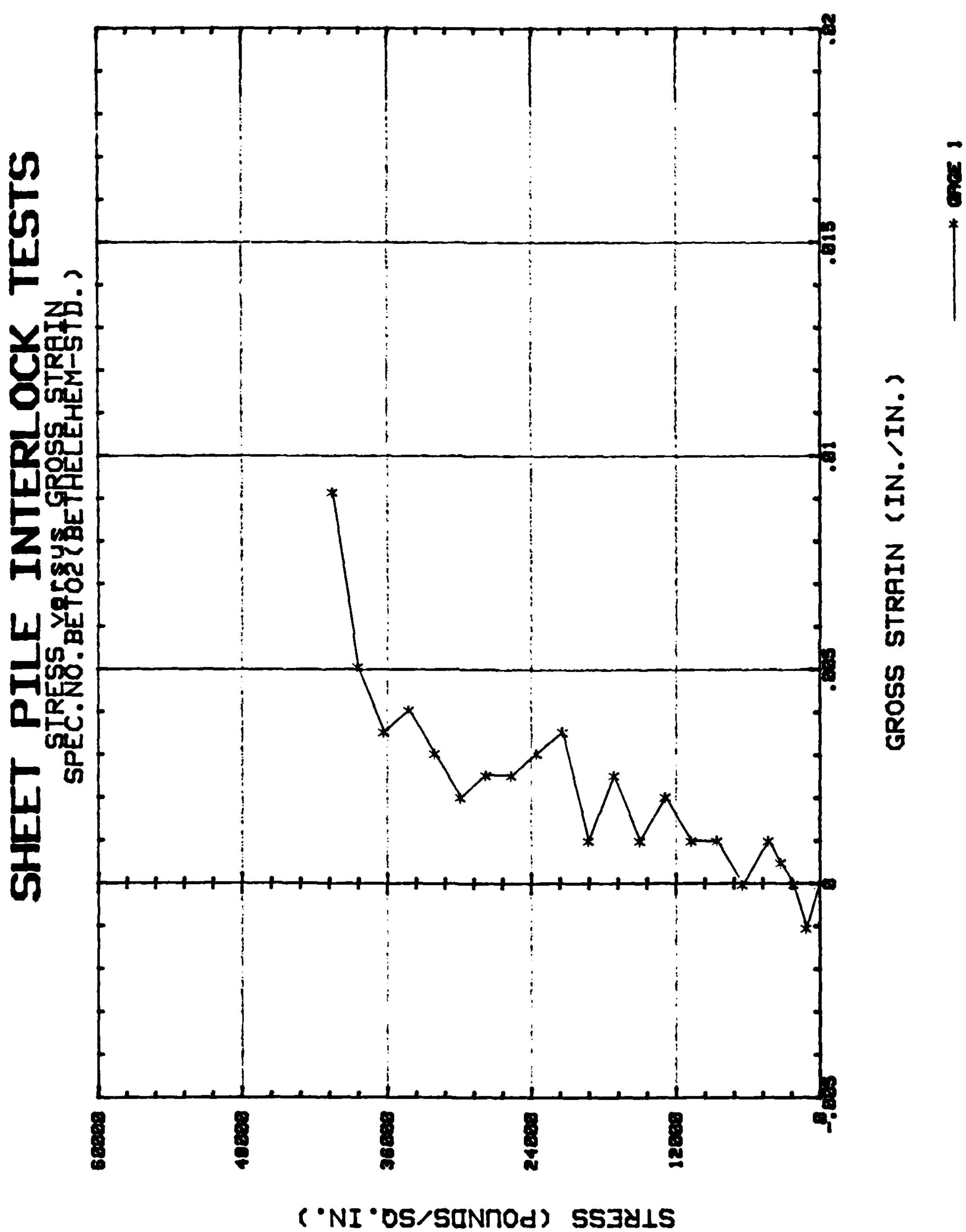
SHEET PILE INTERLOCK TESTS
STRESS versus GROSS STRAIN
SPEC.NO.BET02(BETHELEHEM-STD.)
GROSS STRAIN (IN./IN.)
STRESS (POUNDS/SQ.IN.)
GAGE 1
60000
48000
36000
24000
12000
0
-.005
0
.005
.01
.015
.02

FIGURE F2

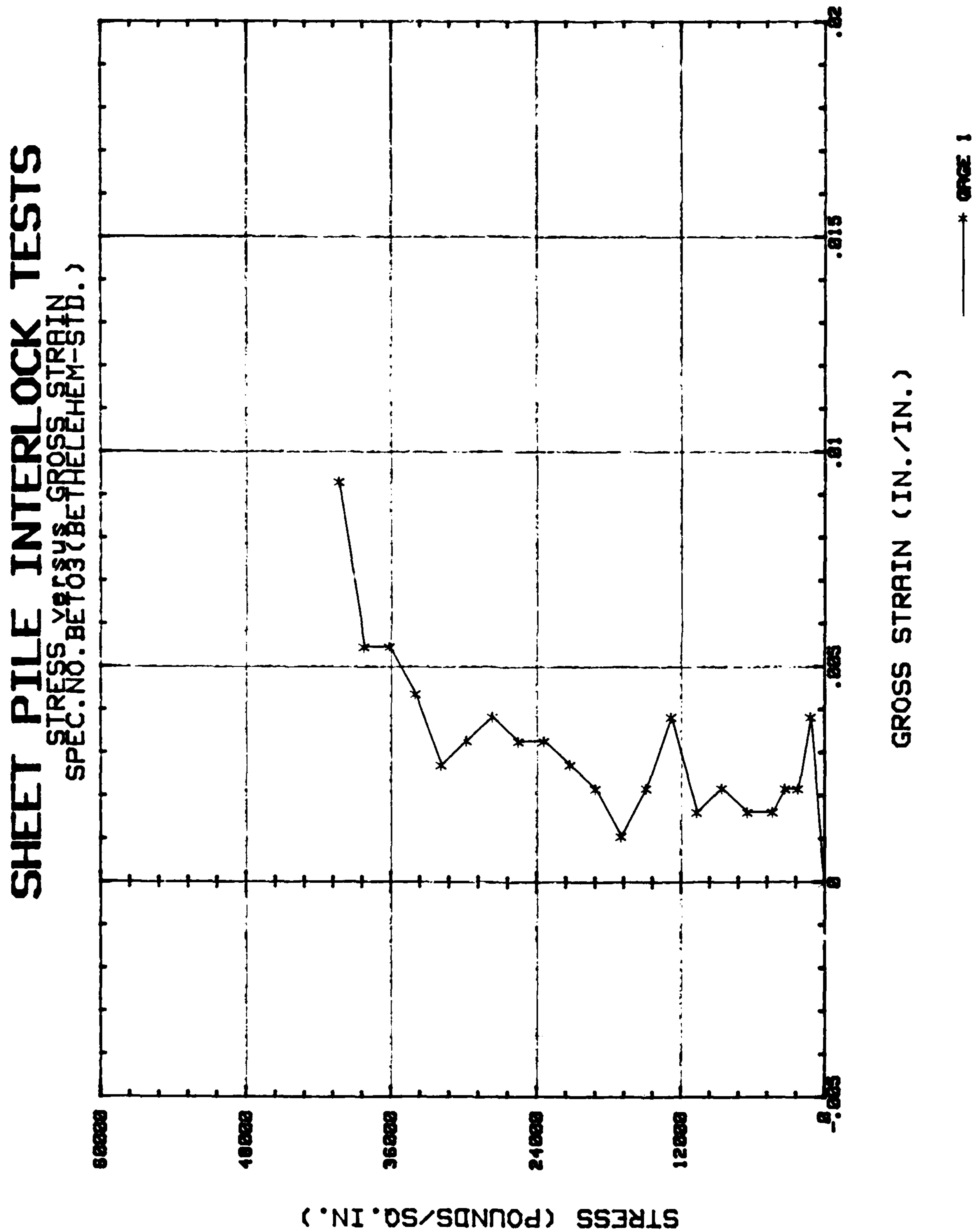
SHEET PILE INTERLOCK TESTS
STRESS versus GROSS STRAIN
SPEC.NO.BET03(BETHELEHEM-STD.)
GROSS STRAIN (IN./IN.)
-.005
0
.005
.01
.015
.02
STRESS (POUNDS/SQ.IN.)
60000
48000
36000
24000
12000
0
GAGE 1

FIGURE F3

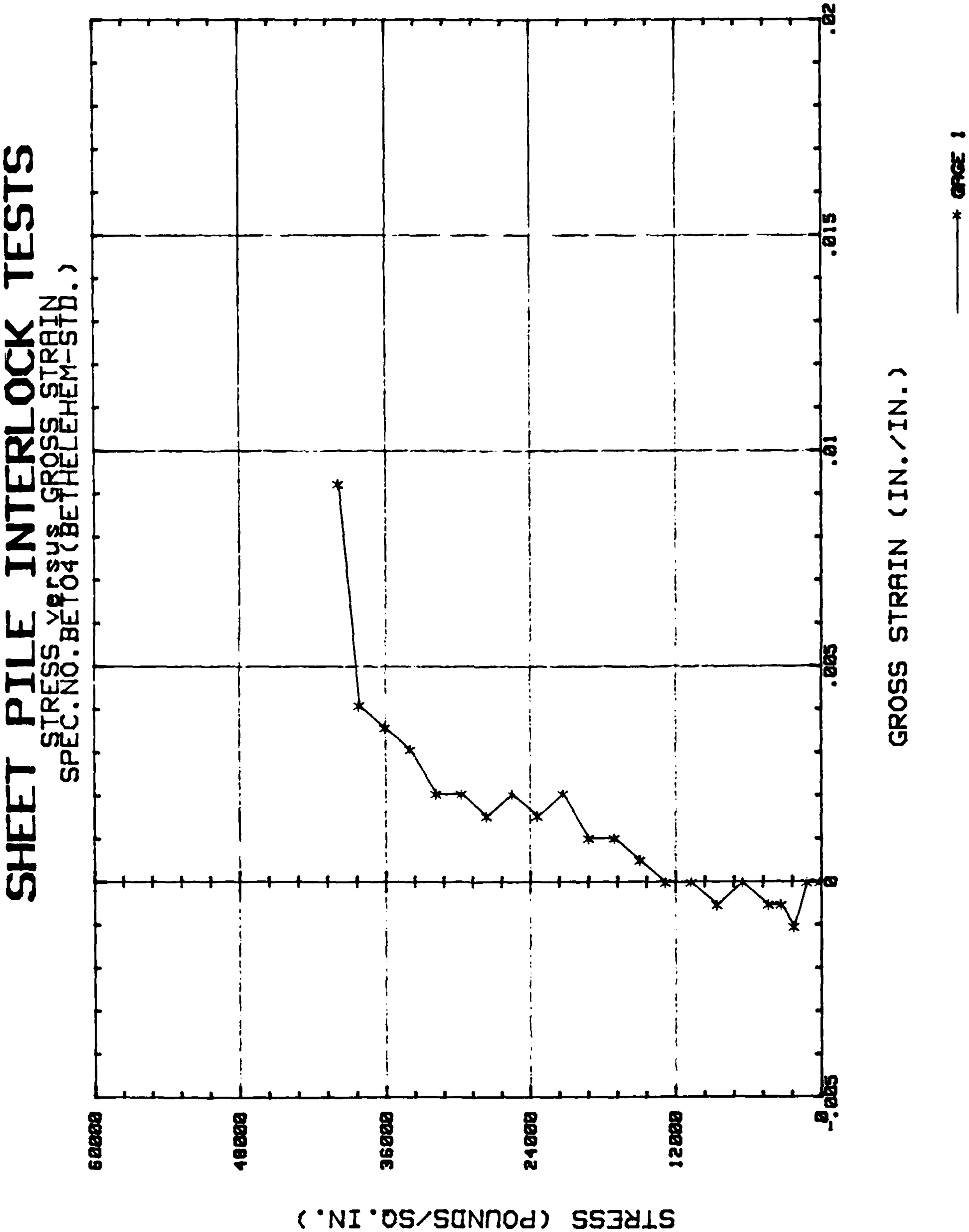

SHEET PILE INTERLOCK TESTS
STRESS versus GROSS STRAIN
SPEC.NO.BET04(BETHELEHEM-STD.)
GROSS STRAIN (IN./IN.)
STRESS (POUNDS/SQ.IN.)
GAGE 1
-.005
0
.005
.01
.015
.02
0
12000
24000
36000
48000
60000

FIGURE F4

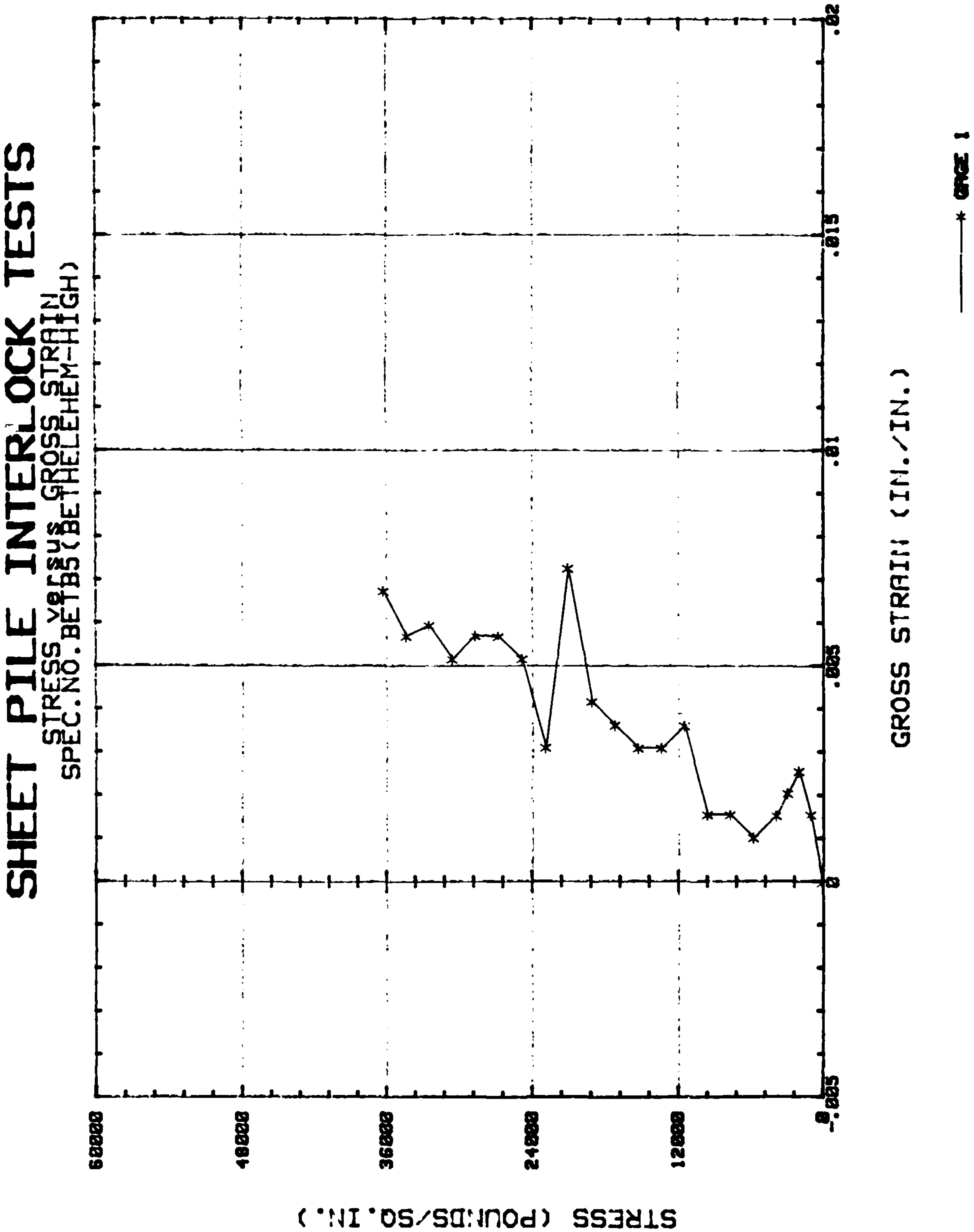
SHEET PILE INTERLOCK TESTS
STRESS versus GROSS STRAIN
SPEC.NO.BETB5(BETHELEHEM-HIGH)
GROSS STRAIN (IN./IN.)
STRESS (POUNDS/SQ.IN.)
-.005
0
.005
.01
.015
.02
0
12000
24000
36000
48000
60000
GAGE 1

FIGURE F5

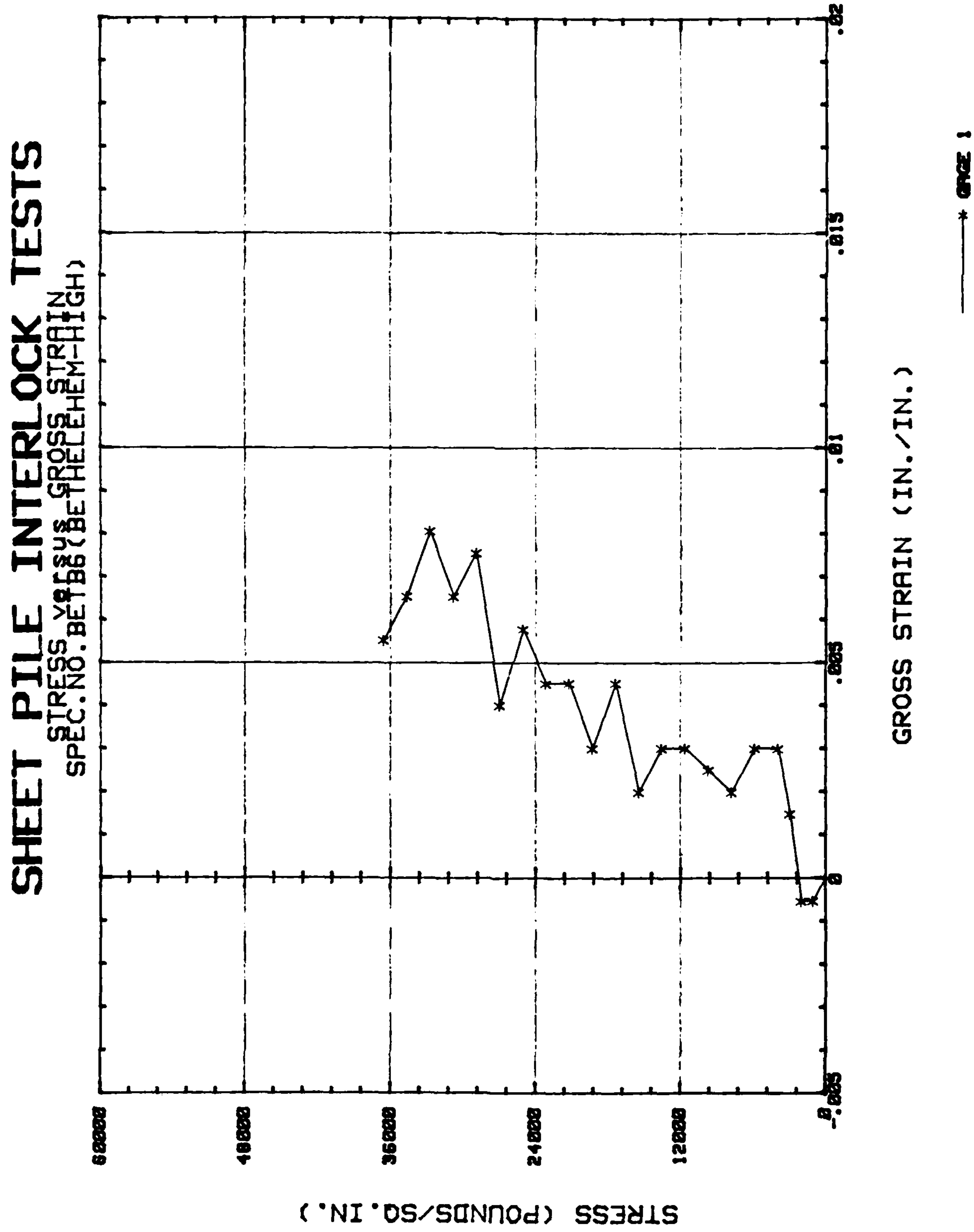
SHEET PILE INTERLOCK TESTS
STRESS versus GROSS STRAIN
SPEC.NO.BETB6(BETHLEHEM-HIGH)
GROSS STRAIN (IN./IN.)
STRESS (POUNDS/SQ.IN.)
GAGE 1
-.005
0
.005
.01
.015
.02
60000
48000
36000
24000
12000

FIGURE F6

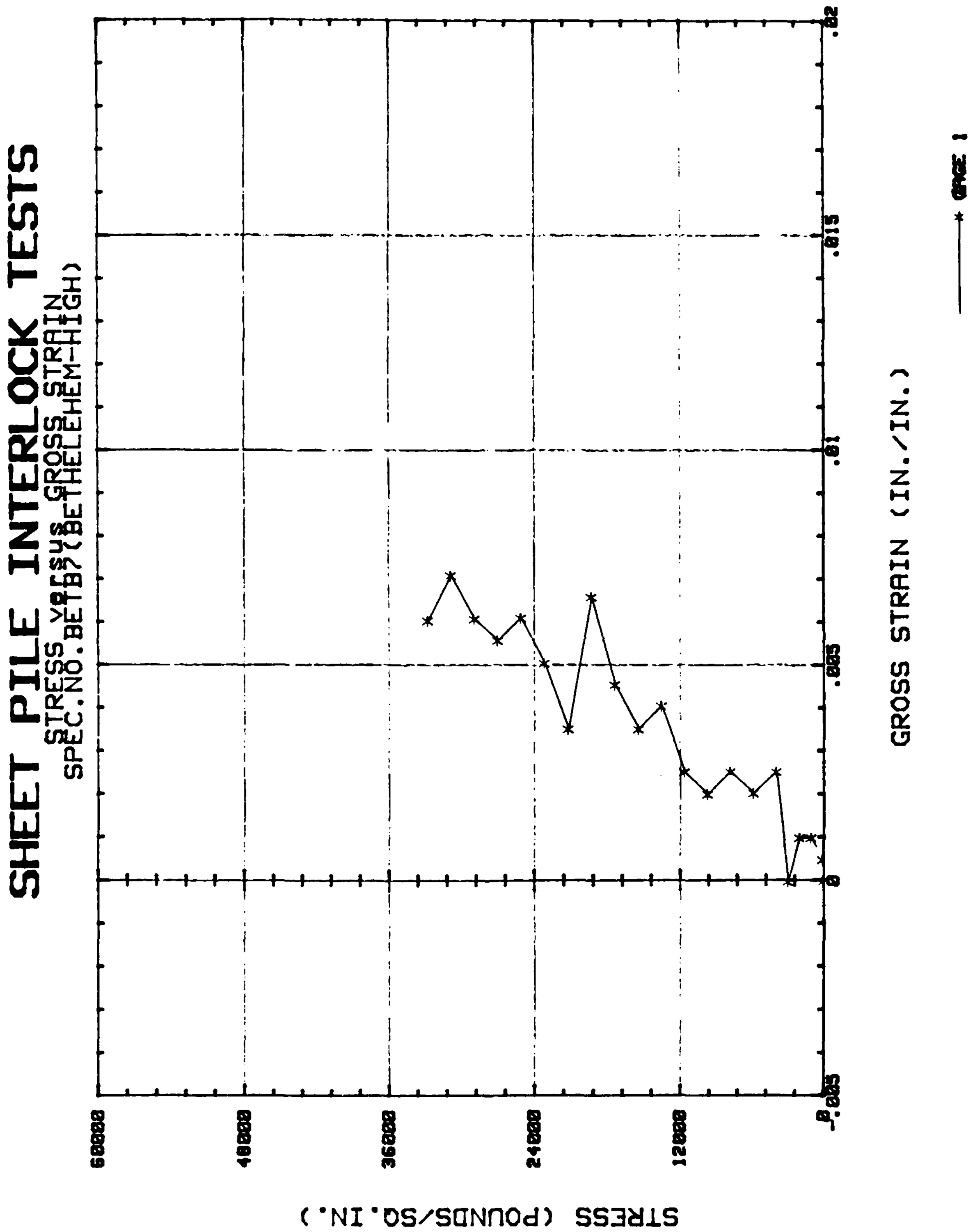
SHEET PILE INTERLOCK TESTS
STRESS versus GROSS STRAIN
SPEC.NO.BETB7(BETHELEHEM-HIGH)
GROSS STRAIN (IN./IN.)
-.005
0
.005
.01
.015
.02
STRESS (POUNDS/SQ.IN.)
0
12000
24000
36000
48000
60000
GAGE 1

FIGURE F7

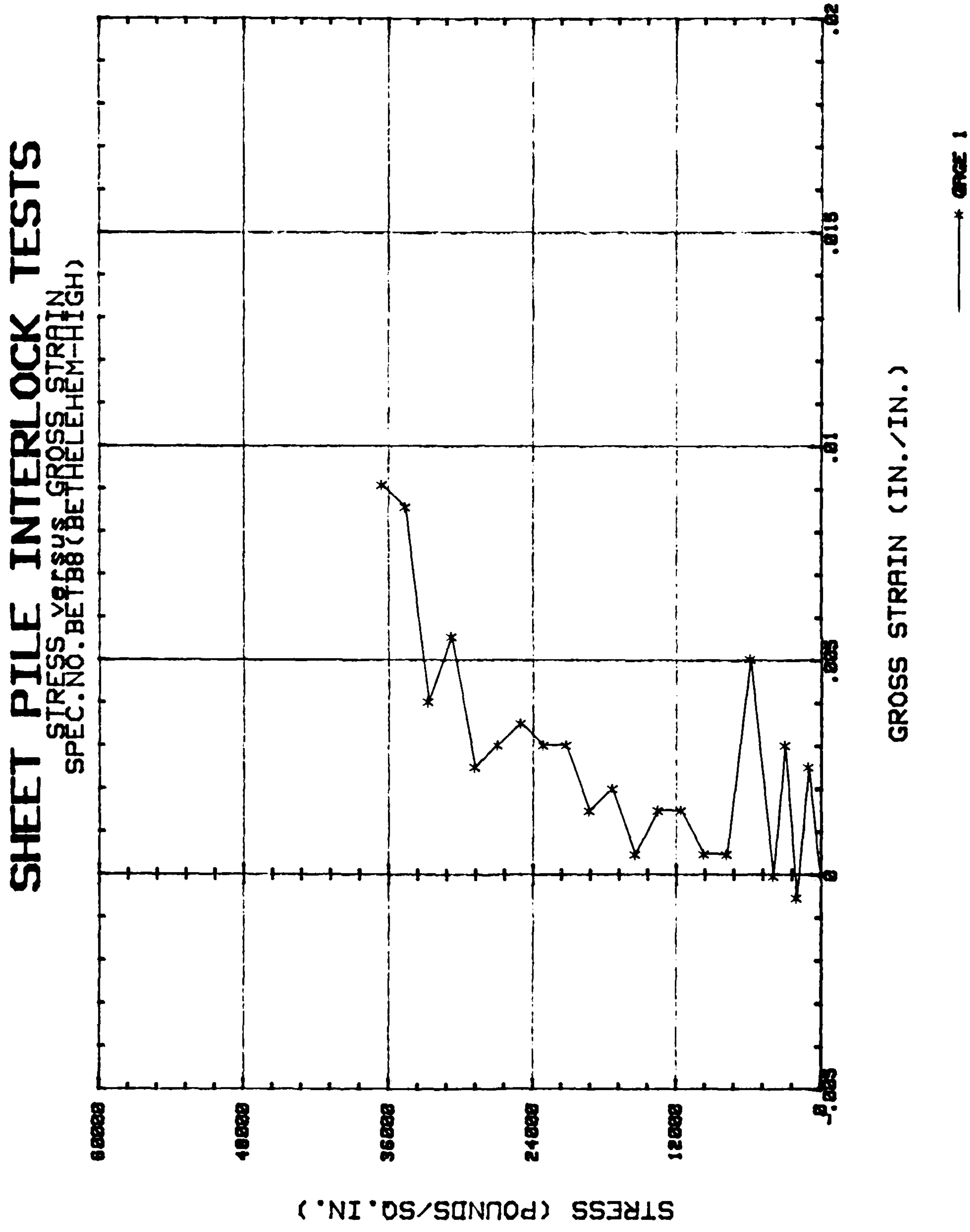
SHEET PILE INTERLOCK TESTS
STRESS versus GROSS STRAIN
SPEC.NO.BETB8(BETHELEHEM-HIGH)
GROSS STRAIN (IN./IN.)
STRESS (POUNDS/SQ.IN.)
60000
48000
36000
24000
12000
0
-.005
0
.005
.01
.015
.02
GAGE 1

FIGURE F8

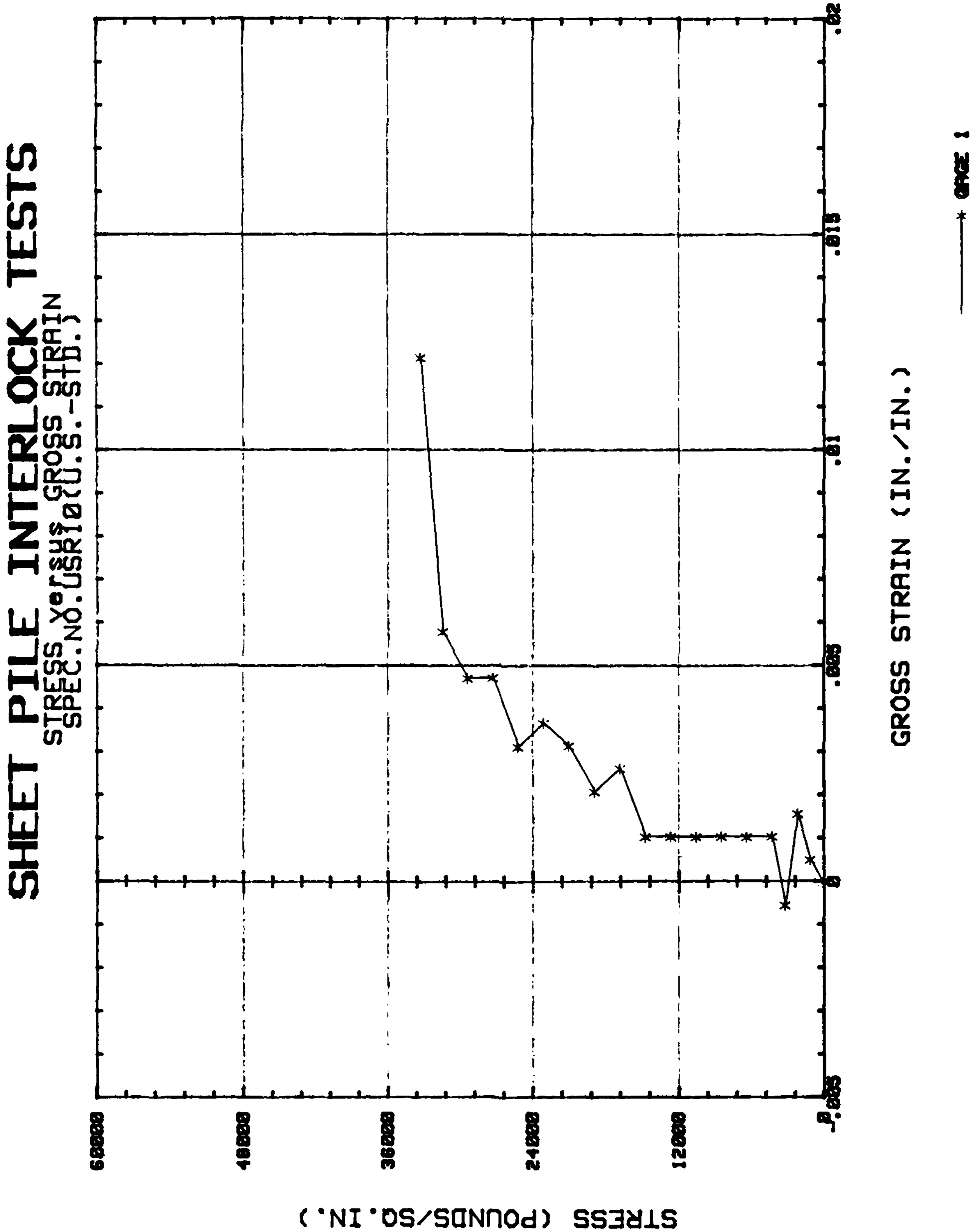
SHEET PILE INTERLOCK TESTS
STRESS VERSUS GROSS STRAIN
SPEC.NO.USR10(U.S.-STD.)
GROSS STRAIN (IN./IN.)
STRESS (POUNDS/SQ.IN.)
GAGE 1
60000
48000
36000
24000
12000
0
-.005
0
.005
.01
.015
.02

FIGURE F9

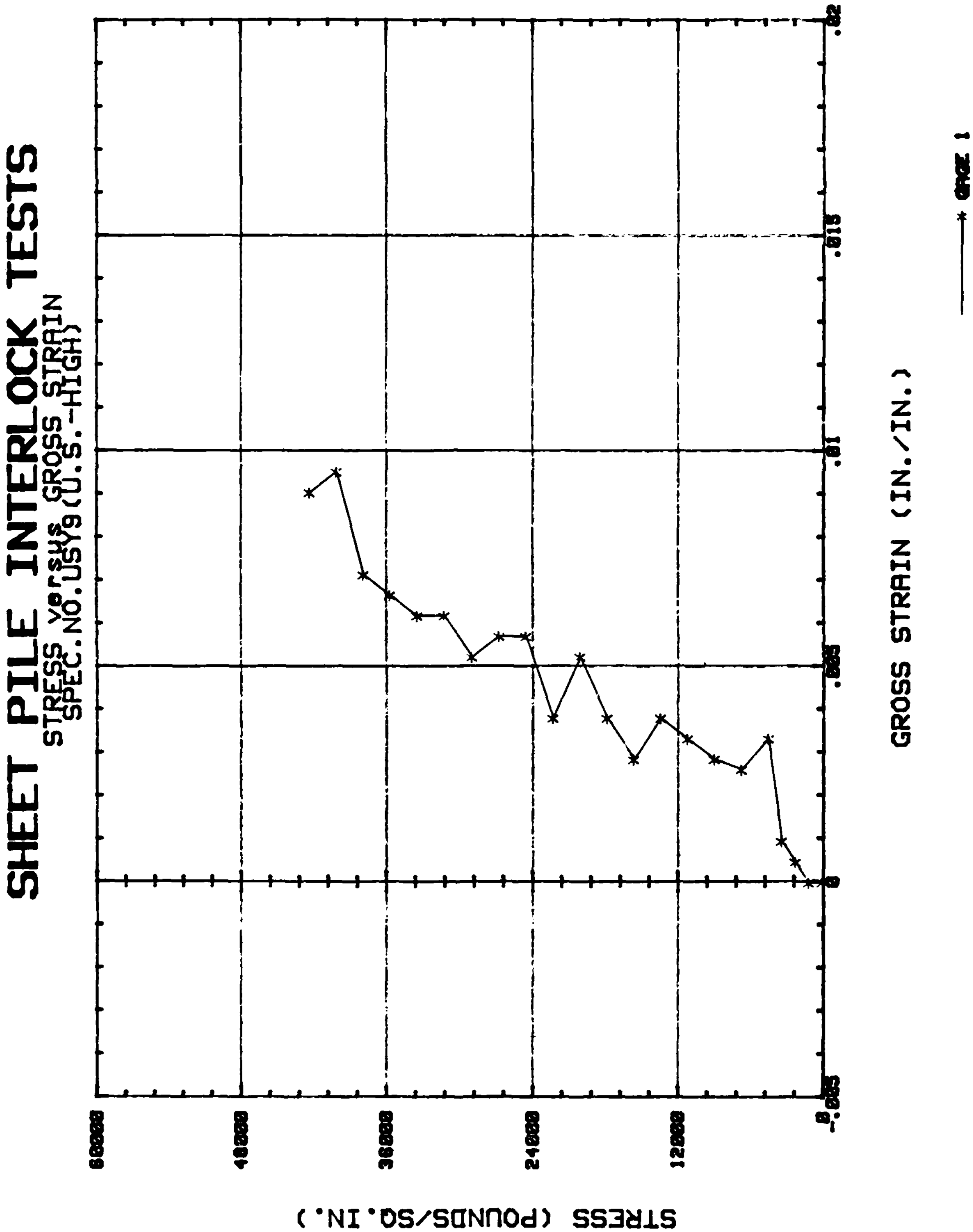
SHEET PILE INTERLOCK TESTS
STRESS versus GROSS STRAIN
SPEC.NO.USY9(U.S.-HIGH)
STRESS (POUNDS/SQ.IN.)
GROSS STRAIN (IN./IN.)
GAGE 1
60000
48000
36000
24000
12000
0
-.005
0
.005
.01
.015
.02

FIGURE F10